RATES OF ELEMENTAL SULPHUR OXIDATION AND ASSOCIATED OXYGEN AND SULPHUR ISOTOPE FRACTIONATION

A Thesis Submitted to the College of
Graduate Studies and Research
In Partial Fulfillment of the Requirements
For the Degree Master of Science
In the Department of Geological Sciences
University of Saskatchewan
Saskatoon

By
LAURA A. SMITH

PERMISSION TO USE

In presenting this thesis in partial fulfillment of the requirements for a Postgraduate degree from the University of Saskatchewan, I agree that the Libraries of this University may make it freely available for inspection. I further agree that permission for copying of this thesis in any manner, in whole or in part, for scholarly purposes may be granted by the professor or professor who supervised my thesis work or, in their absence, by the Head of the Department or the Dean of College in which my thesis work was done. It is understood that any copying or publication or use of this thesis or parts thereof for financial gain shall not be allowed without my written permission. It is also understood that due recognition shall be given to me and to the University of Saskatchewan in any scholarly use which may be made of any material in my thesis.

Requests for permission to copy or to make other use of material in this thesis in whole or part should be addressed to:

Head of the Department of Geological Sciences
University of Saskatchewan
114 Science Place
Saskatoon, Saskatchewan
Canada
S7N 5E2

ABSTRACT

Elemental sulphur (S^0) is removed from sour gas deposits (high H_2S) during refinement. The resulting S^0 is often stored onsite when the costs of shipping S^0 to market exceeds the costs of storing it in large above ground blocks. With the aid of acidiphilic bacteria, atmospheric air and water oxidize S^0 to sulphate (SO_4^{2-}). Long term storage is under consideration; however, oxidation rates and the role of each oxygen source ($O_{2(g)}$ and H_2O) is not clear.

S^0 oxidation experiments were conducted over a range of temperatures (6-32°C) to investigate reaction rates and isotopic fractionation of O and S isotopes during oxidation. The experiments also investigated the effect of integrating S^0 oxidizing microorganisms and available nutrients on both the reaction rates and isotope fractionation. Results indicated > 95% of total SO_4^{2-} generated can be attributed to autotrophic microbial activity. Experiments conducted in a nutrient rich mineral solution showed rates increase with temperature from 0.16 (6°C) to 0.98 (32°C) μg S^0 cm^{-2} d^{-1} ($Q_{10} \approx 1.7 - 1.9$). Experiments conducted in a nutrient poor solution (deionized water) showed oxidation rates did not increase with temperature (0.06 to 0.08 μg S^0 cm^{-2} d^{-1}) between 12 and 32°C. Oxygen isotope analysis of the generated SO_4^{2-} indicated essentially all oxygen incorporated into the SO_4^{2-} originated from H_2O. In addition, effluent samples obtained from S^0 block effluent at SCL indicated $\delta^{18}O_{(SO4)}$ generally reflected the $\delta^{18}O_{(H2O)}$ in the system at the time of oxidation. While covering the S^0 blocks with an impermeable cover would undoubtedly minimize total SO_4^{2-} accumulation in block effluent, the results of this study suggest $\delta^{18}O_{(SO4)}$ can also be used to track water movement through the block.

ACKNOWLEDGEMENTS

I would like to thank my supervisor Dr. M. Jim Hendry for his continued support, guidance and encouragement throughout the duration of my thesis.

Also, thank you to Dr. Leonard Wassenaar for providing thought-provoking comments and suggestions.

Thank you to Dr. Kevin Ansdell and Dr. Yuanming Pan for serving as department chairs on my committee; and to Dr. Rich Farrell for providing valuable comments and suggestions as my external examiner.

The advice and laboratory assistance from John Lawrence and George Swerhone was an invaluable resource regarding all aspects of microbiology in this thesis.

To Dr. Bernhard Meyer and Steve Taylor at the University of Calgary, thank you for advice and isotope analysis. And to the people at Syncrude Canada Ltd., thank you for diligently taking weekly samples and shipping them to the University.

Without the financial support of Syncrude Canada Ltd. and the NSERC-CRD program, this thesis would not have been possible.

I am greatly appreciative of the people I have met in the Geological Sciences department, students, employees, and professors alike. You all have made my time in the department truly memorable.

To my friends, thank you for the countless late nights of listening and attempting to offer advice when you had no idea what I was talking about.

Finally, a special thank you to my family for supporting me in everything I've chosen to do. Your unwavering encouragement, patience and love made everything seem easier.

TABLE OF CONTENTS

LIST OF FIGURES

LIST OF TABLES

1.0 INTRODUCTION

1.1 Overview

The Alberta oil sands are one of the largest petroleum deposits in the world. The sand deposits currently account for approximately 40% of Canada's crude oil production, but this is expected to increase to 70% by 2015 (Timilsina et al., 2005). The estimated volume of crude oil bitumen in place is 400 billion cubic meters, of which 49 billion cubic metres is recoverable using current technology (approximately 174 billion barrels) (Timilsina et al., 2005; NEB, 2000).

The long-term increasing price of oil and declining availability of conventional oil resources allows for continued exploration, recovery, and refinement of the deposits. Unlike conventional deposits, the oil sand extractions are high in hydrogen sulphide (H_2S) content (several mole % or more). Refinement of these high H_2S reservoirs (coined 'sour gas' reservoirs) produces elemental sulphur (S^0) as a byproduct. In 2006, 66 million tonnes of S^0 were produced as auxiliary waste during oil sands refinement, comprising approximately 90% of total world sulphur production (Crescenzi et al., 2006; Ober, 2006).

Since the early 1990's, increased production of oil from sour gas reservoirs has created a surplus of S^0 in the world market, driving down its commodity price (McKenna, 2004). As a result, the cost of shipping S^0 offsite from the oil sands region of western Canada often exceeds the costs of storing it onsite. Further, continued and increasing production of S^0 virtually ensures that its economic value will not recover in the near future. Canada, for example, will likely increase its oil sands production by 100-150% in the next five years (Crescenzi et al., 2006). The alternative to shipping S^0 to market is storing it on-site in large, above ground blocks. These sulphur depositories are anticipated to last up to 100 years or more; however, long-term storage creates multiple concerns for producers in the oil sands.

In 2004, the University of Saskatchewan initiated a study of stored S^0 blocks at Syncrude Canada Ltd (SCL) near Fort McMurray, AB. A key objective of this study was to assess the production rate of sulphuric acid (H_2SO_4) via the oxidation of S^0. This objective was addressed by a multidisciplinary group of researchers, focusing on aspects of the geochemical, biochemical, hydraulic and physical properties that govern the production and redistribution of H_2SO_4 in the storage blocks. The findings of this assessment will be used to address the long-term impacts of existing S^0 blocks, as well as to explore alternative storage methods. The focus

of the current study is the oxidation of S^0 to sulphate (SO_4^{2-}), which is present in the low pH effluent from onsite storage blocks.

1.2 Research Objectives

The production of H_2SO_4 via the abiotic and biotic oxidation of S^0 has been studied extensively. However, most research to date has focused on understanding and improving the efficiency of S^0 oxidation in soils for crop fertilization (Germida and Janzen, 1993; Watkinson, 1989; Laishley et al., 1986; Lawrence et al., 1988; Janzen and Bettany, 1987a; Janzen and Bettany, 1987b; Attoe et al., 1966). Considerable knowledge also exists on the rates and controls of the oxidation of sulphide minerals in mine tailings with a strong emphasis on mineral pyrite oxidation (Balci et al., 2007, Gleisner et al., 2002, 2006; Bernier and Warren, 2005; Taylor and Wheeler, 1984). However, laboratory and field studies are needed to focus on the key factors controlling the oxidation of S^0 and subsequent production of SO_4^{2-} in S^0 blocks.

Stable isotopes of S and O can be used to understand how sulphur reactions progress (Balci et al., 2007; Taylor and Wheeler, 1984a, 1984b; Lloyd, 1967). The majority of research in this field is focused on sulphide mineral (pyrite) oxidation in acid mine drainage (AMD). While AMD provides a good model for comparative purposes, the oxidation of sulphide minerals can be achieved in anaerobic environments via pathways unavailable for S^0 oxidation. Further, limited research exists on the application of stable isotopes to the oxidation of S^0 relating directly to commercial scale S^0 blocks.

The production of H_2SO_4 in the blocks is complex because the blocks are in direct contact with the atmosphere and external variables such as temperature, moisture content, surface area, microorganisms, and the availability of both essential nutrients and molecular oxygen can all exert a control on the rate of H_2SO_4 production. To draw conclusions regarding the long-term storage of S^0 and minimizing impact on the surrounding environment, the relationship between changing environmental conditions and the oxidation of S^0 was investigated.

The goal of the current research was to assess whether the application of O and S isotopes of aqueous SO_4^{2-} could be used to provide insight into the process and controls on the oxidation of S^0 in sulphur blocks. To achieve this goal, four research objectives were defined:

1) Measure the abiotic and biotic oxidation of S^0 to SO_4^{2-} in laboratory controlled S^0 oxidation experiments as a function of temperature and varying nutrient availability;

2) Quantify the partitioning of oxygen (from molecular O_2 and H_2O) into SO_4^{2-} during abiotic and biotic oxidation of S^0 to identify the proportion of oxygen originating from each source;

3) Collect field SO_4^{2-} and S^0 samples from S^0 blocks to compare with lab results and relationships determined in objective 2 to determine if lab conditions can be considered analogous to field conditions.

2.0 SITE LOCATION

2.1 Syncrude Canada Ltd. (SCL)

The Syncrude Mildred Lake Operation is located on Oil Sands Lease 17/22, 35 km north of Fort McMurray Alberta, Canada (57°N, 111°W, 302 metres elevation above sea level) (Syncrude, 2004). The climate of the area is continental and sub-humid, with long, cold winters and short, hot summers. Annual precipitation averages 450 mm, with half falling as snow. Mean annual air temperature is about -1°C and ranges from -51 to +37°C (Environment Canada website).

Mining operations focus on the McMurray Formation, a lower Cretaceous oil-bearing quartz sandstone. The McMurray Formation overlies a Devonian limestone of the Beaverhill Lake Group, and underlies marine clays of the Clearwater Formation. While the origin of the oil in the McMurray Formation is controversial, the principal theory is that it evolved in highly organic Cretaceous shales in the southern portion of the Alberta Sedimentary Basin. Due to underground pressure, the oil migrated into the silt and sand bodies of the McMurray Formation, where they are now mined (Syncrude, 2008).

The oil sands of the McMurray Formation are a combination of sand, bitumen, mineral-rich clays, and water (NEB, 2000). The useable oil is recovered from the bitumen, a black naphthenic-based hydrocarbon. Bitumen has a consistency much like molasses, and is 4-6% sulphur. The recovered bitumen is upgraded to Syncrude Sweet Blend (SSB), a high-quality, light, sweet crude oil (Syncrude, 2008).

In the third quarter of 2007, SCL produced approximately 348,400 barrels of SSB per day. For every barrel of SSB produced, about 7.5 kg of S^0 is created, which results in a daily production of approximately 2625 tonnes. Current projections estimate SCL will produce one million tonnes of S^0 per year for the remaining 50 year lifespan of the reservoir (Syncrude, 2004). Using present extraction techniques, roughly 175 billion barrels of oil are recoverable; however, new refinement processes could increase the projected production of SSB, and accordingly increase S^0 production (Syncrude, 2008).

2.2 SCL sulphur storage

SCL stores the excess S^0 produced during SSB processing in large, above ground storage blocks (Figure 2.1). The Phase I block was poured between 1994 and 2004, and is approximately 380 m long × 170 m wide × 17 m high. An additional 0.5 m was added in 2005. In total, the Phase I block contains 895,000 m^3 (1.7 million tonnes) of 99.8% purified S^0 (Syncrude, 2004). The phase II block is located approximately 100 m west of the Phase I block. Constructed between 1997 and 2005, it contains approximately 2,000,000 m^3 of S^0, and is 260 m long × 335 m wide × 25 m high. SCL is currently in the process of constructing a third block, named Phase III, located 300 m west of the Phase II block and 400 m west of Phase I. The three blocks are considered large by international standards; where most sulphur blocks range in size between 100-400 m long, 50-200 m wide, and 6-15 m high (McKenna, 2004).

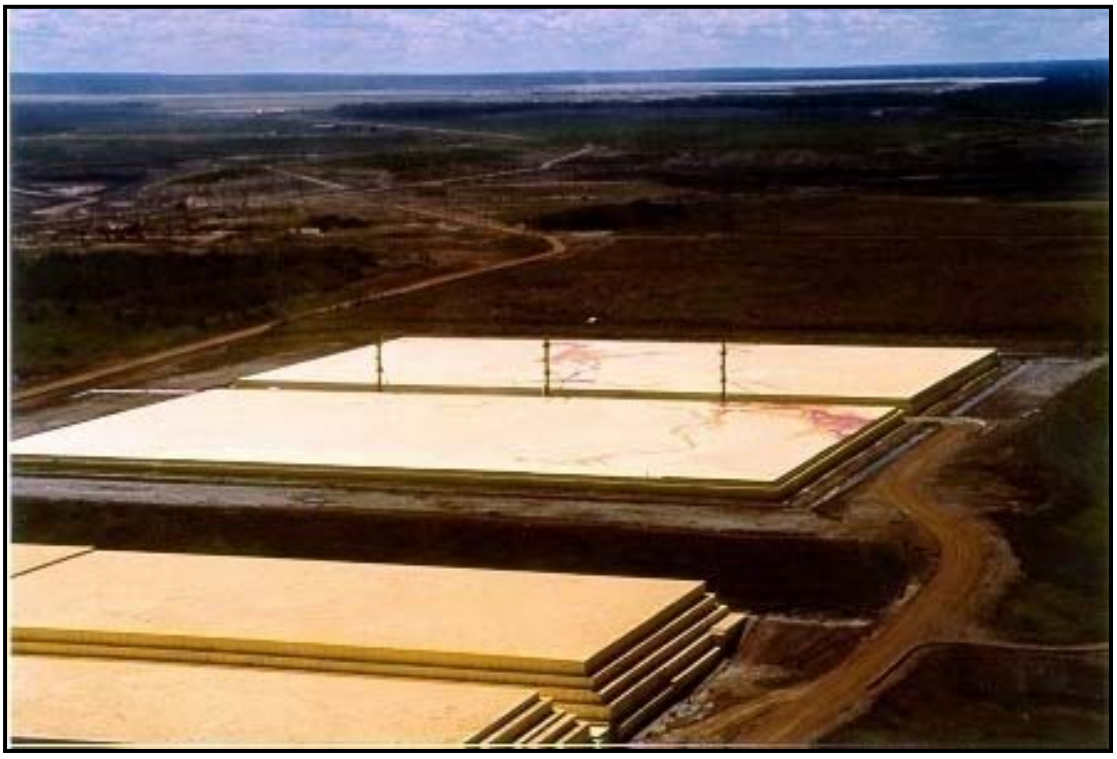

Figure 2.1. Phase I (lower left) and II (center) blocks at SCL Mildred Lake Site (2006).

3.0 Background and Literature Review

3.1 S^0 block construction

Understanding the physical properties of S^0 is essential to constructing large, above ground blocks. Table 3.1 summarizes some important properties of sulphur during progressive cooling phases.

Table 3.1. Physical Properties of S^0 (Meyer, 1977).

Phase	**Melting Point (°C)**	**Density (g cm^{-3})**	**Notes:**
Molten	-	1.82	Temperature range >115°C
Monoclinic	119	1.96	Long, needlelike crystals Stable between 96-199°C
Orthorhombic	113	2.07	Temperature <96°C Stable (stored)

S^0 blocks are constructed by pouring thin lifts (a few cm at most) of molten sulphur (150°C) on a prepared surface of a compacted clay liner at least 5 m deep with a permeability of less than 1×10^{-8} m/s (Golder, 1999). Contained by portable aluminum panels fixed along the entire perimeter of the block, each lift is allowed to solidify/freeze before a successive lift is poured (Figure 3.1). During the first stage of cooling, the molten sulphur converts to a monoclinic crystal form, resulting in a volume loss of approximately 7%. Within a month, the monoclinic sulphur converts to a more stable orthorhombic crystal form, resulting in an additional 5.5% volume loss (SCL Research Dept. Progress Report, 2000). During cooling, the sulphur is vulnerable to cracks and fissures; the blocks undergo the majority of the fracturing observed at both large and small scales during the cooling process. Even with proper construction and maintenance, both horizontal and vertical fracturing occur (Clark, 2005; Golder, 1999).

Figure 3.1. Construction of a S^0 block: pouring of molten sulphur from a pouring tower and subsequent cooling.

Fractures are a dominant factor controlling the migration of gas and water through S^0 blocks (Birkham et al., 2009; Bonstrom, 2007). In addition to increasing the interconnected surface area of the block and exerting a control on gas and water migration, the fractures also provide an environment where sulphur oxidizing microbes are protected from direct sunlight and wind (Figure 3.2) (Pisz, 2008). Therefore, the fractures likely exert an important control on the production, transport and fate of H_2SO_4.

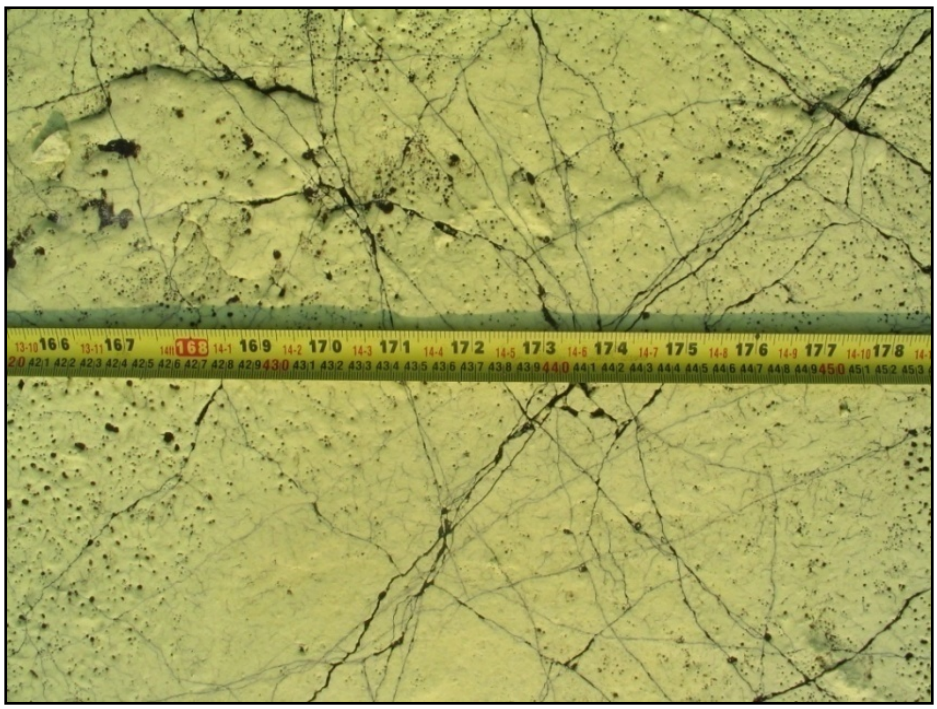

Figure 3.2. Surface fractures in the Phase I block.

3.2 Oxidation of S^0

Sulphur exists in the environment in various oxidation states in both organic and inorganic compounds, and is an essential nutrient for all living plants, animals and microorganisms (Howarth et al., 1992). This study was concerned with the oxidation of zero-valent elemental sulphur (S^0) to sulphate (SO_4^{2-}). When exposed to molecular oxygen and water, reduced sulphur compounds such as sulphide (S^{2-}) and S^0, undergo oxidation in a two part reaction as defined by Lloyd (1967). Sulphite (SO_3^{2-}) is an important intermediate produced in the first step (Equation 3.1), which is then further oxidized to SO_4^{2-} (Equation 3.2). When SO_4^{2-} combines with hydronium ions (H^+), H_2SO_4 acid is produced. The two reactions are expressed in terms of the production of H_2SO_4 by the oxidation of S^0 (Equation 3.3) (Lloyd, 1967):

$$S^0 + H_2O + O_2 \rightarrow SO_3^{2-} + 2H^+ \quad (3.1)$$

$$SO_3^{2-} + 1/2\,O_2 \rightarrow SO_4^{2-} \quad (3.2)$$

$$S^0 + H_2O + 3/2\,O_2 \leftrightarrow H_2SO_4 \quad (3.3)$$

3.2.1 Abiotic

Theoretically, abiotic oxidation of S^0 can occur to a limited extent; however, few attempts to define the rate of abiotic reaction have been reported (Germida, et al., 1993). Previous work regarding the microbial oxidation of sulphur compounds (S^0, H_2S and FeS_2) in laboratory settings always employ sterilized abiotic controls. Comparative results show negligible amounts of SO_4^{2-} produced with time in both long and short term experiments, making rate calculations difficult and often inaccurate (Balci et al., 2007; Gleisner et al., 2006; Germida et al., 1993; Chapman, 1989).

3.2.2 Biotic

Exposed S^0 surfaces during and after block construction are vulnerable to windblown dirt and coke. Sulphur oxidizing microorganisms present in the local soils may colonize the sulphur lifts, allowing microbial habitation to occur. Common features of S^0 blocks are darkly pigmented areas following a layering trend (Figure 3.3). McKenna (2004) suspected these could be indicative of bacterial growth, but no further work was conducted. S^0 stored in areas where fractures are not prevalent and therefore not in direct contact with the atmosphere is bright yellow and free of any darkened areas (matrix sulphur).

Figure 3.3. Horizontal black layer between S^0 lifts of the Phase I block.

Sulphur blocks are characteristically nutrient-poor and subject to the varying seasonal climate of northern Canada. However, it is expected that sulphur oxidizing microorganisms are present and active. The pH of S^0 block effluent waters generally ranges from 2-0.5. Given the particularly slow abiotic oxidation of S^0, sulphur oxidizing microorganisms likely contribute to acid production. Brooks (1989) suggests 90% of the acid generated from mine tailings can be attributed to microbial activity. In addition, Laishley and Bryant (1987) indicate sulphur oxidizing microorganisms thrive under both aerobic and anerobic, and light or dark conditions.

Both autotrophs and heterotrophs are capable of oxidizing S^0. Heterotrophs use molecular O_2 as an electron acceptor, and require carbon from organic matter (Germida and Janzen, 1993). Autotrophs also require O_2, but are capable of fixing carbon from carbon dioxide (CO_2) from energy gained by oxidizing S^0 or other reduced sulphur compounds. This enables S^0 oxidizing autotrophs to survive in nutrient poor environments, where heterotrophs are less likely to find sufficient organic sources for their carbon requirements. In nutrient rich environments where organic compounds are abundant, heterotrophs are generally dominant (Germida, 1991).

Microbial oxidation of S^0 follows a similar reaction pathway as abiotic oxidation. The enzymatic reactions involved in the biotic oxidation of S^0 differ among sulphur oxidizing microorganisms, but all processes end with a (sulphite) SO_3^- group. Suzuki (1992) reports the enzymatic reaction producing SO_3^- is completely dissociated from the reaction producing SO_4^{2-}. This is identical to the abiotic chemical step-wise reaction (Equations 3.1-3.3).

Acitithiobacilli (a chemolithotrophic autotroph) is a common bacteria found in AMD and other systems where S^0 and FeS_2 are prevalent. *Acidithiobacillus thiooxidans* (a rod shaped bacterium) exclusively oxidizes S^0, and can grow in both mesophilic and extremely acidic conditions (Takckuwa, 1992; Konishi et al., 1995). *A. thiooxidans* is a good model for sulphur oxidation reactions and is commonly used as the chief S oxidizing microorganism in sulphide mineral and S^0 oxidation experiments (Kelly and Wood, 2000; Kelly et al., 1997; Konishi et al., 1995; Pronk, et al., 1990).

A recent study of the microbial communities inhabiting the S^0 blocks reveal autotrophs concentrated heavily in the upper 0.6 m, and heterotrophs present in higher populations at greater depths (Pisz, 2008). Further, the majority of SO_4^{2-} is speculated to be produced in the top 1 m of the S^0 block (Birkham et al., 2009). This is not surprising given that acidiphilic autotrophs such as *A. thiooxidans* oxidize S^0 at a faster rate than heterotrophs in the same growing medium under

similar conditions (Germida and Janzen, 1993; Pepper and Miller, 1978). Current understanding indicates heterotrophs present at depth utilize autotroph exudates and possibly windblown organic material that settled during lift cooling as a carbon source (Mahmoud et al., 2005; Johnson and Hallbert, 2003). Microorganisms may be re-distributed throughout the block by the continued flow of water and gas influx through fractures (Pisz, 2008).

3.2.2.1 Oxygen and nutrient availability

Abiotic and biotic oxidation of S^0 require O_2 to produce SO_4^{2-}; therefore, molecular oxygen is a key limiting factor in acid production. According to Equation 3.3, 1.5 tonnes of O_2 is required to completely oxidize 1.0 tonne of S^0 (Golder, 1999; Lloyd, 1967). In addition, essential nutrients such as nitrogen, carbon, phosphorous, and magnesium are required for microorganisms to perform at optimal levels; however, the ability of autotrophs to fix carbon from CO_2 using energy from S^0 oxidation enables them to survive in nutrient poor environments. The amount and availability of nutrients in a sulphur block are largely dependent upon the local environment and precipitation events that introduce these nutrients into the block.

3.2.2.2 Temperature

Temperature is one of the most important factors influencing sulphur oxidation. Assuming about 90% of the H_2SO_4 produced in S^0 blocks is attributed to microbial oxidation, understanding the influence of temperature on microbial growth is important. Autotrophic and heterotrophic microorganisms have minimum temperature requirements to maintain growth rates (Ehrlich, 1996; Germida et al., 1993; Laishley et al., 1985). Generally, the rate of S^0 oxidation peaks between 29 and 33°C, and becomes negligible below 5°C for most S^0 oxidizing microorganisms (Laishley, et al. 1985). As average temperatures at SCL are above 5°C between the months of May and September, acid production is expected to occur throughout these months (Golder, 1999).

3.2.2.3 Surface area

The oxidation of S^0 is a surface reaction; meaning only S atoms directly exposed to chemical or biological activity are vulnerable to oxidation. Laishley et al. (1983) report that even when pure cultures of *thiobacilli* are integrated into experiments, oxidative activity does not

penetrate the core of S^0 grains. Further, hydrophobic surfaces of sulphur grains may inhibit transport of nutrients and oxygen to the interior of the grain and prevent microorganisms from entering and occupying the interior (Watkinson, 1987). Therefore, the amount of SO_4^{2-} produced is a function of the exposed S surface area rather than the actual mass of the sulphur present (Janzen, 1987). Particle shape influences the exposed surface area; spherical particles have the lowest surface area to mass ratio, and any variance from sphericity increases the specific surface area (Germida, 1993). The relationship between the amount of SO_4^{2-} produced and the total surface area of S^0 is linear (Koehler and Roberts, 1983; Laishley et al., 1983; Janzen et al., 1982; Fox, 1964).

3.3 Stable isotopes

Stable isotopes of oxygen and sulphur can be used as a tool to help identify the source of oxygen incorporated into SO_4^{2-} produced via S^0 oxidation. Changing environmental conditions play an important role in the isotopic composition of SO_4^{2-} produced. In particular, temperature, oxygen and water availability, microbial activity and pH affect the fractionation of oxygen isotopes during the production of SO_4^{2-} in geologic environments. Generally, the majority of oxygen incorporated into SO_4^{2-} originates from water; however, the controls governing the partitioning of oxygen remain controversial (Van Stempvoort, et al., 1994).

3.3.1 Sulphur

Sulphur has four stable isotopes— ^{32}S, ^{33}S, ^{34}S, and ^{35}S —whose natural abundances are 95.02, 0.75, 4.21, and 0.02%, respectively. Generally, isotope abundance variations are expressed in terms of an abundance ratio of the two principal isotopes, in this case, $^{34}S/^{32}S$. The absolute isotopic composition of a material is difficult to measure directly, therefore isotope ratios of a sample are compared to a standard and referred to in delta notation [per mil (‰); Equation 3.4]. The accepted international standard is the Canyon Diablo Meteorite which has a $^{34}S/^{32}S$ value of 0.0450 (Clark and Fritz, 1997).

$$\delta^{34}S\ [‰] = \frac{[(^{34}S/^{32}S\ sample) - (^{34}S/^{32}S)standard]}{(^{34}S/^{32}S)standard} * 1000 \qquad (3.4)$$

Regardless of anthropogenic influences, a large range of sulphur isotope compositions exist in the natural environment (Thode et al., 1949) (Figure 3.4). Generally, $\delta^{34}S_{SO4}$ values of surface waters fall between -20 and +20‰. The variance of terrestrial sulphur isotope compositions is the result of a wide range of sulphur valance states (+6 to -2), with the greater valance states tending to be enriched in the heavier isotope (Krouse, 2000).

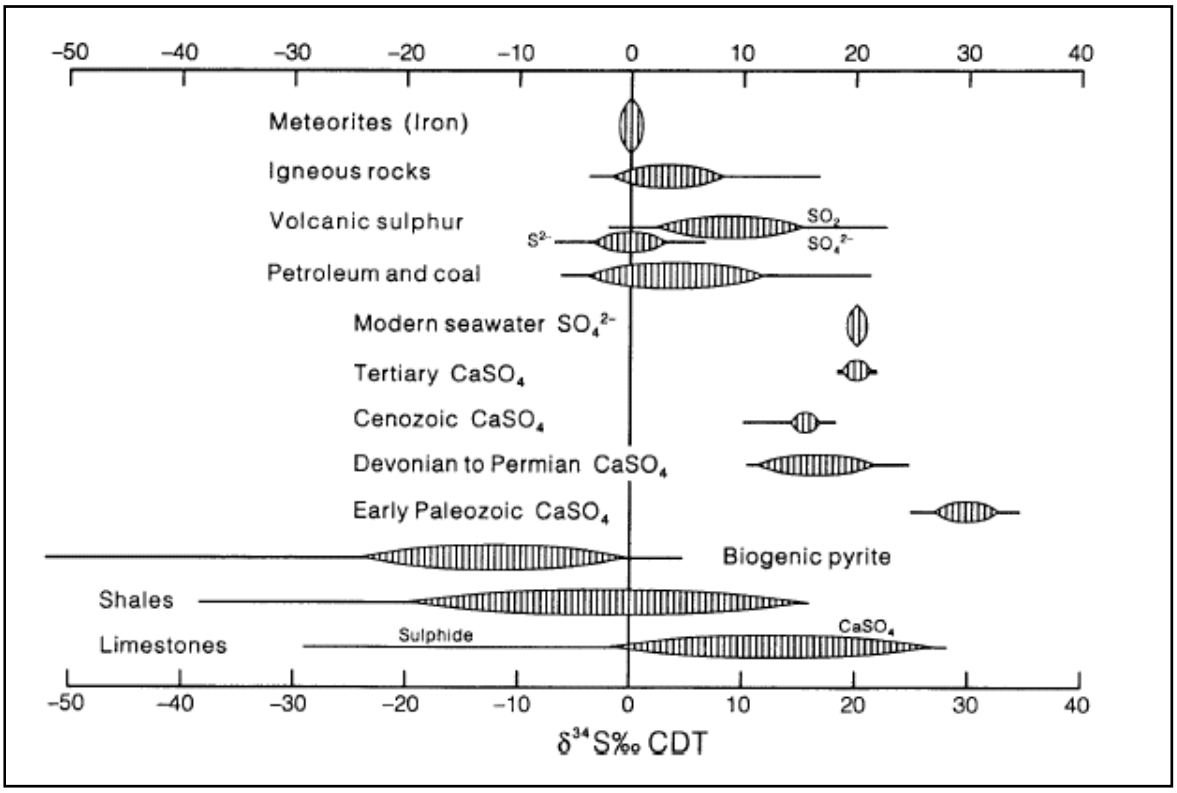

Figure 3.4. Ranges in $\delta^{34}S$ contents of sulphur and sulphur compounds in different materials and environments (Krouse, 1980).

3.3.2 Oxygen

Oxygen has three stable isotopes— ^{16}O, ^{17}O and ^{18}O—with natural abundances of 99.76, 0.038, and 0.21%, respectively. The abundance ratio is measured with the two most abundant isotopes, ^{16}O and ^{18}O, whose international standard is based on Vienna-Standard Mean Oceanic Water (VSMOW) at 2.0052 x 10^{-3} (Equation 3.5; Clark and Fritz, 1997).

$$\delta^{18}O\ [‰] = \frac{[(^{18}O/^{16}O\ sample) - (^{18}O/^{16}O)standard]}{(^{18}O/^{16}O)standard} * 1000 \qquad (3.5)$$

3.3.3 Oxygen isotope composition of SO_4 ($\delta^{18}O_{SO4}$)

The oxidation of reduced sulphur compounds such as H_2S or S^0 produce highly variable $\delta^{18}O_{SO4}$ values. Lloyd (1968), Taylor, Wheeler & Nordstrom (1984), and Van Everdingen & Krouse (1985) suggest the variability occurs because the oxygen is derived from two sources (molecular O_2 and H_2O) in an 'oxidation-hydrolysis' reaction. The oxygen isotope composition of SO_4^{2-} is accordingly influenced by both the $\delta^{18}O$ of molecular oxygen and water oxygen. The observed $\delta^{18}O_{SO4}$ value is the result of contributions from both sources and any kinetic isotope fractionation effects.

3.3.3.1 The SO_4^{2-}- H_2O system

The rate of oxygen isotope exchange between dissolved SO_4^{2-} and water is remarkably slow in circum-neutral pH solutions, and hence, in most normal geological environments (Mizutani and Rafter, 1969; Hoering and Kennedy, 1957; Teis, 1957). The rate of isotopic exchange increases with increasing acidity and temperature of the solution (Mizutani and Rafter, 1969; Hoering and Kennedy, 1957).

Lloyd (1967) estimates the time required for 97% equilibration of ocean-water and SO_4^{2-} oxygen exchange to be close to 250,000 years. Experiments by Zak et al. (1980) show no sign of SO_4^{2}–H_2O exchange in porewaters of deep marine sediments, and deduce an exchange half-life ($t^{1/2}$) > 5 x 10^9 yr. Chiba and Sakai (1985) conclude the ocean water – sulphate oxygen exchange rate has a $t^{1/2} \approx 10^9$ yr at temperatures ranging from 100-300^{o}C and at pH values between 2 and 7 in laboratory experiments.

The slow rate of exchange between oxygen isotopes of SO_4^{2-} and H_2O has important implications with respect to the $\delta^{18}O$ of SO_4^{2-}. A slow oxygen exchange indicates the $\delta^{18}O$ value of the SO_4^{2-} produced during the oxidation of S^0 reflects the source of the oxygen, with little influence from subsequent exchange reactions with H_2O. However, as previously mentioned, SO_3^- is the key intermediate during both abiotic and biotic oxidation of sulphide minerals and S^0. Unlike SO_4^{2-}, which exchanges oxygen with water slowly, SO_3^- undergoes isotopic exchange with water much faster (by as much as a factor of 10^5). In addition to contributing oxygen during oxidation, water influences the oxygen isotopic composition of SO_4^{2-} through exchange reactions with intermediates. Lloyd (1967) suggests the isotopic composition of SO_4^{2-} is influenced by a competition between the rate of SO_3^- oxygen exchange with water and the rate

that SO_3^- is oxidized to SO_4^{2-}. This is further examined by Schwarcz and Cortecci (1974) who state the relationship between $\delta^{18}O_{(SO4)}$ and $\delta^{18}O_{(H2O)}$ during pyrite oxidation in neutral waters is caused by the rapid exchange of oxygen isotopes between SO_3^- and H_2O.

3.3.4 Sulphur isotope composition of SO_4^{2-} ($\delta^{34}S_{SO4}$)

Sulphur isotope fractionation during the oxidation of reduced sulphur compounds with lower valence states tends to be relatively small (Fry, 1988). The $\delta^{34}S$ of SO_4^{2-} produced during oxidation in soils is often indistinguishable from the parent S^0 (Krouse, 2000). Previous work surrounding the oxidation of metal sulphides and other reduced sulphur compounds indicates the fractionation of sulphur isotopes is minimal, especially when compared to the fractionation of oxygen isotopes in the same system (Balci et al., 2007, Taylor et al., 1984ab; McCready and Krouse, 1982; Nakai and Jensen, 1964).

The relationship between $\delta^{18}O$ and $\delta^{34}S$ in naturally occurring sulphates is linear (Thode, 1949). Oxygen and sulphur isotopic compositions of naturally occurring sulphates (Mayer, 1998; van Stempvoort & Krouse, 1994; Holt & Kumar, 1991; Newman & Forrest, 1991; Neilson, 1974) are plotted as $\delta^{18}O_{(SO4)}$ vs. $\delta^{34}S_{(SO4)}$ and result in linear or near linear trends (Figure 3.5).

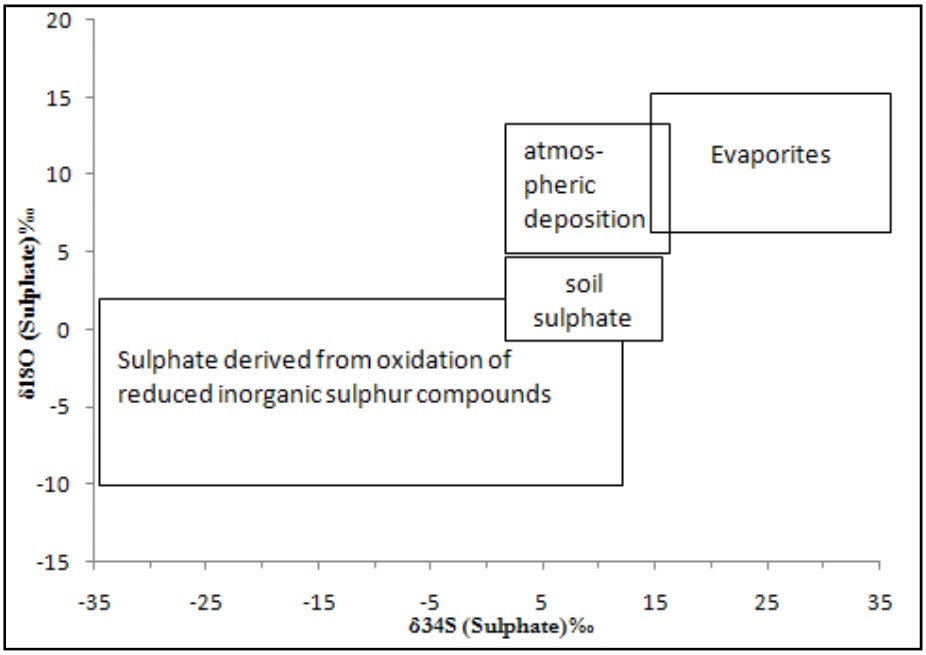

Figure 3.5. Commonly observed ranges for atmospheric, pedogenic and lithogenic SO_4^{2-} (redrawn from Krouse, 1991).

3.4 Environmental considerations for long-term S^0 storage

Possibly the most important unresolved environmental issue concerning sulphur storage is the oxidation of S^0 and subsequent production of SO_4^{2-} enriched, low pH (circa 2-0.5) effluent (Figure 3.6). Drainage waters are collected and neutralized before discharge from the S^0 blocks; however, this is not only costly, but presents management problems and a long-term liability for the sulphur block's owner (Crescenzi et al., 2006). In addition, H_2SO_4 can be transported to the surrounding environment by heavy rainfall and leaching. The input of H_2SO_4 to the environment can be damaging to the local biota if the acid produced exceeds local buffering capacity (Crescenzi et al., 2006). Accumulation of H_2SO_4 lowers the overall pH of groundwaters, causing metal solubility to increase. As acidic groundwater moves through the sub-surface, it can leach metals from the soil and bedrock, potentially transporting metals considerable distances away from the storage site (Golder, 1999). In some cases, the contaminated groundwater can seep into beds of nearby creeks where the pH change can cause bright red iron and manganese oxides to precipitate in the creek beds. The seepage can also lead to increased SO_4^{2-} and heavy metal concentrations in the creek water (Golder, 1999). Extreme acidity can directly damage the local flora ecosystem and render plants incapable of any nutrient uptake. Ultimately, increased levels of H_2SO_4 in the groundwater can create a less diverse community of heterotrophic organisms in the surrounding environment (Laishley and Bryant, 1987).

S^0 blocks are subject to extreme temperature changes, which results in both physical and chemical weathering. Erosion compromises the structural integrity of the block, and can lead to failure of the block walls (Crescenzi et al., 2006). All blocks are susceptible to slumping and crumbling, as evidenced by a tour of S^0 blocks in western Canada by SCL in 2003. S^0 dust can be blown kilometres away from the storage site, and settle on the ground surface. Once the S^0 dust is deposited, it can be incorporated into the biological cycle as SO_4^{2-} after oxidation occurs. Eventually, acidic groundwaters and increased SO_4^{2-} uptake can render the soil barren and unproductive (Golder, 1999).

Figure 3.6. Collection trough for effluent from the Phase I block at SCL.

4.0 EXPERIMENTAL METHODS

A series of S^0 oxidation experiments were conducted to investigate the oxidation rate of solid S^0 to aqueous SO_4^{2-} over a range of temperatures. Stable isotopes of $\delta^{18}O$ were used to determine how oxygen is partitioned and incorporated into the resulting SO_4^{2-}. By systematically varying the $\delta^{18}O$ values of H_2O and O_2 during each series of experiments, the contribution of each oxygen source to the resulting SO_4^{2-} was determined. A total of 13 series experiments were conducted, each with a constant but different temperature, and a range of ^{18}O in both the water and O_2. The experiments also investigated the effect of integrating S^0 oxidizing microorganisms in a nutrient rich mineral solution (MS) vs. a nutrient poor solution (deionized water; DI). Results provided in this study were from four series of experiments, referred to as MS-A (mineral solution reaction media with atmospheric air at 32, 21, 12 and 6°C); MS-C (mineral solution with custom mixed ^{18}O- enriched air at 32, 21, and 12°C), DI-A (DI solution with atmospheric air at 32, 21, and 12°C), and DI-C (DI solution with custom mixed ^{18}O-enriched air at 32, 21, and 12°C).

4.1 S^0 preparation

Samples of solid S^0 were obtained from the Mildred Lake Site of Syncrude Canada Ltd. (SCL), a sour gas plant in northern Alberta. During construction of the Phase II block in 2005, 99% pure molten S^0 was poured into a 20 L metal bucket, sealed, and stored at 15-17^{o}C. Prior to use, the S^0 was ground and sieved to a grain size < 4 mm to provide maximum surface area for oxidation without powdering the S^0. Once sieved, the grains were washed with DI three to five times to remove any S^0 powder remaining on the surface. No effort was made to sterilize the sulphur used in the experiments, as the intended purpose of these experiments was to observe the oxidation of S^0 as it occurs naturally. Surface bacterial sterilization of sulphur used in the controls of each series was achieved by rinsing and soaking the S^0 in a 70% ethanol solution for ten minutes, rinsing with DI, and then soaking in a 5% bleach solution for five minutes. The S^0 was then rinsed three to five times with DI to remove all traces of bleach and ethanol. The S^0 grains were blocky in shape (Figure 4.1). The dimensions (length, width, and height) of 200 grains were measured using a digital caliper and the mean calculated.

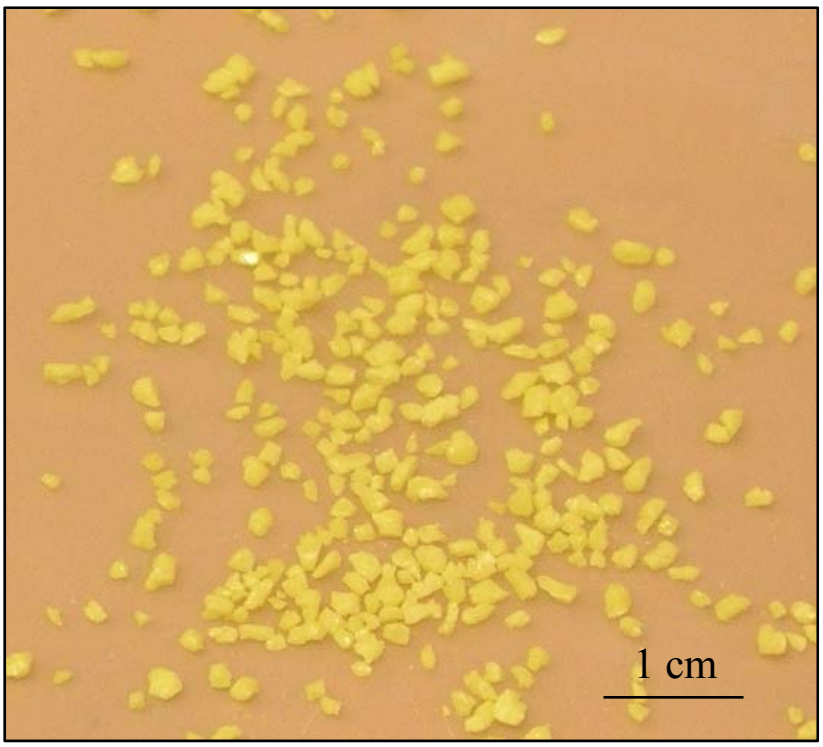

Figure 4.1. 1 g of non-spherical S^0 grains used in oxidation experiments.

4.2 Reaction medium

One hundred mL of either a mineral solution (A, B, C or D) or DI (E, F, G or H) was used as the primary reaction medium. A low SO_4^{2-} mineral solution that substitutes Cl^- for SO_4^{2-} was adapted from the ATCC 125 growth medium (0.52 g NH_4Cl, 0.25 g $MgSO_4 \cdot 7H_2O$, 0.07 g $CaCl_2$, 0.28 g KH_2PO_4 per 1 L of DI water) to lower the background SO_4^{2-} concentration to an initial value of 1.0 mM in the MS series. Solutions were pH adjusted to between 5 and 5.5 using dilute HCl, and then filtered through 0.2 µm Millipore filters to sterilize the solution and remove impurities. The solutions were mixed with varying volumes of a 10 % $H_2{}^{18}O$ water spike to achieve distinctly different $\delta^{18}O$ (Table 4.1), using equations 4.1a and 4.1b:

$$X = \frac{f^{18}O_{(t)} * V_{(t)} + f^{18}O_{(w)} * V_{(w)}}{V_{(t)} + V_{(w)}} \quad (4.1a)$$

$$\delta^{18}O = \left[\left(\frac{x}{0.002005}\right) - 1\right] * 1000 \quad (4.1b)$$

where $f^{18}O_{(t)}$ is the fraction of ^{18}O in the tracer, $f^{18}O_{(w)}$ is the fraction of ^{18}O in the water, $V_{(t)}$ is the volume of tracer used (mL), $V_{(w)}$ is the volume of water used, and X is the isotope ratio ($^{18}O/^{16}O$).

The ^{18}O isotopic composition of the water was determined using off-axis integrated-cavity output spectroscopy (OA-ICOS), which measures D/H and $^{18}O/^{16}O$ isotopic ratios of natural waters. For this study, sample analyses were done using a Los Gatos Research Liquid Water Analyzer model 908-0008. For operating conditions of the liquid water analyzer, see Lis et al., 2008.

Table 4.1. $\delta^{18}O$ of water in the aqueous phases used in S^0 oxidation experiments.

Solution	Volume of 10% ^{18}O solution per 10L H_2O (mL)	Mineral solution $\delta^{18}O$ (‰)	Solution	Volume of 10% ^{18}O solution per 10L H_2O (mL)	Deionized water $\delta^{18}O$ (‰)
A	205	+957 (±3.0)	E	90	+427 (±3.0)
B	115	+533 (±3.7)	F	45	+210 (±1.4)
C	55	+234 (±3.6)	G	25	+98 (±2.2)
D	0	-19 (±0.2)	H	0	-19 (±0.1)

4.3 Inoculant preparation

To achieve a microbial consortium similar to the S^0 storage blocks at SCL, effluent from the Phase I block was the primary medium used to prepare the inoculum. The inoculant was prepared by George Swerhone at Environment Canada. To increase the number of S^0 oxidizing microbes per mL of inoculant, the effluent was filtered using a 0.2 μm vacuum filter apparatus, then re-suspended in a pH 5.4 mineral salts medium (ATCC 125 mineral salts mixture: 0.2 g $(NH_4)_2SO_4$, 0.5 g $MgSO_4 \cdot 7H_2O$, 0.25 g CaCl, 3.0 g KH_2PO_4, and 5.0 mg $FeSO_4$ per 1 L water) (ATCC website). This was repeated twice more to concentrate the sulphur oxidizing organisms by a factor of 10. The low pH water was then removed and replaced with the mineral salts medium described above. Approximately 300 mL of effluent was used to produce 30 mL of inoculant.

Prior to adding the prepared inoculant to the experiments, a population survey was conducted to determine the types of microorganisms present in the inoculant. The most probable number (MPN) technique was used to enumerate the number of autotrophic S^0 oxidizing microorganisms (Oblinger et al., 1975). A mineral salts medium designed for autotrophic S^0 oxidizing bacteria and 0.03 g of a colour indicator (Bromocresol green) was used to measure bacterial growth. In-situ hybridization of the flocs formed in flasks containing ATCC #125 medium, colloidal S^0, and S^0 block effluent were used to determine the species of bacteria present.

Total heterotrophic fungal populations in the inoculant were enumerated using 10% trypticase soy agar ($^1/_{10}$ TSA). To investigate the influence of heterotrophic populations on the production of SO_4^{2-} in the S^0 oxidation experiments, a heterotrophic growth medium (1 g peptone, 0.5 g yeast extract, 0.03 g bromothymol blue, 100 mL water and 1 g S^0; pH 6.8) was mixed for the oxidation of S^0 after inoculating the system with S^0 block effluent water.

4.4 S^0 oxidation experiments

Each series was composed of eight or ten 500 mL Erlenmeyer flasks, all of which contained 40 g of prepared S^0 grains. One mL of inoculant was added directly to the S^0 and left unshaken for six to eight hours to ensure ample time for the microorganisms to attach to the surface of the S^0 prior to the addition of a reaction solution (Yu, 2001). To minimize the addition of SO_4^{2-} to the flasks via the inoculant, only one mL of inoculant was added to each flask. While the microorganisms may only initially be in contact with a fraction of the S^0 grains, one mL was a sufficient volume to inoculate the flasks with S^0 oxidizing microorganisms without adding excess SO_4^{2-} to the solution. One hundred mL of the prepared DI or mineral solution was added to the Erlenmeyer flask by pouring the solution down the sides of the flask to minimize directly wetting the sulphur. As a result, the hydrophobic S^0 grains floated at surface until the flasks were shaken to settle the S^0 grains to the bottom of the flasks (occurred after 24 hours) and ensure all surfaces of the S^0 were in contact with the solution. Each flask was shaken for 1 min every 48 h after the initial 24 h stasis to re-distribute the S^0 grains, and encourage O_2 circulation in the headspace and standing water. In series utilizing DI as the reaction solution, 100 mL of DI was added in 20 mL increments every 24 hours to prevent the microorganisms from being overwhelmed in a nutrient deficient environment. Abiotic control experiments were

performed under identical conditions as their biotic counterparts. All experiments were performed in duplicate.

Once the reaction media was added, flasks were immediately placed at one of four temperatures: 32±1, 21±1, 12±1, and 6±1°C. Temperatures were maintained by a water bath (32±1°C), ambient room temperature (20-22°C), and two dedicated refrigerators (12±1°C and 6±1°C). Constant monitoring of the DI series ended after 2200 h (93 days); mineral solution series were run for 1750 h (73 days). The variance in duration corresponds to the expected lag phase of the microorganisms in respective batches.

4.4.1 Open vs. closed cell experiments

Each series was run with either atmospheric O_2 ($\delta^{18}O$ of +23.5‰, Kroopnick and Craig, 1972) (termed open cell experiments) or a custom gas mixture prepared using a 97% ^{18}O gas spike (Cambridge Isotope Lab) (termed closed cell experiments). The open cell experiments were open to the atmosphere but loosely covered with parafilm to minimize evaporation (Figure 4.2). The parafilm was removed during sampling and pH measurements, as well as during agitation of the flask to re-distribute gases. The open cell experiments were conducted to investigate the influence of varying the oxygen isotopic composition of the reaction solution, while the closed cell experiments were intended to investigate the influence of varying the oxygen isotopic composition of the air. Because the S^0 storage blocks are exposed to the atmosphere, the open cell experiments are thought to closely resemble the atmospheric conditions of the blocks.

The experimental methods, results, and conclusions of the closed cell experiments (MS-C and DI-C) are described in Appendix A. The O isotope data are not considered in this portion of the thesis because the resulting data is not considered a correct representation of the experiment intended. What was thought to be an enriched ^{18}O gas being injected into the closed cell experiments was not enriched in ^{18}O at all. Essentially, the closed cell experiments were duplicates of the open cell experiments, as it was atmospheric air was being pumped into the flasks. This was determined after the completion of the experiments when the samples of the flask headspace taken periodically over the entire duration of the experiment, were analyzed for $\delta^{18}O$. The results showed the headspace was not enriched in ^{18}O at any point during oxidation, thus nullifying the objective of the experiment. However, pH and SO_4^{2-} data from the closed cell

experiments (MS-C) provided valuable data regarding the rate of S^0 oxidation in a closed cell environment. These data are presented as duplicate data for MS-A in Chapter 5.

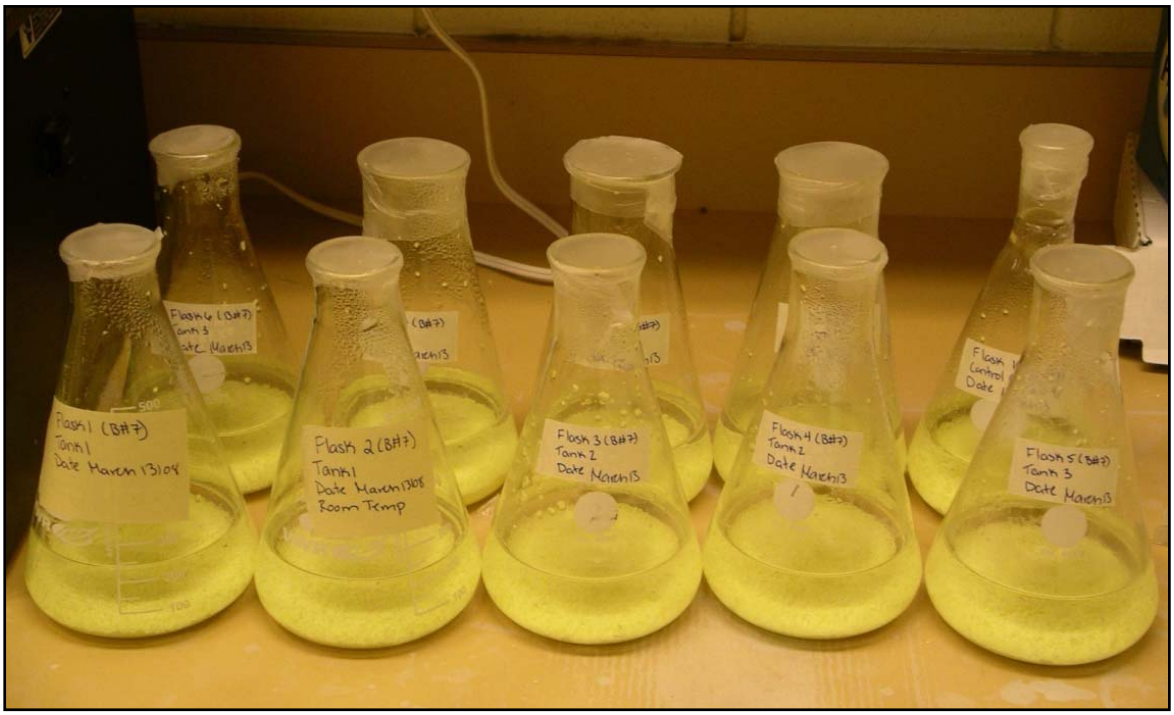

Figure 4.2. Open cell experiments at room temperature (21±1°C).

4.5 Sampling and analysis

Four mL of reaction solution was collected every few days to measure the mass of SO_4^{2-} produced with time. Samples were analyzed for major anions by ion-exchange chromatography. Corresponding pH measurements of the reaction solution were determined using an Orion model 250A pH meter (range: -2 to 19.99; relative accuracy: ±0.02), after three point calibrations using pH 1.00, 4.00, and 7.00 buffers. The pH probe was inserted directly into the reaction medium of each cell open to the atmosphere. Between each reading, the probe was sterilized using a diluted ethanol solution, rinsed with DI, dried with a clean paper towel and stored in a potassium chloride electrode storage solution.

Upon the completion of each experiment, 10 mL of the remaining reaction medium was removed, filtered, and neutralized to a pH of 4-5 using dilute NaOH. $BaSO_4$ was then precipitated by the addition of 5 mL of a 10% (wt/wt) $BaCl_2$ solution and allowed to settle for 16-24 h. The precipitate was recovered on a 0.45 µm Millipore filter and washed with DI water

three times. The dried $BaSO_4$ samples were analyzed for sulphur and oxygen isotope ratios using continuous flow isotope ratio mass spectrometry (CF-IRMS) at the University of Calgary (Balci et al., 2007). Ten samples of the S^0 used for the oxidation experiments were analyzed for isotope composition ($\delta^{34}S$) prior to oxidation. After SO_4^{2-} was recovered and precipitated as $BaSO_4$, 50 samples were analyzed for $\delta^{34}S$. The oxygen and sulphur isotope results stated in this study are expressed relative to the Vienna Standard Mean Ocean Water (V-SMOW), and Canyon Diablo Troilite (V-CDT) standards using δ notation.

4.5.1 Calculation of S^0 oxidation rate

S^0 oxidation rates were calculated based on the linear regression of μg S^0 oxidized with time, producing a rate constant (*k*) (Janzen and Bettany, 1987):

$$k = \frac{dm_a}{dt} \ (\mu g S^0 \, day^{-1}) \tag{4.2}$$

where m_a is the mass of oxidized S^0, and *t* is time (day).

To convert this rate to units eliminating variation of surface area, the following equation from Gleisner et al. (2002) was used:

$$R_{S^0} = \frac{k}{SAmc} \ (\mu g S^0 \, cm^{-2} day^{-1}) \tag{4.3}$$

where SA is the surface area of the S^0 grains ($cm^2\ g^{-1}$), *m* is the mass of sulphur grains (g), and c is the stoichiometric factor (1 for S^0)

4.5.2 Calculation of oxygen source and kinetic isotopic enrichment

The oxidation of S^0 is a dual source reaction during which oxygen from both H_2O and O_2 is incorporated into the resulting SO_4^{2-}. The $\delta^{18}O$ of SO_4^{2-} produced during oxidation will reflect the oxygen isotopic composition of these two sources, the fraction of oxygen derived from each, and any associated kinetic isotope fractionation effects. The slope (X) of the $\delta^{18}O_{(H2O)}$ vs. $\delta^{18}O_{(SO4)}$ linear regression is equal to the fraction of oxygen derived from water, which can be related to the mass balance equation (4.4) (Lloyd, 1967):

$$\delta^{18}O_{SO4} = X\,(\delta^{18}O_{H2O} + \varepsilon^{18}O_{SO4\text{-}H2O}) + (1\text{-}X)\,(\delta^{18}O_{O2} + \varepsilon^{18}O_{SO4\text{-}O2}) \quad (4.4)$$

The y-intercept (b) can be used to describe the relationship between $\varepsilon^{18}O_{SO4\text{-}O2}$ and the other variables (Balci et al., 2007):

$$\varepsilon^{18}O_{SO4-O2} = \left[\frac{b - X(\varepsilon^{18}O_{SO4-H2O})}{1-X}\right] - \delta^{18}O_{02} \quad (4.5)$$

where X is the fraction of oxygen derived from H_2O, (1-X) is the fraction of oxygen derived from O_2, and $\varepsilon^{18}O_{SO4\text{-}H2O}$ and $\varepsilon^{18}O_{SO4\text{-}O2}$ are the kinetic oxygen isotope fractionation effects between SO_4^{2-}–H_2O and SO_4^{2-}–O_2 respectively.

4.6 Statistical methods

4.6.1 Analysis of covariance (ANCOVA)

ANCOVA is a merger of ANOVA and linear regression for continuous variables. In other words, ANCOVA is a general linear model that tests whether certain factors affect the response variable after removing the variance for which quantitative predictors (covariates) account. ANCOVA is appropriate when data are compiled from different groups of subjects or categories that exhibit linear regression, and is used to examine the extent to which the regression relationships differ between the groups. ANCOVA increases the power of comparison by reducing the estimates of experimental error by adjusting the response variables with respect to the covariate. All ANCOVA tests were done using the statistical program Minitab® 15.

Three important variables must be considered when conducting an ANCOVA. Indicator variables are values introduced to the model to represent and separate the different categories in the study. The values associated with the indicator variables are typically 0, 1, or -1 but have no meaning as numerical values. The covariate is the x-axis variable and is independent of the study (e.g., time, age, income, or height). The response variable is the y-axis variable and is dependent on the indicator variable and the covariate (Larson, 2008).

All of the assumptions of a regular ANOVA (1-3) are included in an ANCOVA model, with the addition of two more (4-5) (Minitab® tutorial, 2008):

1) Responses are independent and normally distributed;

2) Response variance is equal for all values of the covariate and independent of the value of the indicator variable (homoscedasticity);
3) No measurement error in independent variables;
4) The relationship between the response variable and covariate is linear; and
5) Homogeneity of regression coefficients (slope).

4.6.2 Student's t-test

A Student's t-test was used to compare the means of two independent groups, under the assumption the subjects of each group are normally distributed with equal variances. Essentially, the t-test is used to test the defined null hypothesis that the means of two groups are equal. If the *p*-value determined for the test is less than the defined level of significance (0.05 for this study), the null hypothesis (H_0) is rejected in favour of the alternative hypothesis (H_a), where the means of the two groups are not the same.

5.0 RESULTS AND DISCUSSION

5.1 Evolution of pore water chemistry in S^0 oxidation experiments

pH measurements and SO_4^{2-} concentrations presented here are the mean of all flasks in each mineral solution or deionized water series (MS and DI, respectively) at a given test temperature (32, 21, 12, or 6°C). Flask components in each series were identical (40 g of S^0, 100 mL of solution, 1 mL of inoculant), with the only variable being the oxygen isotopic composition of H_2O. At a given temperature, SO_4^{2-} concentrations were similar for flasks from any given sampling period. Therefore, mean pH and SO_4^{2-} concentrations for all flasks at each sampling period were used to represent changes in water chemistry in each series. Error bars of one standard deviation (σ) from these measurements are illustrated in figures constructed using this method. Data collected from individual flasks, as well as supplementary data regarding statistical analysis for all experiments, are presented in Appendix B.

5.1.1 SO_4^{2-} production and pH

Initial SO_4^{2-} concentrations of the MS and DI series were 1 and 0.1 mM, respectively. In all experiments, an initial stasis preceded SO_4^{2-} production, during which time only background aqueous SO_4^{2-} was recovered. Following the initial stasis, SO_4^{2-} concentration in the MS-A, DI-A, and MS-C series increased over the duration of the experiment (Figure 5.1). The strong linear correlation between increasing SO_4^{2-} concentration and time (R^2 of 0.97 to 0.99 for all series and temperatures except DI-A 21°C; R^2=0.78) suggested the S^0 oxidation was a zero-order reaction. Previous literature does not always indicate S^0 oxidation follows zero-order kinetics; however, numerous studies have observed zero-order kinetics during S^0 oxidation experiments (Birkham et al., 2009; Slaton et al., 2001; Janzen and Bettany, 1987b; Li and Caldwell, 1966).

Generally, SO_4^{2-} concentrations at any given sampling period increased with increasing temperature (Figure 5.1). At the final sampling period (1700±48 hr), SO_4^{2-} concentrations were 90, 52, 36 and 3 mM at 32, 21, 12 and 6°C, respectively, in the MS-A series; and 100, 58, and 52 at 32, 21 and 12°C, respectively, in the MS-C series. At 2150±48 hr, SO_4^{2-} concentrations in the DI-A series were 10.4 (32°C), 7.6 (21°C), and 6.9 mM (12°C). The abiotic control flasks for all series produced minimal SO_4^{2-} (< 2 mM); implying > 95% of SO_4^{2-} produced in the biotic trials was the result of microbial activity. An additional sample was removed from all flasks at each temperature in the MS-A series at 3024 hours to assess whether the SO_4^{2-} was continuing to

increase. These four data points are not shown in Figure 5.1, but confirm continued production of SO_4^{2-} at all temperatures.

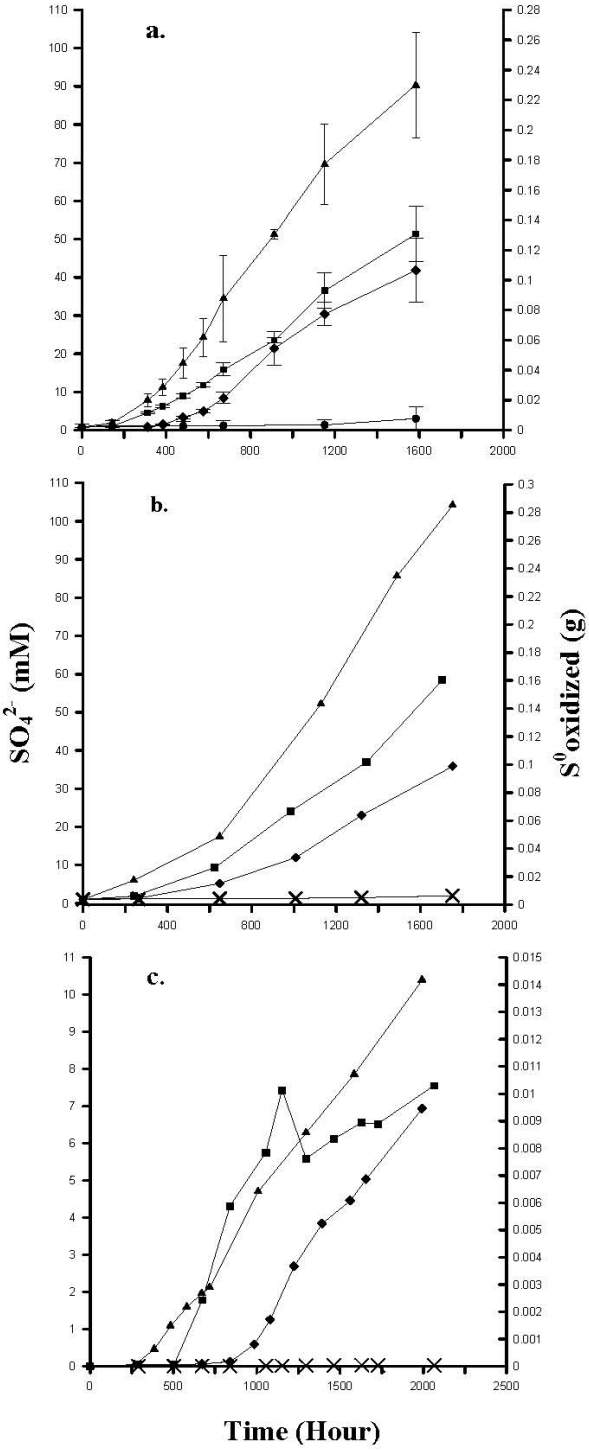

Figure 5.1. SO_4^{2-} (mM) production and S^0 oxidized (g) with time for MS-A (a), MS-C (b), and DI-A (c) at incubation temperatures of 32 (▲), 21 (■), 12 (♦), and 6°C (●). Abiotic controls for DI-A and MS-C at 32°C (x). Error bars are 1σ.

With increasing production of SO_4^{2-}, pH decreased with time from the initial conditions (4.5 to 5.5). The rate of change (dpH/dt (day^{-1})) slowed below pH 1–1.5, but continued to decrease; no further changes in pH were observed once the pH of the reaction solution measured between 0.8 and 0.5 (Figure 5.2).

In this study, excess S^0 was incorporated into each cell to reduce the inhibitory effect of decreasing S^0 available for oxidation. To confirm the lack of control exerted by limited S^0, a simple running stoichiometric calculation indicated < 1 g (2.1%) of S^0 was converted to SO_4^{2-} after 3000 hours.

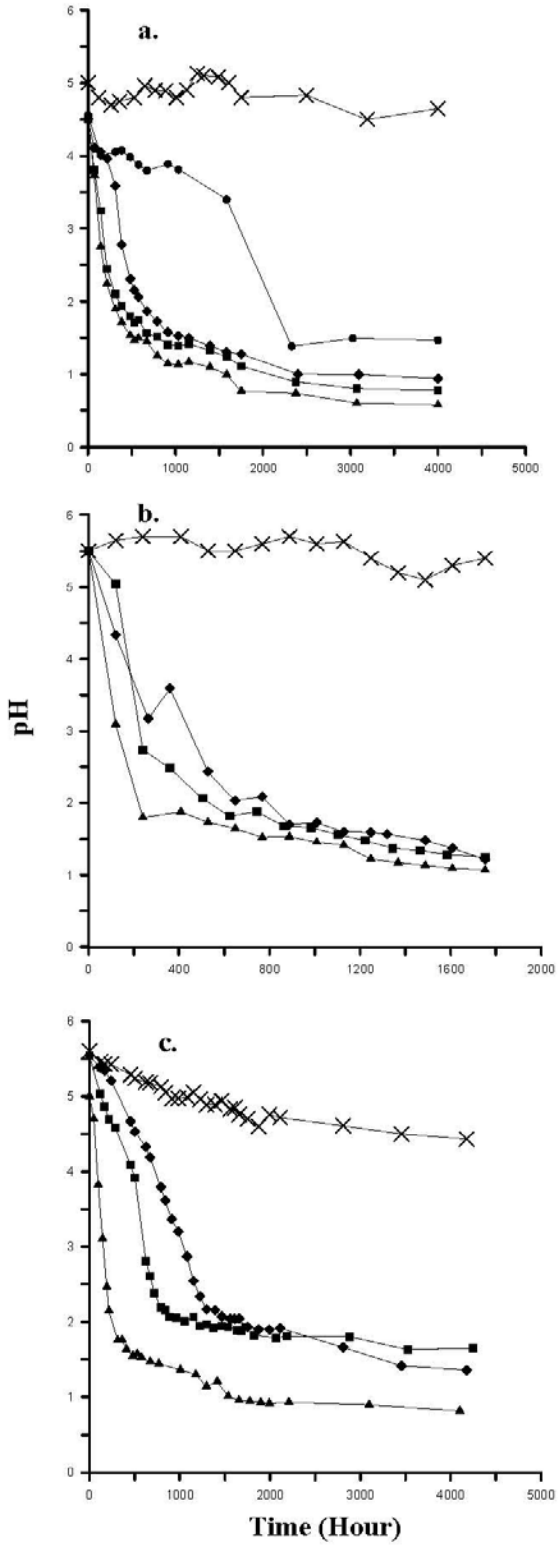

Figure 5.2. pH vs. time for MS-A (a), MS-C (b), and DI-A (c) for incubation temperatures of 32 (▲), 21 (■), 12 (♦), and 6°C (●). Abiotic controls for DI-A and MS-C at 32°C (x). Error bars are smaller than plot points.

5.1.2 Population survey of inoculant

Prior to the S^0 oxidation experiments, a population survey of the inoculant was conducted to determine the types of microorganisms present. Most probable number (MPN) plates indicated the inoculant contained approximately 1.0×10^4 autotrophic S^0 oxidizers per mL. *In situ* hybridization of the flocs indicated > 90% of the bacteria present were *Acidithiobacillus thiooxidans* (personal communication, George Swerhone), an acid-tolerant sulphur oxidizing bacterium (Kuenen et al., 1992). *A. thiooxidans* oxidize S^0 between a pH of 1 and 9, but can only grow under acidic conditions (between a pH of 1 and 5) (Suzuki, 1999). Below pH 1.3, *A. thiooxidans* will continue to acidify the solution medium to a pH of 0.5 although at a decreasing rate (Konishi, 1995; Kuenen et al., 1992; Ahonen and Touvinen, 1991). These findings are consistent with the pH profiles in the current study (Figure 5.2).

All flocs present in the flasks designed for heterotrophic growth were determined to be fungi (Figure 5.3) (personal communication, George Swerhone). Total heterotrophic fungal populations in the inoculant were estimated at 1.1×10^4 colony forming units (CFU) (Figure 5.4). No SO_4^{2-} was recovered from these flasks, indicating the heterotrophic fungi have the ability to lower the pH of a solution to 3.5, but do not produce SO_4^{2-} (personal communication, John Lawrence and George Swerhone).

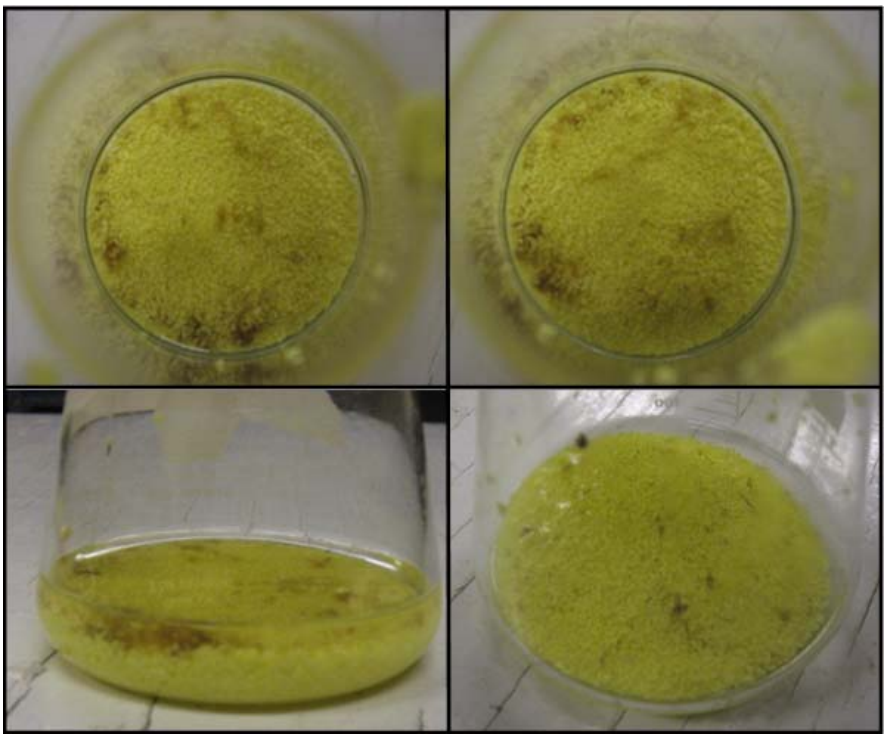

Figure 5.3. Visual evidence of flocculent growth in MS and DI S^0 oxidation experiments.

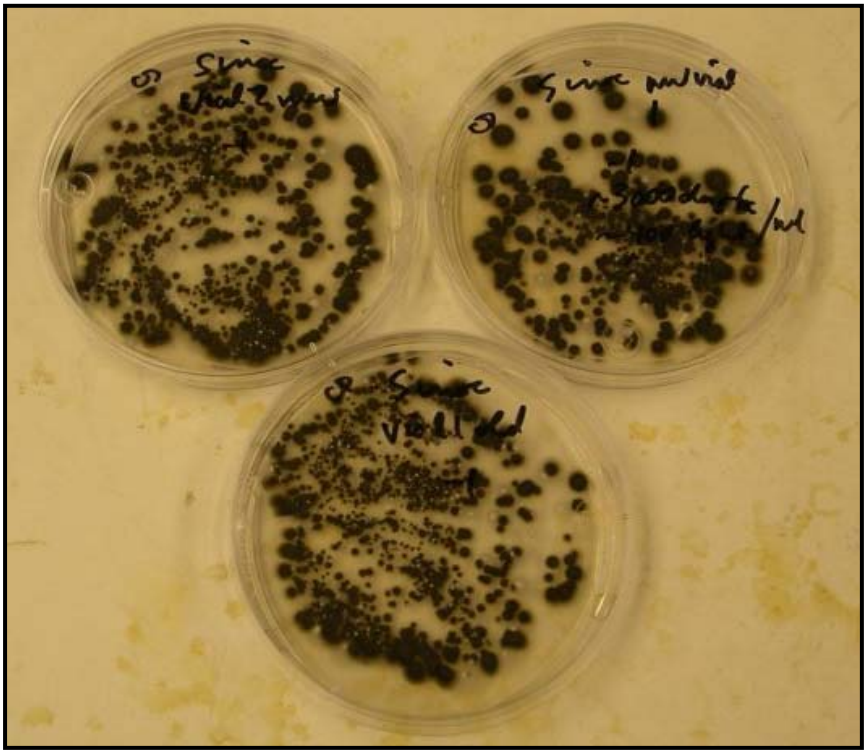

Figure 5.4. Trypticase soy agar (TSA) spread plated with inoculant prior to the start of oxidation experiments. Plates were incubated for one week at room temperature (21°C).

5.1.3 Lag phase

The initial stasis observed in each of the oxidation experiments was identified as a lag phase. A lag phase is the first of three stages of microbial growth, and is generally observed when bacterial cells are inoculated into a new growth medium (Yu, 2001; Lim, 2003). A stasis period is common during S^0 oxidation experiments (Slaton, 2001; Chapman, 1989; Janzen and Bettany, 1986; Nor and Tabatabai, 1977; and Li and Caldwell, 1966), and its length depends upon a variety of factors, including temperature, pH, nutrient availability, differences between the experimental growth medium and the medium the bacteria of interest originated from, and the growth stage of the culture when re-inoculated (Yu, 2001; Lim, 2003; Swinnen et al., 2004). Of these factors, temperature was the only variable altered in each series of the current study, and was therefore the dominant factor controlling the length of the lag phase and any variation between respective batches.

The length of each lag phase was determined by extrapolating the linear exponential growth phase to the x-axis (n_1) (Figure 5.5). The estimated lag phases for the MS-A and MS-C series were 216 and 264 hr (32°C), 264 and 288 hr (21°C), 384 and 504 hr (12°C), and 1200 hr (6°C), respectively. Estimated lag phases for the DI-A series were 300 (32°C), 360 (21°C), and 840 hr (12°C). Such long lag phases for S^0 oxidation incubation experiments are unusual, but have been reported (Yu, 2000; Baldi et al., 1992; Wainwright et al., 1986), and confirmed the duration of the lag phase decreased with increased temperature when all other factors remained unchanged (Yu, 2000; Chapman, 1989).

Microbial oxidation of S^0 by *A. thiooxidans* requires direct contact between the microbial cells and the S^0 grains (Takakuwa et al., 1979; Schaeffer et al., 1963; Vogler and Umbreit, 1941). Before growth on the S^0 can occur, the sulphur-oxidizing bacteria must penetrate the hydrophobic barrier (Knickerbocker et al., 2000). Therefore, the time required for *A. thiooxidans* to colonize the hydrophobic S^0 grains delays the start of the exponential growth phase (Yu, 2001). Generally, oxidation experiments are designed with a small amount (< 1 g) of S^0 available for oxidation with soil as the main constituent (> 10 g) (Chapman, 1989; Janzen and Bettany, 1987a; Li and Caldwell; 1966). The presence of soil provides more suitable (less hydrophobic) colonization surfaces for the microorganisms, which in turn would be expected to reduce the lag phase.

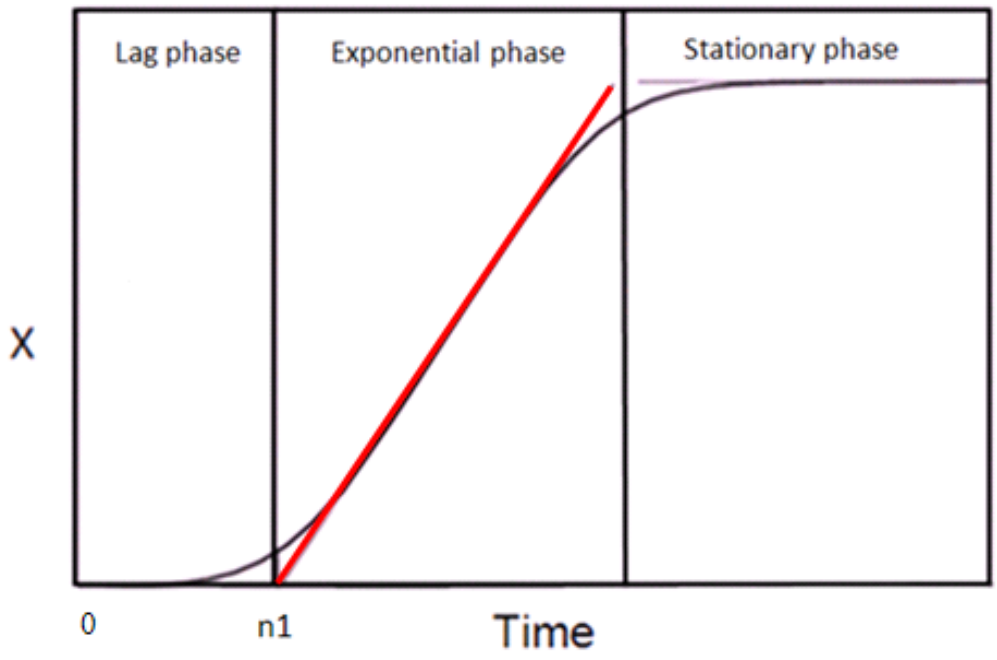

Figure: 5.5. The three phases of microbial growth, where n_1 is the extrapolated point of linear regression for the exponential phase (redrawn from Swinnen et al., 2004).

5.2 Rate of S^0 oxidation

Rate constants (*k*) for all temperatures in the MS-C, MS-A, and DI-A series were estimated from the slope of the linear regression of a plot of mass of S^0 oxidized with time (Figure 5.1) (Equation 4.3). To account for the lag phase at the onset of incubation, the slope was determined for the exponential growth phase of each flask (n_1). The mass of S^0 oxidized was calculated by converting SO_4^{2-} concentrations (mg L^{-1}) to mass of SO_4^{2-} (g) produced and correcting for the volume of solution removed at each sampling period.

Rate constants ranged from 753 (6°C) to 3910 (32°C) µg S^0 oxidized day^{-1} for the MS-A series and 1910 (12°C) to 4700 (32°C) µg S^0 oxidized day^{-1} for the MS-C series. Rate constants for the DI-A series were 371, 287, and 348 µg S^0 oxidized day^{-1} for temperatures of 12, 20, and 32°C, respectively (Table 5.1). To eliminate variation due to particle size, *k* was converted to µg S^0 oxidized cm^{-2} day^{-1} (Equation 4.4) (Janzen and Bettany, 1987a). These surface area based rates are presented in Table 5.1. S^0 oxidation rates increased with increasing temperature in both the MS-A and MS-C series. Oxidation rates for the MS-A and MS-C series ranged from 0.16 (6°C) to 0.78 (32°C) µg S^0 cm^{-2} d^{-1} and 0.40 (12°C) to 0.98 (32°C) µg S^0 cm^{-2} d^{-1}, respectively.

Estimated oxidation rates for the DI-A series did not increase with increasing temperatures and ranged from 0.06 to 0.08 μg S^0 cm^{-2} d^{-1} between 12 and 32°C. The considerably slower S^0 oxidation rates in the DI series implied microbial productivity was inhibited by lack of nutrients.

The oxidation rates calculated for all series were much lower than estimates of previous authors. Janzen and Bettany (1987b) report a mean rate of 4.8±1 μg S^0 cm^{-2} d^{-1} for S^0 oxidation in 40 different types of Canadian soils at 23°C (range 2.3-8 μg S^0 cm^{-2} d^{-1}) and Chapman (1989) reports values between 4.3 and 40 μg S^0 cm^{-2} d^{-1} for S^0 oxidation in three types of Scottish soils at 20°C. Birkham et al. (2009) determined a mean reaction rate for the oxidation of S^0 in liquid water reaction cells of 9 μg S^0 cm^{-2} d^{-1} at 23°C.

Comparable moisture content is of major importance when comparing oxidation rates from S^0 from prior studies. S^0 oxidation in soils is optimal when the water holding capacity of the soil does not exceed 50% (Iistedt, 2000; Janzen and Bettany, 1987a, b). Both Chapman (1989) and Janzen and Bettany (1987b) oxidized S^0 in soils at near optimal moisture content (45-55%). The study by Birkham et al. (2009) introduced enough water to the system to ensure the S^0 grains were in contact with water but not submerged (10 mL of water per 20 g S^0). The Birkham et al. study was also conducted without soil, and as a result is considered the most appropriate model for comparison to the current study. Notably, however, S^0 grains in the current study were completely submerged for the duration of the experiment (100 mL water per 40 g S^0). The extreme hydrophobicity of the S^0 ensured the system was not saturated; however, the volume of water in the flask far exceeded the amount required for optimum oxidation.

In addition, the parafilm cover on the 'open cell' experiments described here may have limited gas (O_2 and CO_2) migration into the flask between sampling periods. This is further compounded by the complete submergence of the S^0 in water, where molecular O_2 may have already been limited. O_2 is necessary for the growth and productivity of both the heterotrophic fungi and autotrophic bacteria. If fungal populations in the reaction solution increase (evidenced by visual growth, Figure 5.3) and consume a portion of the available O_2 in the system, the supply of O_2 for autotrophic activity would decrease, and consequently lower the rate of S^0 oxidation. Furthermore, fungi can consume extensive amounts of SO_4^{2-}, resulting in immobilization of free SO_4^{2-} released by oxidation (personal communication, John Lawrence; and Killham, 1994). Therefore, the comparatively slow oxidation rate in this study may be the result of surplus of

water in the system, limited O_2 available for oxidation, and uptake of SO_4^{2-} by fungal populations.

5.2.1 Activation energy (Ea) and temperature coefficient (Q_{10})

Activation energy was calculated by constructing an Arrhenius plot (Figure 5.6) from the rate constant values (k) and using the Arrhenius equation:

$$k = Ae^{-Ea/RT} \quad (5.1)$$

where A is the special constant, R is the universal gas constant, and T is temperature in Kelvin.

The calculated Ea values for the MS-A (6 to 32°C) and MS-C (6 to 32°C) series were 39 and 32 kJ mol^{-1}, respectively (Table 5.1). These estimates are slightly lower than the estimated range of 43-78 kJ mol^{-1} for S^0 oxidation in soils by Chapman (1989) and 65 kJ mol^{-1} from S^0 oxidation in a mineral salts media (0.4 g each of $(NH_4)_2SO_4$, K_2HPO_4, and $MgSO_4 \cdot 7H_2O$ per litre) reported by Ahonen and Tuovinen (1990).

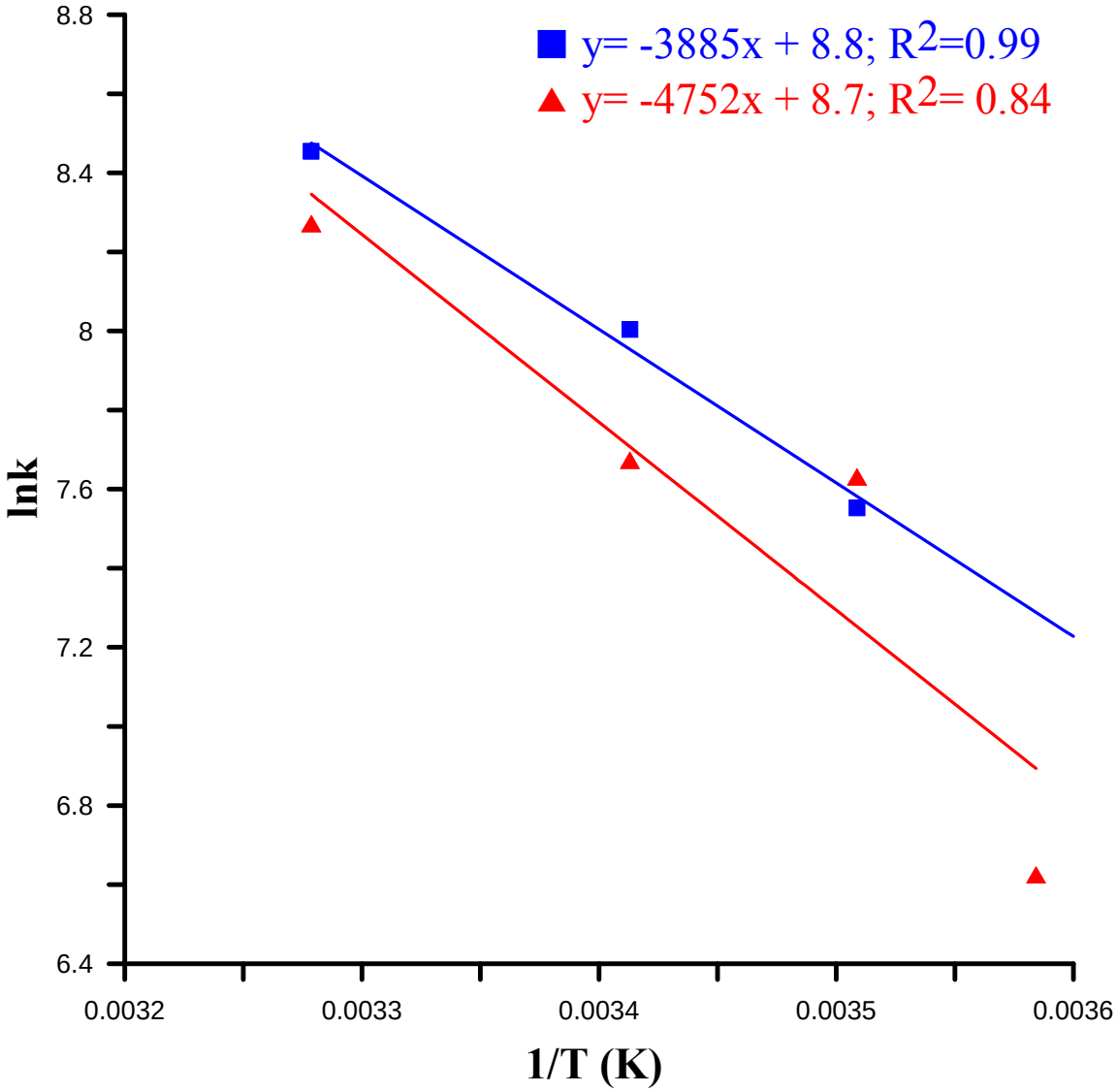

Figure 5.6. Arrhenius plot of rate constants determined for MS-A (▲) and MS-C (■).

Temperature coefficients (Q_{10}) were determined using (Equation 5.2):

$$Q_{10} = \left(\frac{k_a}{k_b}\right)^{\frac{10}{(Ta-T_b)}} \quad (5.2)$$

where k_a and k_b are the rate constants (μgS^0oxidized day^{-1}) for temperatures T_a and T_b (K), respectively.

The Q_{10} values of the MS-A and MS-C series were estimated at 1.9 and 1.6, respectively (Table 5.1). These values are lower than ranges estimated by Janzen and Bettany (1987b) (3.2-4.3) and Chapman (1989) (1.9-3.2) for S^0 oxidation in soils, as well as the value reported by Ahonen and Tuovinen (1990) (2.1) for the oxidation of S^0. However, the values compared well with Q_{10} estimates by Simunek and Suarez (1993) (1.5-3) for soil microbial respiration.

Table 5.1. Summary of S^0 oxidation for S^0 oxidation experiments.

Series	Temperature (±1°C)	Rate constant (*k*) (μgS^0 day^{-1})	R^2	Oxidation rate (μg S^0 cm^{-2} day^{-1})	Activation Energy (kJ mol^{-1})	Temperature coefficient (Q_{10})
MS-A	6	753	0.90	0.16		
	12	2060	0.98	0.43		
	21	2150	0.99	0.45		
	32	3910	0.99	0.78	39	1.9
MS-C	12	1910	0.99	0.40		
	21	2990	0.99	0.62		
	32	4700	0.99	0.98	32	1.6
DI-A	12	372	0.99	0.07		
	21	287	0.85	0.06		
	32	349	0.98	0.08	n.d.	n.d.

n.d. not determined

5.3 Oxygen isotopic composition of SO_4^{2-} in experimental solutions

The $\delta^{18}O_{(SO4)}$ vs. $\delta^{18}O_{(H2O)}$ plots for the MS-A and DI-A series (Figures 5.7 and 5.8, respectively) show excellent linear correlations ($R^2 \geq 0.991$). The slopes indicated essentially all oxygen incorporated into the SO_4^{2-} between 12 and 32°C for both the MS-A and DI-A series was derived from H_2O (Table 5.2). At 6°C, approximately 84% of the SO_4^{2-} oxygen was derived from H_2O, with the remaining 16% from O_2. As only one trial was conducted at 6°C (MS-A series), these results could not be confirmed in the DI-A series but the high R^2 value (0.99), gives confidence that the value of 84% is an accurate approximation for 6°C. After ensuring the data was normally distributed, an ANCOVA test was conducted to test the associative influences of the covariate ($\delta^{18}O_{(H2O)}$) and response ($\delta^{18}O_{(SO4)}$) variables. *p*-values of 0.555 (MS-A) and 0.715 (DI-A) indicate the linear association between temperature and $\delta^{18}O_{(SO4)}$ is not significant between 12 and 32°C. However, *p*-values of 0.00 indicated statistically significant linear association between $\delta^{18}O_{(H2O)}$ and $\delta^{18}O_{(SO4)}$. The results indicated $\delta^{18}O_{(SO4)}$ is not influenced by the temperature under which it was generated.

As previously indicated (Section 5.1.1), the production of SO_4^{2-} in S^0 oxidation experiments is predominantly the result of sulphur oxidizing microorganisms. Despite the consumption of O_2 by *A. thiooxidans* during oxidation, the isotopic composition of the SO_4^{2-} produced indicated that water was the primary source of O. However, this does not imply that $O_{2(g)}$ does not play an important role during oxidation. Kelly (1992) and Suzuki et al. (1994) determined that *A. thiooxidans* oxidizes S^0 exclusively through enzymatic pathways, during which the formation of SO_3^{2-} is a common step prior to oxidation to SO_4^{2-}. Intermediate aqueous phases can be expected to have considerable isotopic interactions if the rates of exchange are fast relative to the residence time of the unstable intermediate species (Seal, 2001). The oxygen isotope exchange rate between SO_3^{2-} and H_2O is considerably faster than the exchange rate between SO_4^{2-} and H_2O (Betts and Voss, 1970). The half life of the oxygen exchange reaction for a 0.3M SO_3^- solution at 24.7°C at a pH of 10.5 is 25.3 hr; if the pH decreases to 8.9, the half life decreases to 1.3 min (Betts and Voss, 1970). Therefore, if SO_3^{2-} is present at any point during S^0 oxidation, any prior incorporation of O_2 would be masked by H_2O-SO_3^- exchange reactions.

Stoichiometrically, three of the fours oxygen atoms in SO_4^{2-} resulting from S^0 oxidation should originate from water, and the fourth from molecular oxygen. However, the results from

this study suggest all oxygen was obtained from water. Further, the findings of this study compare well with the results of Mizutani and Rafter (1969) who report 100% of the oxygen was derived from H_2O during the oxidation of S^0 in a soil and water slurry by unknown sulphur oxidizing microorganisms at room temperature (approximately 20-22°C).

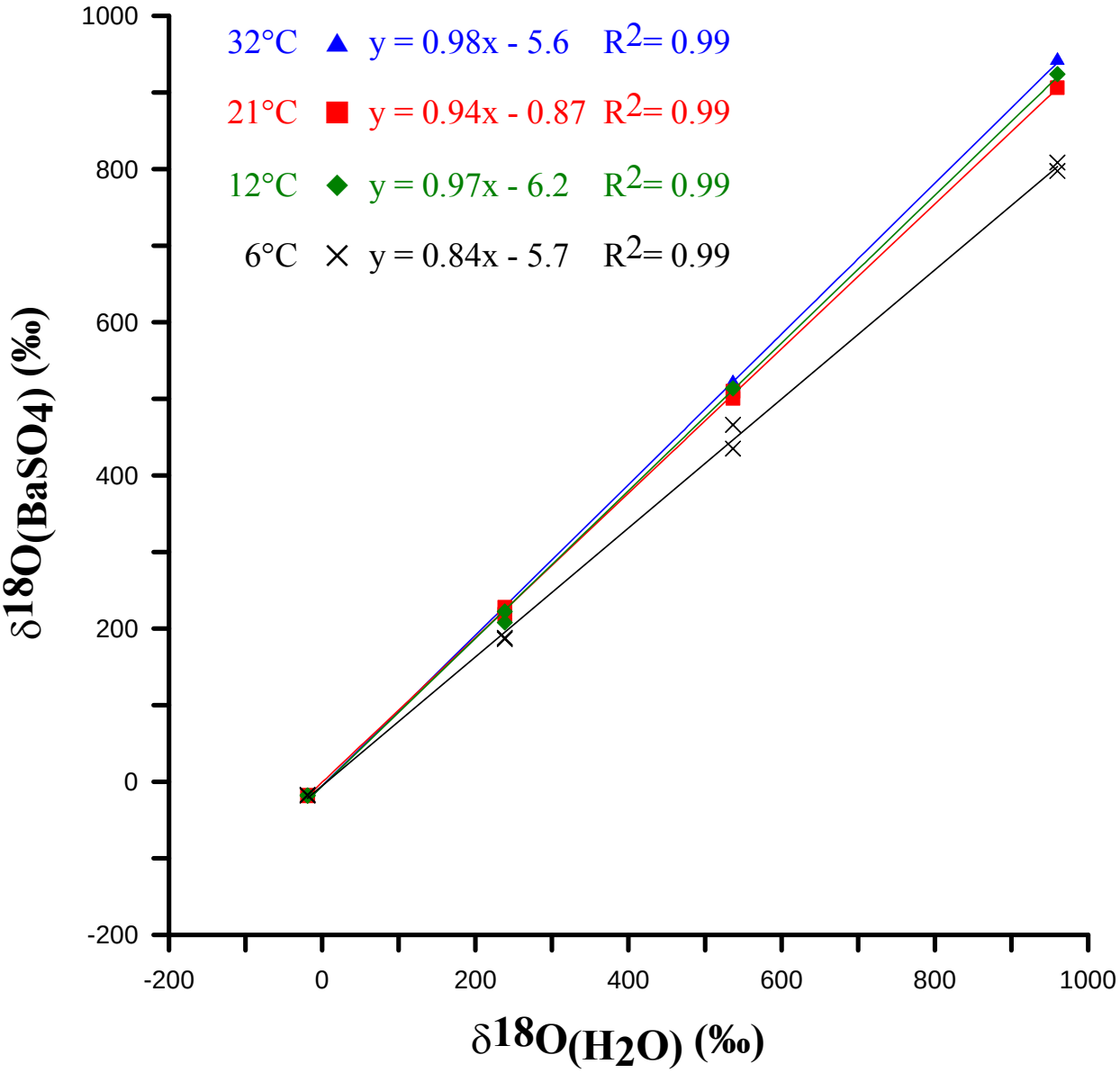

Figure 5.7. $\delta^{18}O$ value of SO_4^{2-} produced during oxidation of S^0 by *A. thiooxidans* vs. the $\delta^{18}O$ of the ambient H_2O at temperatures of 32 (▲), 21 (■), 12 (♦), and 6°C (x) in the MS-A series.

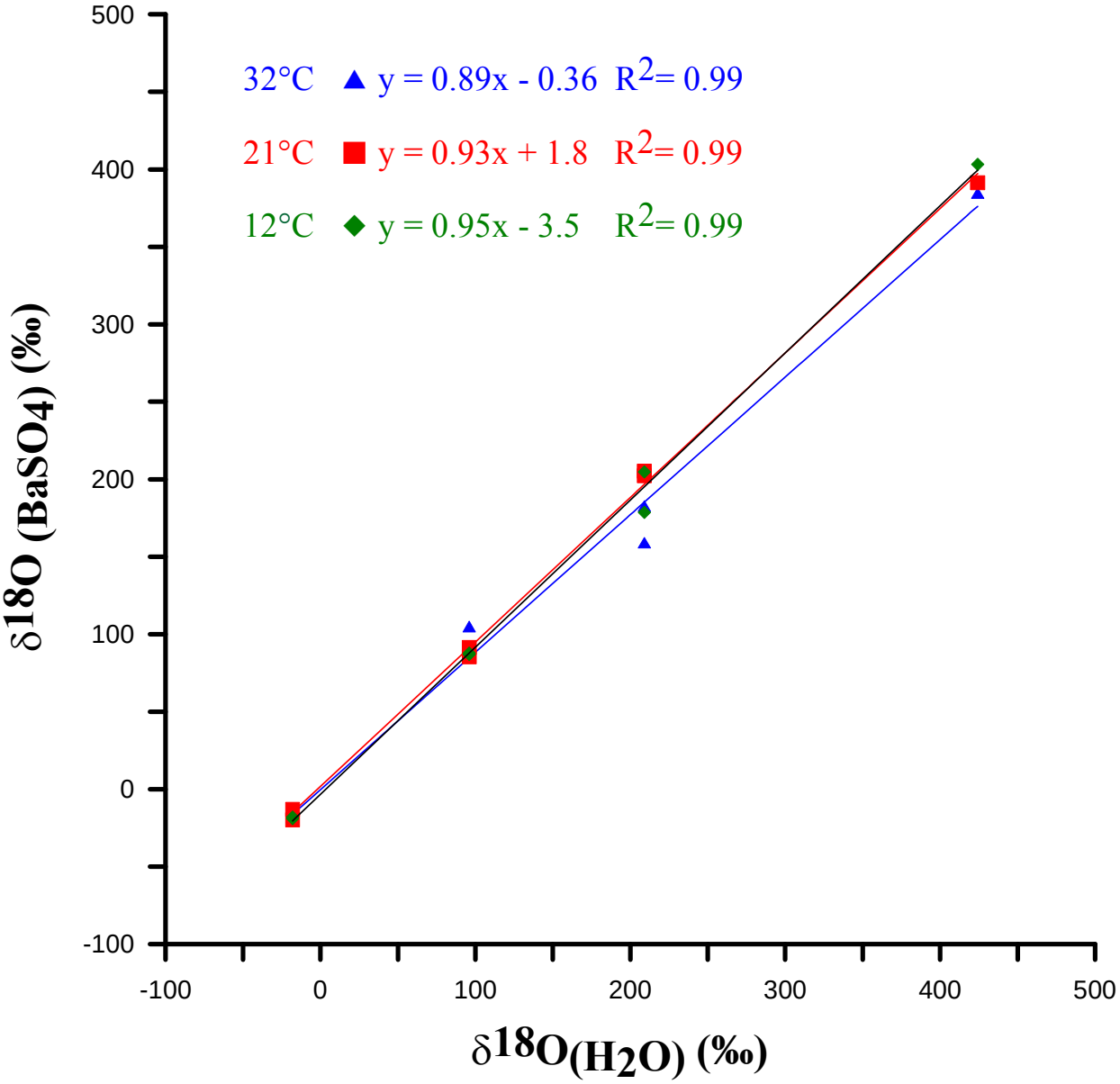

Figure 5.8. $\delta^{18}O$ value of SO_4^{2-} produced during oxidation of S^0 by *A. thiooxidans* vs. the $\delta^{18}O$ of the ambient H_2O at temperatures of 32 (▲), 21 (■), and 12°C (♦) in the DI-A series.

Table 5.2. Summary of calculated oxygen isotope fractionation during oxidation of S^0.

Series	Temperature ±1°C	% Oxygen from H_2O	$\varepsilon^{18}O_{SO4\text{-}H2O}$ (‰)
MS-A	6	84	-5.7
	12	97	-0.9
	21	94	-6.2
	32	98	-5.6
DI-A	12	95	-3.5
	21	93	+1.8
	32	89	-3.6

5.3.1 Kinetic isotope fractionation

Both water and molecular oxygen fractionate from their original isotopic composition during incorporation into SO_4^{2-}. Therefore, determining both fractionation factors and their relative contributions to SO_4^{2-} is not possible from isotope ratios alone (Sessions, 2005). This is true even if the isotopic compositions of both water and molecular oxygen are varied independently (Session, 2005). However, if all oxygen atoms in the generated SO_4^{2-} are from water, Equation 4.6 can be rewritten as $b=\varepsilon^{18}O_{SO4\text{-}H2O}$ (Balci, et al., 2007) and $\varepsilon^{18}O_{SO4\text{-}H2O}$ can be approximated from the y-intercepts of $\delta^{18}O_{(H2O)}$ vs. $\delta^{18}O_{(BaSO4)}$ plots (Figures 5.7 and 5.8). In this case, $\varepsilon^{18}O_{SO4\text{-}H2O}$ ranged from -0.9 to -6.2‰ with a mean of -4.6‰ for the MS-A series, and from +1.8 to -3.6‰ with a mean of -1.7 for the DI-A series (Table 5.2). With the exception of Mizutani and Rafter's (1969) estimate of 0‰, no estimates for $\varepsilon^{18}O_{SO4\text{-}H2O}$ for the oxidation of S^0 have been published. However, results from previous work on sulphide minerals and H_2S are presented in Table 5.3 for comparison (Balci et al., 2007; Van Everdingen, 1985; Taylor and Wheeler, 1984; Schwartz and Cortecci, 1974; Mizutani and Rafter, 1969; Lloyd, 1967).

Table 5.3. Estimates for oxygen sources and enrichment factors for the oxidation of sulphide minerals, H_2S, and S^0.

Source Reactant (Method)	**% Oxygen from H_2O**	**ε_{H2O} (‰)**	**ε_{O2} (‰)**
Lloyd (1969) H_2S (aerated H_2O)	68	0	-8.7
Mizutani and Rafter (1969) S^0 (aerated water/soil slurry)	100	0	n.d.
Schwartz and Cortecci (1974) Pyrite (abiotic/aerated H_2O)	50	n.d.	n.d.
Taylor and Wheeler (1984) Pyrite (*A. ferrooxidans*)	70	+3.5	-11.4
Pyrite (abiotic)		n.d.	-4.3
Van Everdingen et al. (1985) AMD field samples	37-74	+2.6	n.d.
Balci et al. (2007)			
Pyrite (aerated water/biotic/O_2)	85-92	+3.5-4.0	-10 to -11
Pyrite ($Fe(III)_{aq}$)	94-95	+3.6	n.d.
Current study (2009)			
S^0 (Mineral solution/*A.thiooxidans*)	84-98	-3.5 to +1.8	n.d.
S^0 (DI solution/*A.thiooxidans*)	89-95	-6.2 to -0.9	n.d.

n.d. not determined

5.4 Sulphur isotopic composition of SO_4^{2-} in experimental solutions

Ten samples of the S^0 used for the oxidation experiments were analyzed for isotope composition ($\delta^{34}S$) prior to oxidation. The $\delta^{34}S$ values ranged from +4.3 to +6.1‰, with a mean of +5.3±0.53‰. After SO_4^{2-} was recovered and precipitated as $BaSO_4$, 50 samples were analyzed for $\delta^{34}S$ and showed a range between +3.2 and +6.3‰ with a mean of +4.7±0.78‰. After both groups were tested for normality, a two sample t-test was conducted to assess the statistical difference between the means of each group. The calculated *p*-value of the two sample t-test is 0.034, which was below the threshold chosen for statistical significance (0.05). Therefore, the null hypothesis that the two groups do not differ was rejected.

While the t-test indicated the two groups were not the same statistically, the values suggested minimal sulphur isotope fractionation occured during the oxidation of S^0. Few studies identify sulphur isotope fractionation of S^0 during oxidation. Mizutani and Rafter (1969) and

Kaplan and Rittenberg (1964) reported small (<2.3‰) sulphur isotope fractionation between S^0 and resulting SO_4^{2-} during oxidation aided by sulphur oxidizing microorganisms. McCready and Krouse (1982) observed SO_4^{2-} enriched in the lighter ^{32}S isotope by 1‰ during oxidation of S^0 in soils by thiobacilli. The results of the current study were consistent with previous field and laboratory results that conclude the oxidation of sulphide minerals produces SO_4^{2-} with a sulphur isotope composition nearly indistinguishable from the parent sulphide mineral (Balci, et al., 2006; Seal, 2001; Rye et al., 1992; Field, 1966; Nakai and Jensen, 1964; Gavelin et al., 1960).

6.0 SCL FIELD CASE STUDY

A field component was added to this study to determine if the laboratory results could be comparable to field results. In laboratory S^0 oxidation experiments, essentially all oxygen incorporated into the SO_4^{2-} originated from H_2O. If this is true for the field conditions at SCL, the SO_4^{2-} in S^0 block run-off waters should reflect the oxygen isotopic composition of the H_2O in the system at the time of SO_4^{2-} production. Precipitation is the primary source of water infiltrating the S^0 blocks, and oxidizing the underlying S^0. The water enters the system at the top exterior and flows through the block using fractures as conduits (Birkham et al., 2009 and Bonstrom, 2007). Approximately 90% of S^0 oxidation occurs in the top 1 m of the S^0 storage blocks (Birkham, et al., 2009), making collection of water samples directly after the production of SO_4^{2-} impossible. Therefore, while the $\delta^{18}O_{(SO4)}$ should reflect the $\delta^{18}O$ of the water in the system, the water present in the collection tank samples may not be representative of the water present during the production of the SO_4^{2-}. With regular pumping of the collection tanks, the $\delta^{18}O$ of the water and SO_4^{2-} of individual samples should correspond well.

6.1 Pilot blocks

In 2005, five S^0 pilot blocks (approximately 21 × 21 × 3 m) were constructed by Syncrude Canada to assess the controls on acid production from S^0 blocks with varying cover designs (Davis et al., 2008). Each block was constructed on a prepared surface that consisted of a sand layer overlying a 60 mil HDPE liner over ≥ 20 m of compacted clay. The purpose of the sand layer is to collect water moving through the block and direct it towards individual 2100 L fiberglass in-ground storage tanks, where water samples of the effluent chemistry and water discharge can be obtained. General details of the covers (exposed, saturated, insulated, reclamation, and coletanche) on the five blocks are presented below. Additional construction details and rationale for construction are provided in OKC (2005).

Exposed block: The exposed block is a 'worst case end-member' where stored S^0 is subject to water, oxygen, and to temperature fluctuations. It was designed to be a small-scale version of the existing above ground blocks at SCL, and serves as a control to compare the effectiveness of the alternate coverings of the other blocks.

Saturated block: The saturated pilot block was constructed to assess the effectiveness of maintaining a water cover over the S^0 to minimize the ingress of molecular oxygen. A central vertical monitoring well was installed to monitor the water level.

Insulated block: The insulated block was constructed by covering the S^0 with 5 m of sand and a thin layer of gravel to lessen the effects of erosion. The purpose of a thick permeable cover is to maintain temperatures below 10°C in the underlying S^0. Temperatures below 10°C should reduce rates of biologically mediated oxidation of S^0, and thus minimize the production of H_2SO_4.

Reclamation block: The reclamation cover is typical of most covers at SCL, and is composed of 0.3 m of sand, 0.8 m of non-compacted Pg secondary[1] and 0.2 m of peat. The top is vegetated with native grass and shrub seed mix. The sides of the block are sloped at 2% to facilitate collection and measurement of surface runoff. The reclamation cover system sheds surface water from precipitation, and stores and releases water as evapotranspiration during the growing season. The S^0 is not in contact with the atmosphere.

Coletanche block: The coletanche cover is a bituminous geomembrane with low hydraulic conductivity designed to prevent ingress of meteoric water, while allowing the underlying S^0 to drain. The geomembrane is composed of non-woven polyester and oxidized bitumen. The geomembrane is sandwiched between a 0.3 m sand cover in contact with the S^0 below, and 0.3 m sand, 0.2 m till, and 0.15 m of peat above.

6.2 Sampling and analysis

Effluent samples were collected from the reclamation, insulated, exposed, and coletanche pilot blocks over a 15 month span during 2006 and 2007 (note: no samples collected from the saturated block). After the pH was measured, samples were filtered through a 0.45 μm cellulose filter and stored at 6°C for further analysis. Twenty-five samples from each collection tank were analyzed for major anions using ion-exchange chromatography. Eighteen of the 25 samples were analyzed for water isotopes using off-axis integrated-cavity output spectroscopy (OA-

[1] Pg secondary- Pleistocene deposits with relatively high clay content (called secondary materials when used for reclamation covers) (R. McMillan et al., 2007).

ICOS; Lis et al., 2008). Four samples from each block were precipitated as $BaSO_4$ and analyzed for $\delta^{18}O$ using continuous flow isotope ratio mass spectrometry (Balci, 2007).

Due to inconsistent pumping of the percolation tanks in 2006, the samples collected during this time were not included in the following SO_4^{2-} accumulation and $\delta^{18}O_{(SO4)}$ discussions. Because meteoric water cannot penetrate the coletanche cover, irregular pumping of the percolation tank would have no influence on the SO_4^{2-} recovered in the effluent. For this reason, all samples from the coletanche block were considered in this study. Data from individual samples for pH, SO_4^{2-} concentration, and S and O isotope analysis are presented in Appendix D.

6.3 Results and discussion

6.3.1 Local meteoric water line (LMWL)

Oxygen and hydrogen isotopes can be used to determine the role of evaporation in any naturally occurring system. Because most surface waters and groundwaters originate as meteoric water, they can be expected to fall on the local meteoric water line (LMWL; Clark and Fritz, 2001). In addition, seasonal changes should be observed due to variations in temperature of precipitation. If evaporation is occurring, hydrogen and oxygen isotopes of the residual water will become more enriched in heavy isotopes ^{18}O and ^{2}H, and depart from the LMWL along a positive trend. The slope of this trend will depend upon the temperature and relative humidity associated with evaporation (Clark and Fritz, 2001). While evaporation causes $\delta^{18}O_{(H2O)}$ to shift to higher values, $\delta^{18}O_{(SO4)}$ will remain unchanged once produced due to the slow oxygen exchange between H_2O and SO_4^{2-} (Seal, 2001). It was important to determine if evaporation is occurring in S^0 blocks because if the $\delta^{18}O_{(H2O)}$ of the ambient H_2O in the system becomes progressively heavier, the $\delta^{18}O_{(SO4)}$ produced after evaporation occurs will also become heavier. Depending on where in the block evaporation is occurring and where the SO_4^{2-} is being produced, the SO_4^{2-} recovered from the effluent may not reflect the water infiltrating the system, but rather a range of $\delta^{18}O$ as the H_2O gets progressively heavier. Therefore, evaporation could create considerable error in identifying the source of oxygen incorporated into the SO_4^{2-}.

All samples collected during the 15 month period were plotted on the Edmonton LMWL (Figure 6.1). The LMWL for Edmonton ($\delta D = 7.67\ \delta^{18}O - 1.4$) was constructed using samples from the precipitation station in Edmonton provided by the Global Network of Isotopes in

Precipitation (IAEA, 2006). The resulting trend produced from the pilot block samples indicated evaporation is occurring to a limited extent, but does not likely play an important role in the S^0 block system. In addition, the volume of water collected as effluent was comparable to the estimated volume of water entering the system, indicating evaporation in the block is negligible (Birkham et al., 2009).

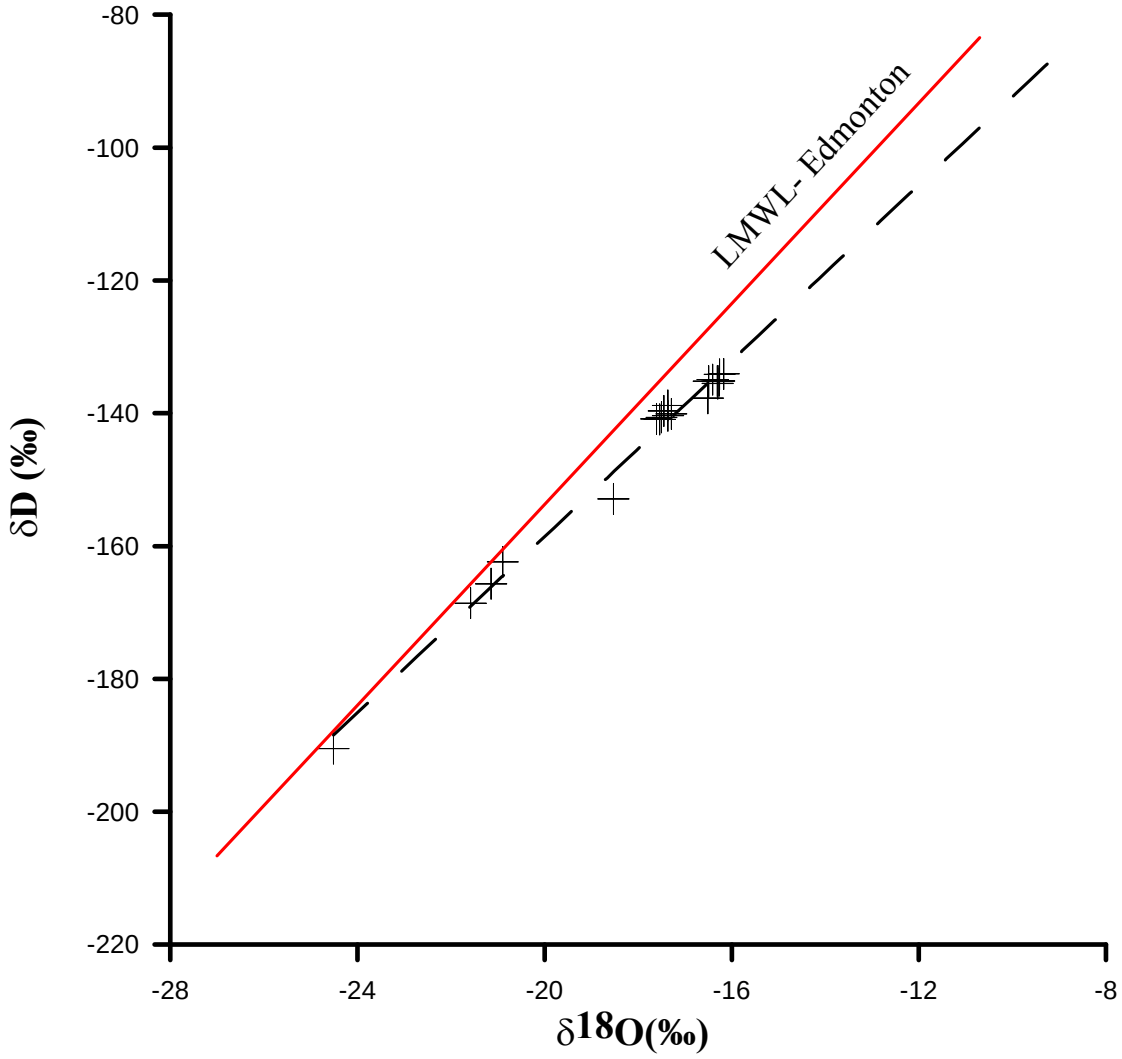

Figure 6.1. LMWL for Edmonton (red; $\delta D = 7.67\ \delta^{18}O - 1.4$) and pilot blocks (+).

6.3.2 SO_4^{2-} loading in effluent

SO_4^{2-} concentrations from each sampling period in 2007 were measured in mg L^{-1}. To determine the cumulative mass of SO_4^{2-} produced in each pilot block, the measured concentration was multiplied by the volume of water outflow (L). However, the volume of the drainage water was not measured directly, and therefore the outflow volume was approximated based on the measured depth of water in the tank at each sampling period.

The cumulative mass of SO_4^{2-} produced from the coletanche block was considerably less than from the reclamation, insulated, or exposed blocks (Figure 6.2). If minimal water penetrates the coletanche cover, the mass of SO_4^{2-} produced via S^0 oxidation in the coletanche block should be less than SO_4^{2-} accumulation in the remaining pilot blocks. However, the limited mass of SO_4^{2-} recovered in the coletanche drainage water may not be the result of S^0 oxidation, but rather residual collection of SO_4^{2-} present in the water during block construction. Because the exposed block is completely vulnerable to the ingress of atmospheric O_2 and meteoric H_2O, the mass of SO_4^{2-} accumulated with time would be expected to be greater than the insulated or reclamation blocks. The observation that the pilot blocks with the greatest and least mass of accumulated SO_4^{2-} with time are the exposed and coletanche blocks, respectively, adds validity to the assumption they represent worst and best case end-members for block coverings.

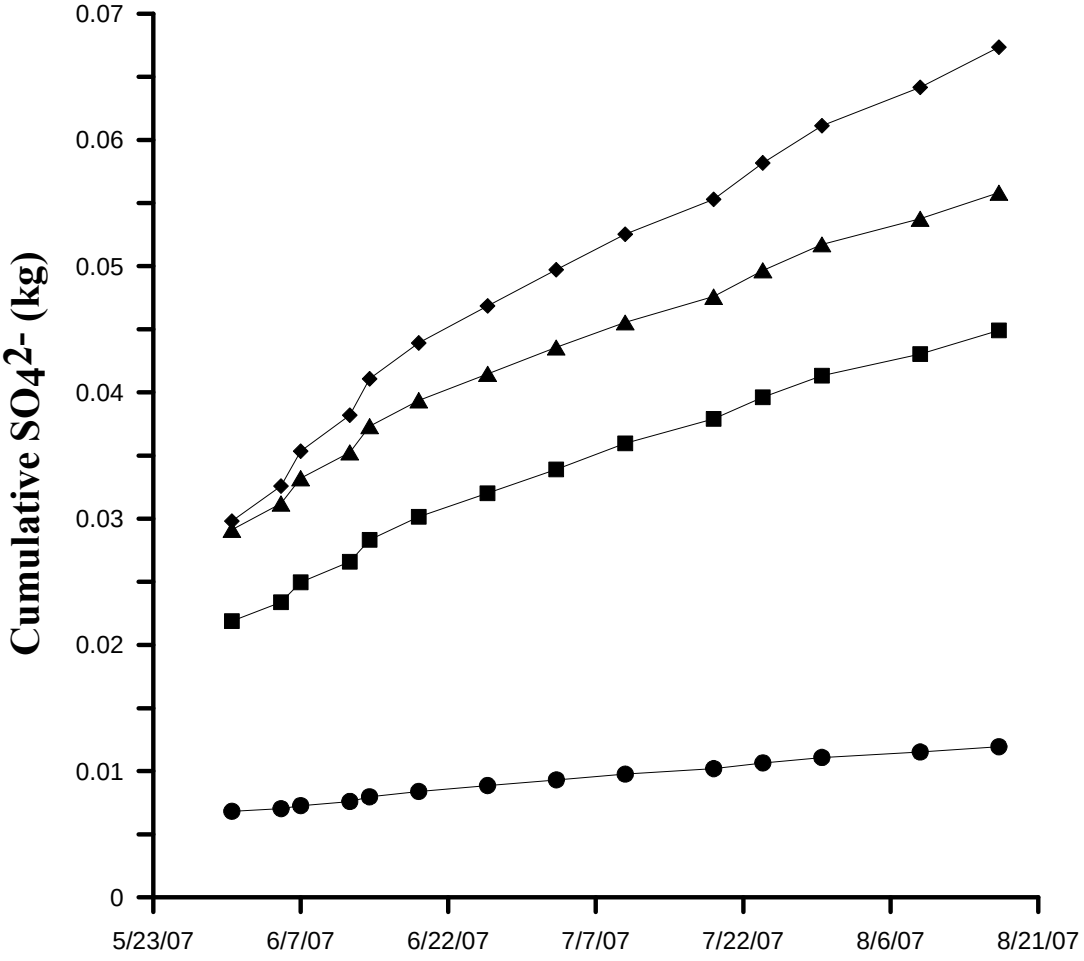

Figure 6.2. Cumulative SO_4^{2-} recovered in the effluent of the four sampled pilot blocks: exposed (♦), insulated (▲), reclamation (■) and coletanche (●).

6.4 Oxygen isotopes of SO_4^{2-} present in block effluent

S^0 blocks with permeable covers (reclamation and insulated) or no cover (exposed and Phase II) allow meteoric water to migrate through the underlying S^0. Data from these blocks should thus reflect a trend in $\delta^{18}O_{(SO4)}$ in response to seasonal variations of precipitation. However, the coletanche block was constructed to prevent the ingress of water, while allowing the underlying S^0 to drain. Therefore, $\delta^{18}O_{(SO4)}$ in the coletanche effluent should not show a trend in response to changing meteoric water $\delta^{18}O$ values.

Two samples from each of the above ground pilot blocks (exposed, insulated, and reclamation), along with two samples from the Phase II block and four samples from the coletanche pilot block, were used to construct Figure 6.3. The $\delta^{18}O_{(SO4)}$ of the coletanche

samples ranged from -13.6 to -14.1‰ with a mean of -13.6±0.36; the $\delta^{18}O_{(H2O)}$ ranged from -15.5 to -18.5‰ with a mean of -16.4±1.36‰. The $\delta^{18}O_{(SO4)}$ values confirmed the SO_4^{2-} was created using water with a similar $\delta^{18}O$ composition, and indicated either the SO_4^{2-} recovered in the coletanche effluent was produced using water present in the block prior to the application of the cover, or the source of SO_4^{2-} in the effluent was not S^0 oxidation in the block. The variation in $\delta^{18}O_{(H2O)}$ values may have been caused by subsequent draining of the block or dilution and mixing from precipitation events.

Birkham et al. (2009) indicate the time required for water to flow through the commercial scale Phase II block is a matter of days. Given the small scale of the pilot blocks, water collected in the percolation tanks likely entered the blocks shortly before collection. While the collected water may be a mixture of a few days drainage, if the tanks are pumped regularly, samples should provide a good record of oxygen isotopic composition of H_2O and SO_4^{2-} with time.

The $\delta^{18}O_{(SO4)}$ values of the pilot block effluent samples were linearly related to the $\delta^{18}O_{(H2O)}$ values, with a slope of 1.04 and an R^2 of 0.73 (Figure 6.3). This suggested all oxygen incorporated into the SO_4^{2-} originated from H_2O, which was consistent with results from the laboratory series experiments.

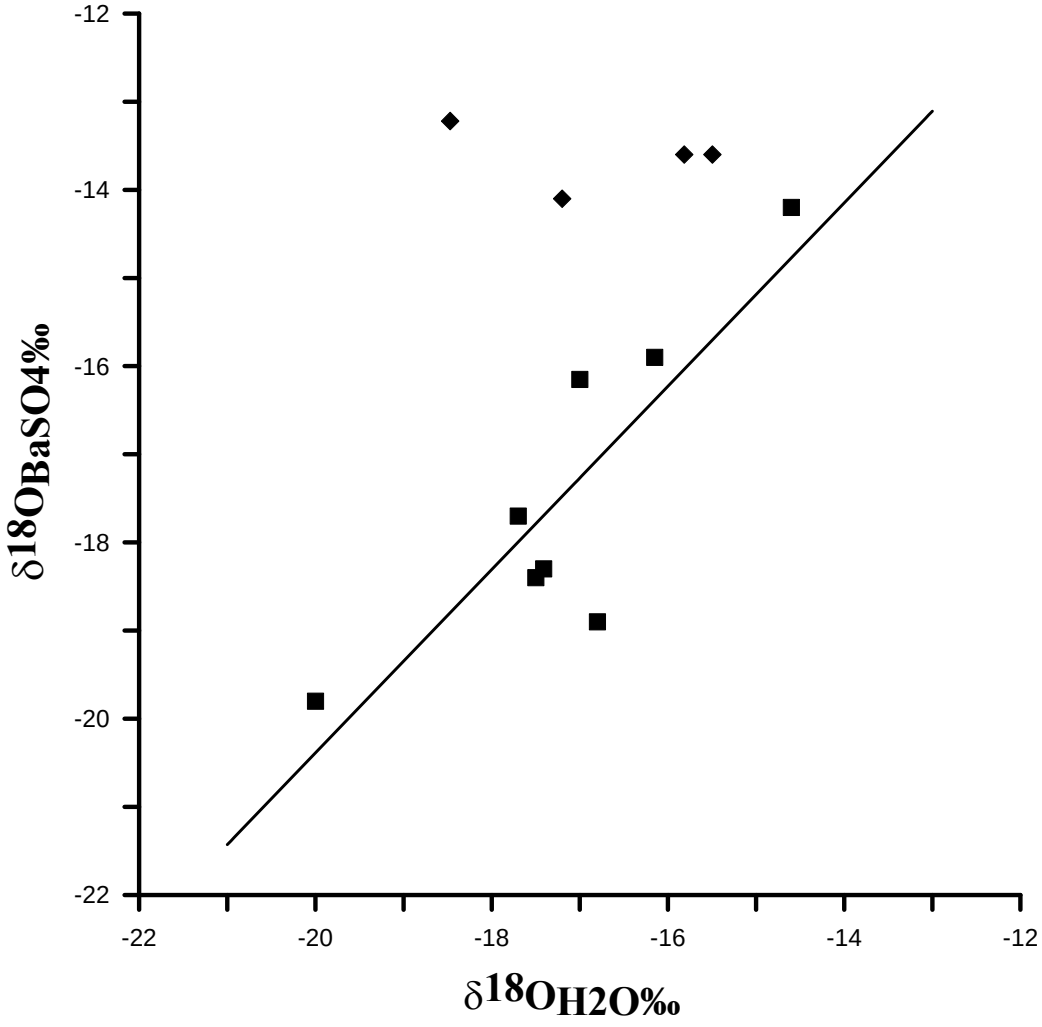

Figure 6.3. $\delta^{18}O_{(H2O)}$ vs $\delta^{18}O_{(SO4)}$ of effluent samples from the reclamation, exposed, insulated and Phase II blocks (■; y= 1.04x + 0.41; $R^2 = 0.73$), and the coletanche block (♦). Error bars are smaller than plot points.

7.0 SUMMARY AND CONCLUSIONS

The goal of this thesis was to investigate the controls on the oxidation of S^0 using stable isotopes of O and S in aqueous SO_4^{2-} and provide insight into the processes and controls on the oxidation of S^0 in sulphur blocks. Specifically, the objectives were to: i) assess abiotic and biotic oxidation reactions in controlled experiments as a function of temperature and nutrient availability; ii) quantify the partitioning of oxygen (from molecular O_2 and H_2O) into SO_4^{2-}; and iii) compare the results of lab experiments to the results of field samples to determine if lab and field conditions can be considered analogous.

The laboratory component of this study was conducted using a series of S^0 oxidation experiments to measure the abiotic and biotic rate of S^0 oxidation at temperatures 6, 12, 20, and 32°C in both mineral salt (MS), and deionized water (DI) solutions. In addition, by systematically varying the $\delta^{18}O$ values of H_2O during each series of experiments, the contribution of each oxygen source to the resulting SO_4^{2-} was determined. Results from batch testing provided oxidation reaction rates, activation energy, temperature coefficients, and insight into the stable isotope chemistry of abiotic and biotic S^0 oxidation.

The field component of this study involved collection of effluent water samples from the percolation tanks of four pilot S^0 blocks at Syncrude Canada Ltd., located near Fort McMurray, Alberta, Canada. The samples were analyzed for SO_4^{2-} concentration, pH, and stable isotopes of H_2O and SO_4^{2-}. Results of this study were compared with the results of the S^0 oxidation experiments to determine if O_2 was similarly fractionated. The summary and conclusions for these objectives are presented below.

7.1 S^0 oxidation as a function of temperature and nutrient availability

To determine the influence of microorganisms on the oxidation of S^0, experiments were conducted with and without a microbial inoculant. The inoculant was prepared from SCL S^0 block effluent to ensure the microbial community was representative of the community inhabiting the blocks onsite. At all incubation temperatures, abiotic controls produced only minor amounts of SO_4^{2-} (< 2 mM SO_4^{2-} after 3000 hours), indicating > 95% of SO_4^{2-} produced in the biotic trials was the result of microbial activity.

In all biotic series, a lag phase preceded SO_4^{2-} accumulation in the reaction solution. The lag phase decreased with increasing temperature, indicating the acid producing microorganisms

(*Acidithiobacillus thiooxidans*) adapted to the new reaction solution faster with increasing temperature. The lag phases observed in the MS series were markedly shorter than observed in the DI series, suggesting the SO_4^{2-} producing microorganisms required additional time to adapt to the nutrient deficient environment. After the initial lag phase, SO_4^{2-} concentrations (mM) increased linearly, indicating the biotic oxidation of S^0 is a zero-order reaction. Estimated oxidation rates for the MS-A and MS-C series ranged from 0.16 (6°C) to 0.78 (32°C) μg S^0 cm^{-2} d^{-1} and 0.40 (12°C) to 0.98 (32°C) μg S^0 cm^{-2} d^{-1}, respectively, indicating S^0 oxidation increased with temperature. Temperature coefficients of 1.9 and 1.6 were calculated for the MS-A and MS-C series, respectively. Estimated oxidation rates for the DI-A series did not increase with temperatures and ranged from 0.06 to 0.08 μg $S^0 cm^{-2} d^{-1}$ between 12 and 32°C. Q_{10} and Ea estimates could not be calculated due to the small differences in SO_4^{2-} production between temperatures. The considerably slower rates of S^0 oxidation in the DI series indicated the productivity of microorganisms, as measured by SO_4^{2-} production, substantially increased when nutrients such as PO_4, Mg, Ca, NH_4, and Cl were present.

The oxidation rates calculated for all series are lower than estimates of previous authors. However, previous studies measuring S^0 oxidation often represent soils with optimal water content or free water cells with less than 10 mL water per 10 g S^0. Excess water (100 mL per 40 g S^0), limited available molecular O_2, and increasing fungi populations in the flasks likely contributed to the slower oxidation rates observed in the current study.

7.2 Quantify the partitioning of oxygen into SO_4^{2-}

Oxygen isotope analyses conducted on SO_4^{2-} recovered in the reaction solution of all S^0 oxidation experiments showed essentially all oxygen incorporated into the SO_4^{2-} originated from H_2O in all cases conducted above 6°C. The oxygen isotope fractionation effect between SO_4^{2-} and water was determined to be -5.7 (6°C), -0.9 (12°C), -6.2 (20°C) and -5.6 (32°C) for the MS series, and -3.5 (12°C), +1.8 (20°C) and -3.6 (32°C) for the DI series. Sulphur isotope analysis indicated a small (< 0.4‰) but significant fractionation between S^0 and SO_4^{2-}.

Data reflecting SO_4^{2-} accumulation in the four studied pilot blocks indicated that limiting water ingress to the S^0 blocks would minimize SO_4^{2-} production (Figure 6.3). The cumulative mass of SO_4^{2-} produced from the block covered by an impermeable geomembrane cover (coletanche block) was considerably less than the remaining four blocks. In addition, the block

completely vulnerable to meteoric water and atmospheric air (exposed block) accumulated the greatest mass of SO_4^{2-} with time. With H_2O oxygen identified as the major source of oxygen incorporated into SO_4^{2-} during S^0 oxidation in laboratory and field environments, limiting water to the system would minimize the production of H_2SO_4.

7.3 Isotope comparison of laboratory and field samples

To determine if laboratory conditions could be scaled to field conditions, samples from percolation tanks were subjected to oxygen isotope analysis. If the processes partitioning oxygen into SO_4^{2-} produced in the S^0 blocks are similar to those in the lab, nearly 100% of the SO_4^{2-} oxygen would be obtained from associated water. Results indicated $\delta^{18}O_{(SO4)}$ recovered from the effluent samples were linearly related to $\delta^{18}O_{(H2O)}$ of the system. A slope of 1.04 ($R^2 = 0.73$) indicated 100% of the oxygen incorporated into the generated SO_4^{2-} originated from H_2O, which was consistent with results from laboratory S^0 oxidation experiments.

7.4 Implications

Recognizing that H_2O plays an important role in the generation of SO_4^{2-} during S^0 oxidation has implications for S^0 storage which go beyond the recommendation of limiting H_2O to the blocks. While covering the S^0 blocks with an impermeable cover would undoubtedly minimize total SO_4^{2-} accumulation in block effluent, the results of this study suggest $\delta^{18}O_{(SO4)}$ can be used to track water movement through the block. Because > 90% of SO_4^{2-} is generated in the top 1 m of the S^0 block (Birkham et al., 2009), and both laboratory and field results indicated nearly 100% of oxygen incorporated into SO_4^{2-} during S^0 oxidation originated from water, $\delta^{18}O_{(SO4)}$ could be used as a tracer to estimate the time required for the H_2O (and aqueous SO_4^{2-}) to migrate through the block. With continuous sampling of H_2O entering and exiting the block and frequent $\delta^{18}O$ analyses of inflowing H_2O and out-flowing aqueous SO_4^{2-} estimates of H_2O migration could be highly accurate.

8.0 RECOMMENDATIONS FOR FUTURE WORK

1. Results of isotope analyses from the oxidation experiments indicated nearly all oxygen incorporated into SO_4^{2-} originated from H_2O. However, the stoichiometry of S^0 oxidation indicates one atom of molecular oxygen and three atoms of water oxygen should be incorporated into the produced SO_4^{2-}. This discrepancy between the observed and theoretical results may be caused by exchange reactions with intermediate species not identified in this study. Therefore, to clarify the processes occurring during oxidation, experiments should be carried out to sample and analyze S^0 oxidation intermediates.

2. While the results of this study indicate that molecular oxygen plays a minor role in the oxidation of S^0, an aspect not investigated was intentionally varying or controlling the concentration of dissolved oxygen in the reaction solution. Because the solubility of O_2 in water varies between approximately 13 and 7 mg/L between temperatures 6 and 32°C, respectively (Figure 8.1); the concentration of available O_2 could impact both the oxidation rate, and the oxygen isotopic composition of the produced SO_4^{2-}. To fully assess the importance of O_2 during S^0 oxidation, closed cell experiments designed to vary O_2 concentration should be considered.

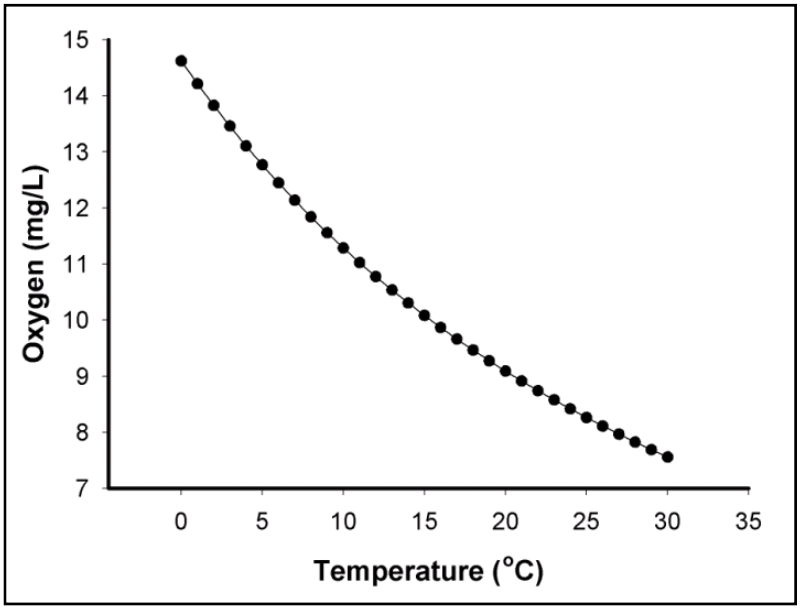

Figure 8.1. Oxygen solubility curve in water (Food and Agriculture Organization 2009).

3. An initial objective of this study was to systematically vary the $\delta^{18}O$ values of O_2 and inject the spiked ^{18}O mix into closed cell experiments. This was an important aspect, as a limited number of studies have approached this problem by varying the gas component of the experimental design. However, due to a manufacturing error, the custom mixed gas was not enriched in ^{18}O. Future work should focus on varying the $\delta^{18}O_{(O2)}$ used in S^0 oxidation experiments to confirm the results obtained in this study by varying the $\delta^{18}O_{(H2O)}$ in open cell experiments.

4. The bulk of the information presented in this study is the result of work conducted in a laboratory setting. Relating laboratory results to field scale systems is inherently difficult. Samples removed from the percolation tanks in 2006 were not included for analysis due to irregular pumping of the tanks; therefore, additional samples should be obtained for oxygen isotope analysis and added to Figure 6.3. Additional data will ideally increase the correlation coefficient of the linear regression of $\delta^{18}O_{(H2O)}$ vs. $\delta^{18}O_{(SO4)}$, and increase confidence in scaling up the results of laboratory experiments to a field situation.

9.0 REFERENCES

Ahonen, L. and Tuovinen, O. (1991) Kinetics of sulfur oxidation at suboptimal temperatures. *Applied and Environmental Microbiology* **56** (2), 560-562.

American Type Culture Collection. (2009) Available at: www.atcc.org. Last accessed June, 2009.

Attoe, O. and Olson, R. (1966) Factors affecting rate of oxidation in soils of elemental sulfur and that added in rock phosphate-sulfur fusions. *Soil Science* **101** (4), 317-325.

Balci, N., Shanks III, W.C., Mayer, B. and Mandernack, K. (2007) Oxygen and sulfur isotope systematics of sulfate produced by bacterial and abiotic oxidation of pyrite. *Geochimica et Cosmochimica Acta* **71**, 3796-3811.

Baldi, F., Clark, T., Pollack, S.S. and Olson, G. J. (1992) Leaching of pyrites of various reactivities by Thiobacillus ferrooxidans. *Applied and Environmental Microbiology* **58**, 1853-1856.

Bernier, L. and Warren, L. (2007) Geochemical diversity in S processes mediated by culture-adapted and environmental-enrichments of Acidithiobacillus spp. *Geochimica et Cosmochimica Acta* **71**, 5684-5697.

Bernier, L. and Warren, L. (2005) Microbially driven acidity generation in a tailings lake. *Geobiology* **3**, 115-133.

Betts, R. and Voss, R. (1970) The kinetics of oxygen exchange between sulfite ion and water. *Canadian Journal of Soil Science* **48**, 2035-2041.

Birkham, T., Hendry, M. and Barbour, S. Controls and rates of acid production in commercial-scale sulphur blocks. *For submission to: Journal of Environmental Quality*.

Blair, G., Lefroy, R.D.B., Dana, M. and Anderson, G.C. (1993) Modeling of sulfur oxidation from elemental sulfur. *Plant and Soil* **155/156**, 379-382.

Bonstrom, K. (2007) Physical controls on water migration in elemental sulphur blocks. Masters of Science thesis, University of Saskatchewan.

Brooks, B., Peters, T. and Winch, J. (1989) *Preparation of a Manual of Methods used in Revegetation of Reactive Sulphide Tailings Basins.* Energy, Mines and Resources Canada. Ottawa, Ontario.

Canfield, D., Mandl, M., Helanova, S. and Kasparovska, J. (2001) Isotope fractionation and sulfur metabolism by pure and enrichment cultures of elemental sulfur-disproportionating bacteria. *Biotechnology and Bioengineering* **78** (1), 24-30.

Chapman, S. (1989) Oxidation of micronized elemental sulphur in soil. *Plant and Soil* **116**, 69-76.

Chiba, H. and Sakai, H. (1985) Oxygen isotope exchange-rate between dissolved sulfate and water at hydrothermal temperatures. *Geochimica et Cosmochimica Acta* **49**, 993-1000.

Clark, I. and Fritz, P. (1997) *Environmental Isotopes in Hydrogeology.* Lewis Publishers, New York.

Clark, P. (2005) Surface block storage of elemental sulphur: a simple strategy to prevent all emissions. *Sulphur* **297**, 23-27.

Crescenzi, F., Crisari, A., D'Angeli, E. and Nardella, A. (2006) Control of acidity development on solid sulfur due to bacterial action. *Environmental Science and Technology* **40**, 6782-6786.

Davis, P. and Clark, P. (2008) Fossil fuel development requires long-term sulfur strategies. *Oil and Gas Journal*, 45-53.

Edwards, P. (1982) *Report of consultancy at the regional lead center in China for integrated fish farming*. Establishment of a Network of Aquaculture Centers in Asia. Report no. AC257/E.

Ehrlich, H. (1996) *Geomicrobiology*, Marcel Dekker, Inc.

Field, C. (1966) Sulfur isotopic method for discriminating between sulfates of hypogene and supergene origin. *Economic Geology* **61**, 1428-1435.

Fox, R., Atesalph, H., Kempbell, D.H. and Rhoades, H.F. (1964) Factors Influencing the Availability of Sulfur Fertilizers to Alfalfa and Corn. *Soil Science Society American Journal* **28**, 406-408.

Fry, B., Ruf, W., Gest, H. and Hayes J.M. (1967) Oxidation of sulphur in soils. *Mineralium Deposita* **2**, 181-187.

Gavelin, S., Parwel, A. and Ryhage, R. (2002) Sulfur isotope fractionation in sulfide mineralization. *Economic Geology* **55**, 510-530.

Germida, J., Wainwright, M. and Gupta, V. (1991) Biochemistry of sulfur cycling in soil. In *Soil Biochemistry*. New York: Marcel Dekker, Inc. pp 1-53.

Germida, J. and Janzen, H. (1993) Factors affecting the oxidation of elemental sulfur in soils. *Fertilizer Research* **35**, 101-114.

Gleisner, M., Herbert, R. and Frogner Kockum, P. (2002) Pyrite oxidation by Acidithiobacillus ferrooxidans at various concentrations of dissolved oxygen. *Chemical Geology* **225**, 16-29.

Gourdon, R. and Funtowicz, N. (1998) Kinetic model of elemental sulfur oxidation by Thiobacillus thiooxidans in batch slurry reactors. *Bioprocess Engineering* **18**, 241-249.

Hallberg, K. and Johnson, D. (2003) Novel acidophiles isolated from moderately acidic mine drainage waters. *Hydrometallurgy* **71** (1-2), 139-148.

Hoering, T. and Kennedy, J. (1957) The exchange of oxygen between sulphuric acid and water. *Journal of American Chemical Society* **79**, 56-60.

Holt, B. and Kumar, R. (1991) *Oxygen isotope fractionation for understanding the sulphur cycle*. Island Press, Washington, DC.

Howarth, R. and Stewart, J. (1992) *The interactions of sulphur with other element cycles in the ecosystem*. Wiley and Sons, United Kingdom, GBR.

IAEA/WMO (2006) Global Network of Isotopes in Precipitation. The GNIP Database. Accessible at: http://isohis.iaea.org. Last accessed July 15, 2009.

Ilstedt, U., Nordgren, A. and Malmer, A. (2000) Optimum soil water for soil respiration before and after amendment with glucose in humid tropical acrisols and a boreal mor layer. *Soil Biology and Biochemistry* **32**, 1591-1599.

Janzen, H. and Bettany, J. (1987) Measurement of sulfur oxidation in soils. *Soil Science* **143** (6), 91-103.

Janzen, H. and Bettany, J. (1986) Release of available sulfur from fertilizers. *Canadian Journal of Soil Science* **66**, 91-103.

Janzen, H. and Bettany, J. (1987) The effect of temperature and water potential on sulfur oxidation in soils. *Soil Science* **144** (2), 81-89.

Johnson, D. and Hallberg, K. (2003) The microbiology of acidic mine waters. *Research in Microbiology* **154**, 466-473.

Kelly, D., Shergill, J.K., Lu, W.P. and Wood, A.P. (1997) Oxidative metabolism of inorganic sulfur compounds by bacteria. *Antonie Van Leeuwenhoek* **71**, 95-107.

Kelly, D. and Wood, A. (2000) Reclassification of some species of Thiobacillus to the newly designed genera Acidithiobacillus gen. nov., Halothiobacillus gen. nov. and Thermithiobacillus gen. nov. *International Journal of Systematic and Evolutionary Microbiology* **50**, 511-516.

Killham, K. (1994) *Soil Ecology*. Cambridge University Press.

Knickerbocker, C., Nordstrong, D. and Southam, G. (2000) The role of "blebbing" in overcoming the hydrophobic barrier during biooxidation of elemental sulfur by Thiobacillus thiooxidans. *Chemical Geology* **169**, 425-433.

Koehler, F. and Roberts, S. (1983) An evaluation of different forms of sulphur fertilizers. In *Proceedings of the International Sulphur '82 conference*. British Sulphur Corporation, London. pp. 833-842.

Konishi, Y., Asai, S. and Yoshida, N. (1995) Growth kinetics of Thiobacillus thiooxidans on the surface of elemental sulphur. *Applied and Environmental Microbiology* **61** (10), 3617-3622.

Kroopnick, P. and Craig, H. (1972) Atmospheric oxygen: Isotopic composition and solubility fractionation. *Science* **175**, 54-55.

Krouse, H.R. (1981) Sulphur isotopes in our environment. In *Handbook of Environmental Isotope geochemistry*, Vol. 1. Elsevier, Amsterdam. pp 435-471.

Krouse, H., Gould, W.D., McCready, R.G.L. and Rajan, S. (1991) ^{18}O incorporation into sulphate during the bacterial oxidation of sulphide minerals and the potential for oxygen isotope exchange between O2, H2O and oxidized sulphur intermediates. *Earth and Planetary Science Letters* **107**, 90-94.

Krouse, H. and Mayer, B. (2000) Sulphur and oxygen isotopes in sulphate. In *Environmental tracers in subsurface hydrology*. Kluwer Academic Publishers, Norwell, Massachusettes. pp 195-232.

Kuenen, J., Robertson, L. and Touvinen, O. (1992) The genera Thiobacillus, Thiomicrospira and Thiosphaera. In *The prokaryotes*. Springer, Berlin.

Laishley, E. and Bryant, R. (1983) *The effect of particle sizes and molecular composition of elemental sulphur on ease of microbiological oxidation*. Alberta Sulphur Research Council. Calgary, AB.

Laishley, E., Bryant, R. and Hynes, J. (1985) *The effect of temperature and biocides on the sulphur oxidizing activity of Thiobacilli.* Alberta Sulphur Research Council. Calgary, AB.

Larsen, P., 2008. Regression and analysis of variance. Available at: http://statmaster.sdu.dk/courses/st111/. Last accessed March, 2009.

Lawrence, J., Gupta, V. and Germida, J. (1988a) Impact of elemental sulfur fertilization on agricultural soils. *Canadian Journal of Soil Science* **68** (3), 475-483.

Lawrence, J., Gupta, V. and Germida, J. (1988b) Relationship between microbial biomass and elemental sulfur oxidation in agricultural soils. *Soil Science Society American Journal* **52** (3), 672-677.

Li, P. and Caldwell, A. (1966) The oxidation of elemental sulfur in soil. *Soil Sci. Soc. Amer. Proc.* **30**.

Lim, D. (2003) *Microbiology* 3rd ed. Kendall/Hunt, Dubuque, Iowa.

Lis, G., Wassenaar, L. and Hendry, M. (2008) High-precision laser spectroscopy D/H and $^{18}O/^{16}O$ measurements of microliter natural water samples. *American Chemical Society*. Published online 11/22/2007.

Lloyd, M. (1968) Oxygen isotope behaviour in the sulfate-water system. *Geophysical Research* **73** (19), 6099-6110.

Lloyd, M. (1967) Oxygen-18 Composition of Oceanic Sulfate. *Science* **156**, 1228-1231.

Mahmoud, K., Leduc, L. and Ferroni, G. (2005) Detection of Acidithiobacillus ferrooxidans in acid mine drainage environments using fluorescent in situ hybridization (FISH). *Journal of Microbiological Methods* **61**, 33-45.

Mayer, B. (1998) Potential and limitations of using sulfur isotope abundance ratios as an indicator for natural and anthropogenic induced environmental change. In *Isotope Techniques in the Study of Past and Current Environmental Changes in the Hydrosphere and the Atmosphere*. Vienna: IAEA, 423-435.

McCready, R. and Krouse, H. (1982) Sulfur isotope fractionation during the oxidation of elemental sulphur by thiobacili in solonetzic soil. *Canadian Journal of Soil Science* **62**, 105-110.

McKenna, G. (2004) *Geo-environmental observations of 17 sulphur blocks in Alberta*, Syncrude Canada Ltd.

McMillan, R., Quideau, S.A., MacKenzie, M.D. and Biryukova, O. (2007) Nitrogen mineralization and microbial activity in oil sands reclaimed boreal forest soils. *Journal of Environmental Quality* **36**, 1470-1478.

Meyer, B. (1977) *Sulphur, Energy, and Environment*. Elsevier, Amsterdam.

Mizutani, Y. and Rafter, T. (1969) Bacterial fractionation of oxygen isotopes in the reduction of sulphate and in the oxidation of sulphur. *New Zealand Journal of Science* **12**, 60-68.

Nakai, N. and Jensen, M. (1964) The kinetic isotope effect in the bacterial reduction and oxidation of sulfur. *Geochimica et Cosmochimica Acta* **28**, 1893-1912.

National Energy Board (2000) *Canada's Oil Sands: A supply and market outlook to 2015*. National Energy Board, Calgary, AB.

Nielsen, H. (1974) Isotopic composition of the major contributers to the atmospheric sulfur. *Tellus* **26**, 213-221.

Nor, Y. and Tabatabai, M. (1977) Oxidation of elemental sulfur in soils. *Soil Science Society American Journal* **41**, 736-741.

Ober, J. (2006) USGS. Available at: http://minerals.usgs.gov/minerals/pubs/commodity/sulfur/index.html#mcs. Last accessed January, 2009.

Oblinger, J. and Koburger, J.L. (1975) Understanding and teaching the Most Probable Number Technique. *Journal of Milk and Food* **38** (9), 540-545.

OKC (2006) *As-built report for the Sulphur block research project: Performance monitoring instrumentation at Syncrude Mildred Lake Operations*. O'Kane Consultants Inc. Report No. 690/18-01.

OKC (2005) *Syncrude sulphur block project: Design rationale summary for five sulphur pilot blocks*. O'Kane Consultants Inc. Report No. 690/6-04.

Pepper, I. and Miller, R. (1978) Comparison of the oxidation of thiosulfate and elemental sulfur by two heterotrophic bacteria and Thiobacillus thiooxidans. *Soil Science* **126**, 9-14.

Pisz, J. (2008) Characterization of extremophilic sulfur oxidizing microbial communities inhabiting the sulfur blocks at Alberta's oil sands. Masters of Science thesis, University of Saskatchewan.

Pronk, J., Meulenberg, R., Hazeu, W., Bos, P. and Kuenen, J.G. (1990) Oxidation of reduced inorganic sulphur compounds by acidophilic thiobacilli. *FEMS Microbiology Reviews* **75**, 293-306.

Rees, C. and Holt, B. (1991) The isotopic analysis of sulphur and oxygen. In *Stable Isotopes: Natural and Anthropogenic Sulphur in the Environment*. SCOPE. John Wiley and Sons. pp 43-64.

Rye, R., Bethke, P. and Wasserman, M. (1992) The stable isotope geochemistry of acid sulfate alteration. *Economic Geology* **87**, 225-262.

Schaeffer, W., Holbert, P. and Umbreit, W. (1963) Attachment of Thiobacillus thiooxidans to sulfur crystals. *Journal of Bacteriol.* **85**, 137-140.

Schwarcz, H. and Cortecci, G. (1974) Isotopic analyses of spring and stream water sulfate from Italian Alpes and Apennines. *Chemical Geology* **13**, 285-294.

Seal, R.R. (2003) Stable-isotope geochemistry of mine waters and related solids. In *Environmental aspects of mine wastes*. Short course Series. Mineralogical Association of Canada. Vancouver, British Columbia. pp 303-334.

Sessions, A. and Hayes, J. (2005) Calculation of hydrogen isotopic fractionations in biogeochemical systems. *Geochimica et Cosmochimica Acta* **69** (3), 239-243.

Slaton, N., Norman, R. and Gilmour, J. (2001) Oxidation rates of commercial elemental sulfur products applied to an alkaline silt loam from Arkansas. *Soil Science Society of America* **65**, 239-243.

Sublette, K. and McInerney, M. (1994) Microbial oxidation of sulfides by Thiobacilli. In *Environmental geochemistry of sulfide oxidation*. American Chemical Society, Washington, DC. pp 68-78.

Suzuki, I., Lee, D., Mackay, B., Harahuc, L. and Key Oh, J. (1999) Effect of various ions, pH, and osmotic pressure on oxidation of elemental sulfur by Thiobacillus thiooxidans. *Applied and Environmental Microbiology* **65** (11), 5163-5168.

Suzuki, I. and Chan, C. (1992) Oxidation of elemental sulfur to sulfite by Thiobacillus thiooxidans cells. *Applied and Environmental Microbiology* **58** (11), 3767-3769.

Suzuki, I. and Takeuchi, T. (1990) Ferrous iron and sulfur oxidation and ferric iron reduction activities of Thiobacillus ferrooxidans are affected by growth on ferrous iron, sulfur or a sulfide ore. *Applied and Environmental Microbiology* **56** (6), 1620-1626.

Syncrude Canada Ltd. (2004) *Geoenvironmental characterization of a large sulphur block at Syncrude: results from the 2003 field investigation*.

Synrude Canada Ltd. website (2008) Syncrude Canada Ltd. Available at: http://www.syncrude.ca/users/folder.asp. Last accessed February, 2008.

Takakuwa, S. (1992) Biochemical aspects of microbial oxidation of inorganic sulfur compounds. In *Organic Sulfur Chemistry*. CRC Press, Bocaa Raton, FL. pp 1-43.

Takakuwa, S., Fujimori, T. and Iwasaki, H. (1979) Some properties of cell-sulfur adhesion in Thiobacillus thiooxidans. *Journal of Gen. Applied Microbiology* **25**, 21-29.

Taylor, B. and Wheeler, M. (1984a) Isotope composition of sulphate in acid mine drainage as measure of bacterial oxidation. *Nature* **308**, 538-541.

Taylor, B. and Wheeler, M. (1984b) Stable isotope geochemistry of acid mine drainage: experimental oxidation of pyrite. *Geochimica et Cosmochimica Acta* **48**, 2669-2678.

Teis, R. (1957) Isotopic composition of oxygen in natural sulphates. *Geochemistry* **156** (3), 257-263.

Thode, H. (1949) Sulphur isotopes in nature and the environment. In *Stable Isotopes: Natural and Anthropogenic Sulphur in the Environment*. SCOPE. John Wiley and Sons. pp 1-26.

Timilsina, G., Prince, J.P., Czamanski, D. and LeBlanc, N. (2005) *Impacts of crude oil production from Alberta Oil Sands on the Canadian economy*. Alberta Economic Development.

Toran, L. and Harris, R. (1989) Interpretation of sulfur and oxygen isotopes in biological and abiological sulfide oxidation. *Geochimica et Cosmochimica Acta* **53**, 2341-2348.

Van Everdingen, R., and Krouse, H.R. (1988) Interpretation of isotopic compositions of dissolved sulphates in acid mine drainage. *U.S. Bureau of Mines Circular 9183 Mine drainage and Surface Mine Reclamation*, 147-156.

Van Everdingen, R. and Krouse, H. (1985) Isotope composition of sulphates generated by bacteria and abiological oxidation. *Nature* **315**, 395-396.

Van Stempvoort, D. and Krouse, H. (1994) Controls of $\delta^{18}O$ in Sulfate: A review of experimental data and application to specific environments. *Environmental Geochemistry of Sulfide Oxidation*, 447-480.

Vogler, K. and Umbreit, W. (1941) The necessity for direct contact in sulfur oxidation by Thiobacillus thiooxidans. *Soil Science* **51**, 331-337.

Wainwright, M., Nevell, W. and Grayston, S. (1986) Effects of organic matter on sulphur oxidation in soil and influence of sulphur on soil nitrification. *Plant and Soil* **96**, 369-376.

Watkinson, J. (1989) Measurement of the oxidation rate of elemental sulphur in soil. *Australian Journal of Soil Res.* **27**, 365-375.

Watkinson, J. (1987) Oxidation rate of elemental sulfur particles with a wide range of sizes. *Australian Journal of Soil Res.* **31**, 67-72.

Yu, J., McGenity, T. and Coleman, M. (2001) Solution chemistry during the lag phase and exponential phase of pyrite oxidation by Thiobacillus ferrooxidans. *Chemical Geology* **175**, 307-317.

Zak, I., Sakai, H. and Kaplan, I. (1980) Factors controlling the 18O/16O and 34S/32S ratios of ocean sulfates from modern deep sea sediments. In *Isotope Marine Chemistry*. Rokakuho, Tokyo. pp 339-373.

APPENDIX A- Closed cell experiments

1. Explanation

At the onset of experimentation, the 97% labeled ^{18}O gas was removed from the tank using a gas tight syringe and injected into a gas impermeable tedlar® bag as described below. Upon O_2 measurement of the headspace gas after the completion of the experiment, the O_2 isotopic composition was only slightly above atmospheric conditions. It is understood that either a faulty gas valve regulator or an experimental design flaw caused mixed gas to equilibrate with atmospheric O_2, or the purchased canister of 97% ^{18}O gas was mislabeled or leaking.

The isotopic data in the MS-C and DI-C series do not show consistent $\delta^{18}O_{O2}$ value with time. Further, the $\delta^{18}O$ of the separate series should have ranged from -23.5 to +190‰. The actual range was -19 to -14.7‰. Therefore, calculating the oxygen source by varying the molecular O_2 of the system is not possible. However, the MS-C series was sampled for SO_4^{2-} production and pH changes which provide valuable duplicate data for reaction rates, activation energy, and temperature co-efficient calculations.

2. Experimental methods

The closed cell experiments were conducted using Erlenmeyer flasks (Exeter Scientific Glass model 522-00500) with an air-tight sampling valve inserted at the base of the flask and a filtering valve at the neck of the flask. Cells were assembled as described in chapter 3, and stoppered. A 3-way valve was attached to PVC tubing, and connected to the upper sampling port. A pinchcock was attached to the tubing between the glass port and the valve. All connections were sealed with Teflon tape. A 1L tedlar® bag filled near capacity with atmospheric air was injected with 50mL of the 97% ^{18}O gas and allowed to mix for 48 hours. Four additional gases were prepared by injecting 0, 10, 25, or 40mL of the mixed gas into 4 separate 10L tedlar® bags filled near capacity with atmospheric air to achieve $\delta^{18}O_{(O2)}$ values of -23.5, +95, +130, and +188‰, respectively.

After these gas mixtures were allowed to mix for 48 hours, the gas was injected into the closed flask through the lower valve and bubbled up through the water and S^0 mixture by attaching the bag to the valve using PVC tubing. To ensure that duplicate cells received identical gas mixtures, half of the volume from each bag was injected into each cell. Once the flasks were

flushed with the spiked gas, all ports were closed and the cell was brought to their respective temperature. Each flask was flushed with similarly spiked gas mixed the way described every 10 days.

3. Sampling and analysis

To ensure the accuracy of the mass balance calculation, periodic samples of the headspace in each cell were removed using evacuated glass gas sampling bottles, and analyzed for the $\delta^{18}O$ of O_2. Four mL of reaction solution were collected every 120 hours to measure the mass of SO_4^{2-} produced with time. Samples were analyzed for major anions by ion-exchange chromatography. A corresponding pH measurement of the reaction solution was determined using an Orion model 250A pH meter, after three point calibrations using 1.00, 4.00, and 7.00 buffers. The pH probe was inserted directly into the unfiltered sample removed from closed cells via the lower sampling port.

4. Results

Anion and pH results from the MS-C series can be found in section 5.1.1. Table A1 provides the measured $\delta^{18}O_{O2}$ gas samples collected throughout the duration of the experiment. The raw data output is corrected using frequent measurements of atmospheric air samples (Table A.2). No further work was conducted using the measured $\delta^{18}O_{(O2)}$ values of headspace air.

Table A.1: $\delta^{18}O$ (‰) values of molecular oxygen from headspace samples (±0.01)

	Hour	12°C	20°C	32°C
Flask 1	**120**	22.6	24.9	24.5
	744	25.6	25.3	28.9
	1248	25.8	25.2	28.1
	1752	25.3	24.2	n.d.
Flask 2	**120**	21.9	25.8	28.6
	744	27.1	23.8	28.1
	1248	23.8	24.0	25.6
	1752	25.6	22.5	27.8
Flask 3	**120**	21.2	24.0	26.5
	744	28.0	n.d.	27.9
	1248	26.6	24.3	27.8
	1752	29.0	25.6	27.2
Flask 4	**120**	26.9	25.3	27.7
	744	24.2	15.5	27.2
	1248	24.7	22.1	29.0
	1752	25.8	26.7	28.6
Flask 5	**120**	27.2	27.8	28.7
	744	28.2	25.1	29.8
	1248	27.9	25.3	29.6
	1752	29.7	26.5	30.2
Flask 6	**120**	29.4	26.46	28.75
	744	28.2	24.36	30.08
	1248	30.9	24.59	27.30
	1752	30.9	25.78	27.52

n.d. Not determined due to error in sampling or analysis.

APPENDIX B: Supplementary data for S^0 oxidation experiments

n.d.- Not determined
Bold values indicate contamination- not used in analysis
Average of SO_4^{2-} concentration does not include control flasks

Table 1B: pH changes of individual cells in the MS-A series at 32°C

Hour	Flask 1	Flask 2	Flask 3	Flask 4	Flask 5	Flask 6	Flask 7	Flask 8	Control	Average	Stdev
0	4.5	4.5	4.5	4.5	4.5	4.5	4.5	4.5	4.5	4.5	0.00
72	3.1	3.7	3.8	3.7	3.81	3.7	4.1	3.9	4.8	3.7	0.27
144	2.3	2.4	2.8	2.8	2.71	2.9	2.6	2.6	4.7	2.8	0.20
216	2.00	2.0	2.2	2.1	2.11	2.2	2.1	2.0	4.8	2.2	0.07
312	1.8	1.8	1.9	1.9	1.83	1.9	1.8	1.8	4.8	1.9	0.04
384	1.7	1.7	1.7	1.7	1.67	1.7	1.7	1.7	5.0	1.7	0.03
480	1.5	1.5	1.6	1.5	1.5	1.5	1.5	1.5	4.9	1.5	0.02
528	1.4	1.4	1.5	1.5	1.45	1.5	1.5	1.5	4.9	1.5	0.02
576	1.5	1.5	1.5	1.5	1.48	1.5	1.5	1.5	4.8	1.5	0.02
672	1.5	1.5	1.5	1.5	1.43	1.4	1.4	1.4	4.9	1.4	0.03
792	1.2	1.3	1.3	1.2	1.24	1.3	1.3	1.3	5.1	1.3	0.01
912	1.2	1.2	1.2	1.2	1.14	1.1	1.1	1.1	n.d.	1.1	0.01
1032	1.1	1.1	1.1	1.1	1.13	1.1	1.1	1.1	5.1	1.1	0.01
1152	1.2	1.2	1.2	1.2	1.14	1.2	1.2	1.2	5.1	1.2	0.02
1392	1.1	1.1	1.1	1.1	0.98	1.1	1.1	1.1	5	1.1	0.05
1584	1.1	1.0	1.0	1.1	0.95	1.0	0.9	1.0	4.8	1.0	0.05
1752	0.8	0.8	0.7	0.8	0.75	0.7	0.8	0.8	4.8	0.8	0.02
2376	0.8	0.8	0.7	0.7	0.7	0.7	0.7	0.8	4.5	0.7	0.03
3072	0.6	0.7	0.5	0.6	0.58	0.6	0.6	0.6	4.7	0.6	0.05

Table 2B: pH changes of individual cells in the MS-A series at 20°C

Hour	Flask 1	Flask 2	Flask 3	Flask 4	Flask 5	Flask 6	Flask 7	Flask 8	Control	Average	Stdev
0	4.5	4.5	4.5	4.5	4.5	4.5	4.5	4.5	4.5	4.5	0.00
72	3.6	3.9	3.7	3.9	3.9	4.0	3.7	3.8	4.8	3.8	0.14
144	3.0	3.4	3.4	3.4	3.3	3.3	3.0	3.0	4.4	3.3	0.18
216	2.3	2.5	2.5	2.5	2.5	2.5	2.4	2.4	4.4	2.5	0.06
312	2.1	2.1	2.1	2.1	2.1	2.1	2.1	2.1	4.2	2.1	0.03
384	1.9	2.0	1.9	1.9	2.0	2.0	1.9	1.9	4.8	1.9	0.02
480	1.8	1.8	1.8	1.8	1.8	1.8	1.8	1.8	4.6	1.8	0.02
528	1.7	1.8	1.7	1.7	1.7	1.7	1.7	1.7	4.3	1.7	0.03
576	1.7	1.8	1.8	1.8	1.8	1.8	1.7	1.7	4.4	1.8	0.02
672	1.6	1.6	1.6	1.6	1.6	1.6	1.6	1.6	4	1.6	0.01
792	1.6	1.5	1.5	1.5	1.5	1.5	1.5	1.5	4.2	1.5	0.02
912	1.5	1.4	1.4	1.4	1.4	1.4	1.4	1.4	4.2	1.4	0.03
1032	1.4	1.4	1.4	1.4	1.4	1.4	1.4	1.4	4.2	1.4	0.03
1152	1.5	1.5	1.4	1.4	1.4	1.4	1.4	1.4	4.2	1.4	0.04
1392	1.4	1.4	1.3	1.3	1.3	1.3	1.3	1.3	4.3	1.3	0.04
1584	1.3	1.3	1.2	1.3	1.2	1.2	1.2	1.2	4.3	1.2	0.05
1752	1.2	1.1	1.1	1.1	1.2	1.1	1.1	1.0	4.2	1.1	0.06
2376	1.0	0.9	0.9	0.9	0.9	0.9	0.9	0.9	4.1	0.9	0.03
3072	0.9	0.9	0.8	0.8	0.8	0.8	0.8	0.8	3.9	0.8	0.05

Table 3B: pH changes of individual cells in the MS-A series at 12°C

Hour	Flask 1	Flask 2	Flask 3	Flask 4	Flask 5	Flask 6	Flask 7	Flask 8	Control	Average	Stdev
0	4.5	4.5	4.5	4.5	4.5	4.5	4.5	4.5	4.5	4.5	0.00
72	4.2	4.2	3.8	4.2	4.2	4.2	4.1	3.9	4.5	4.1	0.16
144	4.2	4.1	3.8	4.2	4.2	4.2	4.0	3.9	4.6	4.1	0.15
216	4.1	4.0	3.7	4.1	4.1	4.1	3.9	3.8	4.6	4.0	0.16
312	3.8	3.6	3.3	3.7	3.7	3.7	3.6	3.4	4.3	3.6	0.15
384	2.9	2.8	2.7	2.8	2.8	2.8	2.8	2.7	4.2	2.9	0.08
480	2.4	2.3	2.2	2.3	2.3	2.3	2.3	2.3	4.1	2.3	0.06
528	2.2	2.1	2.1	2.2	2.2	2.2	2.1	2.1	4.3	2.2	0.04
576	2.1	2.0	2.0	2.1	2.1	2.1	2.1	2.0	4.2	2.1	0.04
672	1.9	1.9	1.8	1.9	1.9	1.9	1.8	1.8	4.3	1.9	0.03
792	1.7	1.8	1.7	1.7	1.8	1.7	1.7	1.7	4.3	1.7	0.03
912	1.6	1.6	1.6	1.6	1.6	1.6	1.6	1.5	4.3	1.6	0.03
1032	1.5	1.6	1.5	1.6	1.5	1.5	1.5	1.5	4.3	1.5	0.03
1152	1.5	1.5	1.5	1.5	1.5	1.5	1.5	1.5	4.2	1.5	0.03
1392	1.4	1.4	1.4	1.3	1.4	1.4	1.4	1.4	4.1	1.4	0.03
1584	1.3	1.3	1.2	1.2	1.3	1.4	1.3	1.2	4.3	1.3	0.06
1752	1.4	1.3	1.4	1.4	1.6	1.3	1.2	1.2	4.2	1.3	0.08
2400	1.1	1.1	1.0	1.0	1.0	1.0	1.0	0.9	4.2	1.0	0.03
3096	1.0	1.0	1.0	0.9	1.0	1.0	1.0	1.0	3.7	1.0	0.02

Table 4B: pH changes of individual cells in the MS-A series at 6°C

Hour	Flask 1	Flask 2	Flask 3	Flask 4	Flask 5	Flask 6	Flask 7	Flask 8	Control	Average	Stdev
0	4.5	4.5	4.5	4.5	4.5	4.5	4.5	4.5	4.5	4.5	0.00
144	4.3	4.1	4.2	3.7	4.0	4.2	3.9	3.9	4.6	4.0	0.21
312	4.4	4.2	4.2	3.7	4.0	4.2	3.9	3.9	4.6	4.1	0.23
384	4.4	4.1	4.2	3.7	4.1	4.3	3.9	3.9	4.6	4.1	0.23
480	4.2	4.0	4.3	3.7	4.0	4.2	3.8	3.8	4.5	4.0	0.20
576	4.2	3.9	4.0	3.5	3.9	4.1	3.9	3.7	4.6	3.9	0.23
672	4.0	3.9	3.9	3.3	3.8	4.1	3.7	3.7	4.2	3.8	0.23
912	4.2	3.9	4.0	3.8	3.8	4.0	3.7	3.7	4.3	3.9	0.18
1032	4.1	3.8	3.9	3.7	4.0	3.7	3.6	3.6	4.3	3.8	0.17
1584	3.3	3.0	3.7	1.8	3.1	3.6	2.5	2.6	4.3	2.9	0.58
2328	1.5	1.5	1.6	1.3	1.3	1.5	1.2	1.2	4.4	1.4	0.15
3024	1.5	1.5	1.5	1.3	1.6	1.6	1.6	1.5	3.8	1.5	0.09

Table 5B: pH changes of individual cells in the MS-C series at 32°C

Hour	Flask 1	Flask 2	Flask 3	Flask 4	Flask 5	Flask 6	Control	Average	Stdev
0	5.5	5.5	5.5	5.5	5.5	5.5	5.5	5.5	0.00
120	2.7	3.3	3.2	3.1	2.9	3.4	5.7	3.1	0.28
240	1.7	1.8	1.7	1.9	1.8	1.9	5.7	1.8	0.09
408	2.0	1.9	1.8	1.9	1.8	1.8	5.7	1.9	0.06
528	1.7	1.6	1.6	2.0	1.9	1.6	5.5	1.7	0.18
648	1.7	1.7	1.7	1.7	1.7	1.5	5.5	1.7	0.04
768	1.4	1.4	1.5	1.7	1.6	1.6	5.6	1.5	0.12
888	1.6	1.4	1.5	1.6	1.4	1.6	5.7	1.5	0.12
1008	1.6	1.3	1.4	1.6	1.3	1.6	5.6	1.5	0.13
1128	1.3	1.3	1.4	1.6	1.3	1.6	5.6	1.4	0.15
1248	1.2	1.2	1.2	1.3	1.2	1.3	5.4	1.2	0.06
1368	1.1	1.2	1.1	1.2	1.1	1.3	5.2	1.2	0.07
1488	1.1	1.1	1.1	1.2	1.1	1.2	5.1	1.1	0.03
1608	1.1	1.1	1.1	1.1	1.0	1.1	5.3	1.1	0.02
1752	1.1	1.1	1.1	1.0	1.0	1.0	5.4	1.0	0.02

Table 6B: pH changes of individual cells in the MS-C series at 20°C

Hour	Flask 1	Flask 2	Flask 3	Flask 4	Flask 5	Flask 6	Control	Average	Stdev
0	5.5	5.5	5.5	5.5	5.5	5.5	5.5	5.5	0.00
120	5.1	5.1	4.9	4.9	5.1	5.1	5.5	5.1	0.10
240	2.7	2.7	2.8	2.7	2.8	2.8	5.5	2.7	0.06
360	2.5	2.5	2.5	2.5	2.5	2.5	5.6	2.5	0.03
504	2.1	2.0	2.1	2.1	2.1	2.0	5.6	2.1	0.05
624	1.9	1.8	1.8	1.8	1.8	2.0	5.4	1.8	0.10
744	1.9	1.9	1.8	2.0	1.9	1.9	5.3	1.9	0.05
864	1.8	1.9	1.7	1.7	1.5	1.5	5.4	1.7	0.16
984	1.6	1.6	1.6	1.8	1.8	1.6	5.4	1.7	0.13
1104	1.5	1.5	1.5	1.7	1.8	1.5	5.5	1.6	0.13
1224	1.5	1.5	1.7	1.4	1.5	1.4	5.4	1.5	0.10
1344	1.4	1.3	1.4	1.3	1.4	1.4	5.5	1.4	0.05
1464	1.4	1.3	1.4	1.3	1.4	1.3	n.d	1.3	0.04
1584	1.3	1.3	1.3	1.3	1.3	1.3	n.d.	1.3	0.03
1752	1.3	1.2	1.2	1.2	1.3	1.3	5.3	1.3	0.04

Table 7B: pH changes of individual cells in the MS-C series at 12°C

Hour	Flask 1	Flask 2	Flask 3	Flask 4	Flask 5	Flask 6	Control	Average	Stdev
0	5.5	5.5	5.5	5.5	5.5	5.5	5.5	5.5	0.00
120	4.3	4.5	4.2	4.4	4.4	4.3	5.5	4.3	0.10
264	3.1	3.5	2.9	3.3	3.3	3.0	5.5	3.2	0.20
360	3.3	3.7	3.7	3.5	3.4	4.0	5.7	3.6	0.26
528	2.5	1.7	2.5	2.5	2.5	3.0	5.8	2.4	0.43
648	1.8	1.8	2.1	2.1	2.2	2.3	5.8	2.0	0.21
768	1.9	2.1	2.0	2.0	2.3	2.2	5.5	2.1	0.14
888	n.d.	1.7	1.7	1.7	1.7	1.8	5.5	1.7	0.07
1008	n.d.	1.7	1.7	1.7	1.7	1.7	5.6	1.7	0.02
1128	n.d.	1.6	1.6	1.6	1.6	1.6	5.7	1.6	0.00
1248	n.d.	1.6	1.5	1.6	1.7	1.7	5.5	1.6	0.06
1320	n.d.	1.6	1.5	1.6	1.6	1.6	5.5	1.6	0.04
1488	n.d.	1.5	1.5	1.4	1.5	1.6	5.4	1.5	0.06
1608	n.d.	1.3	1.3	1.4	1.5	1.4	5.5	1.4	0.07
1752	0.9	1.2	1.2	1.3	1.4	1.4	5.4	1.2	0.19

Table 8B: pH changes of individual cells in the DI-A series at 32°C

Hour	Flask 1	Flask 2	Flask 3	Flask 4	Flask 5	Flask 6	Flask 7	Flask 8	Control	Average	Stdev
0	5	5	5	5	5	5	5	5	5	5.0	0.00
48	4.7	4.7	4.7	4.7	4.7	4.7	4.7	4.7	5.1	4.7	0.00
96	4.0	4.2	4.0	3.6	3.6	3.6	4	3.6	4.9	3.8	0.25
144	3.2	3.8	3.1	2.7	2.8	2.9	3.5	2.9	5.0	3.1	0.36
192	2.5	3.3	2.4	2.2	2.3	2.3	2.3	2.5	4.9	2.5	0.36
216	2.2	2.5	2.1	2.0	2.1	2.0	2.0	2.3	4.9	2.2	0.16
312	1.8	1.7	1.7	1.7	1.8	1.8	1.8	1.8	4.8	1.8	0.04
360	1.9	1.8	1.8	1.7	1.7	1.7	1.8	1.8	n.d.	1.8	0.06
408	1.7	1.7	1.6	1.6	1.5	1.6	1.7	1.7	4.7	1.6	0.07
480	1.7	1.6	1.5	1.4	1.6	1.5	1.5	1.6	4.6	1.6	0.07
528	1.7	1.6	1.6	1.5	1.6	1.6	1.5	1.6	4.5	1.6	0.06
576	1.6	1.6	1.5	1.4	1.6	1.5	1.5	1.5	4.3	1.5	0.06
672	1.6	1.5	1.5	1.4	1.5	1.5	1.5	1.5	4.2	1.5	0.05
768	1.6	1.5	1.4	1.4	1.5	1.4	1.4	1.5	4.2	1.5	0.07
1008	1.4	1.4	1.3	1.3	1.4	1.4	1.3	1.4	4.2	1.4	0.04
1176	1.4	1.3	1.2	1.2	1.3	1.3	1.3	1.4	3.9	1.3	0.06
1296	1.2	1.2	1.1	1.1	1.2	1.1	1.1	1.2	4.0	1.1	0.05
1416	1.3	1.3	1.2	1.1	1.2	1.2	1.2	1.2	4.2	1.2	0.05
1536	1.1	1.1	1.0	0.9	1.0	1.0	1.0	1.0	4.3	1.0	0.05
1656	1.0	1.0	1.0	0.8	0.9	0.9	0.9	1.0	4.3	1.0	0.07
1776	1.0	1.0	1.0	0.9	0.9	0.9	0.9	1.0	4.3	0.9	0.07
1896	1.0	0.9	0.9	0.9	0.9	0.8	0.9	1.0	4.3	0.9	0.06
1992	1.0	0.9	0.9	1.0	0.9	0.8	0.9	0.9	4.2	0.9	0.06
2208	0.9	0.9	0.8	1.0	0.9	0.8	0.9	0.9	4.3	0.9	0.10

Table 9B: pH changes of individual cells in the DI-A series at 20°C

Hour	Flask 1	Flask 2	Flask 3	Flask 4	Flask 5	Flask 6	Flask 7	Flask 8	Control	Average	Stdev
0	5.5	5.5	5.5	5.5	5.5	5.5	5.6	5.5	5.5	5.5	0.04
120	5.0	5.1	5.1	5.1	5.0	5.1	5.0	5.0	4.8	5.0	0.06
168	5.0	5.0	4.9	5.0	4.9	5.0	4.7	4.7	4.8	4.9	0.12
216	4.7	4.8	4.8	4.8	4.7	4.8	4.5	4.5	4.7	4.7	0.13
288	4.6	4.7	4.6	4.6	4.6	4.7	4.5	4.5	4.7	4.6	0.09
456	4.1	4.3	4.1	4.2	3.3	4.4	4.1	4.2	4.6	4.1	0.35
504	3.7	4.2	3.8	4.0	3.1	4.2	4.1	4.2	4.6	3.9	0.36
624	2.5	2.7	2.4	2.6	2.3	3.3	2.8	3.9	4.5	2.8	0.53
672	2.3	2.4	2.3	2.4	2.3	3.1	2.5	3.6	4.5	2.6	0.49
720	2.2	2.3	2.2	2.3	2.2	2.7	2.3	2.9	4.4	2.4	0.28
840	2.1	2.1	2.1	2.1	2.1	2.3	2.1	2.3	4.3	2.2	0.08
888	2.0	2.0	2.0	2.0	2.0	2.2	2.1	2.2	4.3	2.1	0.07
960	2.0	2.0	2.0	2.1	2.0	2.2	2.0	2.1	4.3	2.1	0.05
1056	2.0	1.9	2.0	2.1	2.0	2.1	1.9	2.1	4.3	2.0	0.05
1152	2.1	2.0	2.0	2.1	2.1	2.1	2.0	2.1	4.4	2.1	0.03
1224	1.9	1.9	1.9	2.0	2.0	2.0	1.9	2.0	4.3	1.9	0.03
1296	2.0	2.0	2.0	2.0	2.0	2.0	1.9	2.0	4.2	2.0	0.04
1368	1.9	1.9	1.9	1.9	1.9	1.9	1.8	1.9	4.2	1.9	0.04
1464	2.0	1.9	2.0	2.0	1.9	1.9	1.9	1.9	4.2	2.0	0.05
1536	2.0	1.9	1.9	2.0	1.9	1.9	1.8	1.9	4.2	1.9	0.05
1680	1.9	1.9	1.9	1.9	1.9	1.9	1.9	1.9	4.2	1.9	0.03
1728	1.9	1.9	2.0	2.0	1.9	1.9	1.9	1.9	4.1	1.9	0.05
1824	1.9	1.8	1.9	1.8	1.8	1.8	1.8	1.8	4.0	1.8	0.04
2064	1.8	1.8	1.8	1.8	1.8	1.7	1.7	1.7	3.9	1.8	0.07
2184	1.9	1.8	1.9	1.9	1.8	1.8	1.7	1.8	4.0	1.8	0.06
2880	1.8	1.8	1.9	1.9	1.8	1.8	1.7	1.7	3.7	1.8	0.07
3528	1.6	1.7	1.7	1.7	1.6	1.6	1.5	1.6	3.5	1.6	0.08
4248	1.6	1.6	1.7	1.7	1.6	1.6	1.6	1.8	n.d.	1.7	0.07

Table 10B: pH changes of individual cells in the DI-A series at 12°C

Hour	Flask 1	Flask 2	Flask 3	Flask 4	Flask 5	Flask 6	Flask 7	Flask 8	Control	Average	Stdev
0	5.5	5.5	5.5	5.5	5.5	5.5	5.6	5.6	5.6	5.5	0.05
120	5.3	5.4	5.4	5.4	5.4	5.4	5.4	5.3	5.5	5.4	0.03
168	5.4	5.4	5.3	5.4	5.3	5.3	5.4	5.3	5.5	5.4	0.05
240	5.3	5.3	5.2	5.3	5.2	5.2	5.1	5.1	5.4	5.2	0.08
456	4.7	4.7	4.7	4.7	4.7	4.6	4.7	4.6	5.2	4.7	0.05
504	4.6	4.6	4.5	4.6	4.6	4.4	4.5	4.5	5.2	4.5	0.08
624	4.3	4.4	4.2	4.2	4.5	4.2	4.4	4.3	5.2	4.3	0.11
672	4.2	4.3	4.0	4.1	4.4	4.2	4.3	4.2	5.2	4.2	0.14
792	3.9	4.0	3.3	3.4	4.1	3.9	4.0	3.8	5.2	3.8	0.27
840	3.7	3.9	3.2	3.3	3.9	3.7	3.8	3.6	5.1	3.6	0.26
912	3.7	3.7	2.6	2.9	3.7	3.4	3.8	3.1	5.0	3.4	0.44
984	3.6	3.7	2.5	2.7	3.7	3.2	3.6	2.8	5.0	3.2	0.50
1080	3.0	3.4	2.3	2.4	3.6	2.5	3.3	2.4	5.0	2.9	0.49
1152	2.5	2.9	2.3	2.3	3.1	2.3	2.8	2.3	5.2	2.6	0.32
1224	2.4	2.5	2.2	2.2	2.6	2.2	2.4	2.2	4.9	2.3	0.16
1296	2.2	2.3	2.1	2.1	2.4	2.1	2.2	2.1	4.8	2.2	0.11
1392	2.2	2.2	2.1	2.1	2.3	2.1	2.2	2.0	4.8	2.2	0.07
1464	2.1	2.1	2.0	2.0	2.2	2.0	2.1	1.9	4.7	2.1	0.07
1560	2.1	2.1	2.0	1.9	2.1	2.0	2.1	1.9	4.9	2.0	0.06
1608	2.0	2.0	2.0	2.0	2.2	2.0	2.1	2.0	4.9	2.0	0.06
1656	2.1	2.1	2.0	2.0	2.1	2.1	2.1	2.0	4.6	2.1	0.05
1752	1.9	1.9	1.9	1.9	2.0	1.9	1.9	1.9	4.4	1.9	0.05
1872	1.9	1.9	1.9	1.9	2.0	1.9	1.9	1.8	4.4	1.9	0.04
1992	1.9	1.9	1.9	1.9	2.0	1.9	1.9	1.8	4.7	1.9	0.06
2112	2.0	1.9	1.8	1.9	1.9	1.9	1.9	1.9	4.7	1.9	0.04
2808	1.6	1.6	1.7	1.6	1.8	1.7	1.8	1.7	4.5	1.7	0.07
3456	1.4	1.5	1.5	1.4	1.4	1.4	1.5	1.4	3.8	1.4	0.05

Table 11B: SO_4^{2-} concentration (mM) changes of individual cells in MS-A (32°C)

Hour	Flask 1	Flask 2	Flask 3	Flask 4	Flask 5	Flask 6	Flask 7	Flask 8	Control	Average	Stdev
0	n.d.	0.8	0.8	0.8	0.8	0.8	0.8	0.8	0.8	0.8	0
144	3.8	2.6	1.8	1.7	2.1	0.9	2.4	1.9	n.d.	2.2	0.85
312	n.d.	9.9	n.d.	8.1	n.d.	5.9	n.d.	7.5	0.9	7.8	1.65
384	n.d.	13.4	n.d.	11.4	n.d.	8.2	n.d.	12.0	n.d.	11.3	2.19
480	23.4	21.3	19.1	12.9	21.4	13.1	19.1	15.7	0.9	18.3	3.94
576	n.d.	30.9	n.d.	20.6	n.d.	20.3	n.d.	25.2	n.d.	24.3	4.95
672	42.9	35.7	54.6	23.1	45.7	26.0	25.4	31.0	1.2	35.5	11.29
912	n.d.	51.9	n.d.	51.9	n.d.	49.4	n.d.	51.7	1.3	51.2	1.21
1152	89.4	71.7	84.3	71.2	58.0	70.4	61.6	69.7	1.2	72.0	10.46
1584	84.4	115.9	79.6	99.3	81.8	83.3	74.1	98.0	1.4	89.6	13.76
3048	333.9	263.8	617.0	367.4	406.4	492.6	291.5	302.5	n.d.	384.4	118.95

Table 12B: SO_4^{2-} concentration (mM) changes of individual cells in MS-A (21°C)

Hour	Flask 1	Flask 2	Flask 3	Flask 4	Flask 5	Flask 6	Flask 7	Flask 8	Control	Average	Stdev
0	0.8	0.8	0.8	0.8	0.8	0.8	0.8	0.8	0.8	0.8	0.00
144	1.2	1.0	1.1	1.1	1.1	1.1	1.3	1.2	n.d.	1.1	0.11
312	n.d	4.4	n.d	4.9	n.d	4.8	n.d	4.4	0.9	4.6	0.23
384	n.d	6.6	n.d	6.7	n.d	5.9	n.d	6.0	n.d.	6.3	0.39
480	9.8	8.9	9.4	9.8	8.6	8.1	9.4	8.7	1.1	9.1	0.62
576	n.d	12.1	n.d	12.4	n.d	11.2	n.d	11.7	n.d.	11.9	0.53
672	16.5	15.0	17.4	15.3	16.2	13.6	19.0	14.8	1.3	15.9	1.70
912	n.d	23.3	n.d	23.4	n.d	22.9	n.d	24.6	1.3	23.6	0.72
1152	33.6	32.8	39.9	40.6	35.6	28.8	42.3	36.0	1.5	36.2	4.54
1584	42.9	47.6	59.1	52.4	45.0	46.9	53.8	63.5	1.5	51.4	7.16
3024	229.7	208.3	323.8	339.2	308.6	195.2	292.0	224.1	n.d.	265.1	56.80

Table 13B: SO_4^{2-} concentration (mM) changes of individual cells in MS-A (12°C)

Hour	Flask 1	Flask 2	Flask 3	Flask 4	Flask 5	Flask 6	Flask 7	Flask 8	Control	Average	Stdev
0	0.8	0.8	0.8	0.8	0.8	0.8	0.8	0.8	0.8	0.8	0.00
144	1.1	0.8	1.1	0.8	1.2	0.8	1.2	0.9	1.1	1.0	0.17
312	n.d.	0.9	n.d.	0.9	n.d.	0.9	n.d.	0.9	n.d.	0.9	0.03
384	n.d.	1.5	n.d.	1.4	n.d.	1.5	n.d.	1.7	n.d.	1.5	0.14
480	3.3	3.1	4.1	2.8	3.45	3.1	3.8	3.3	1.3	3.4	0.43
576	n.d.	4.9	n.d.	4.8	n.d.	4.6	n.d.	5.7	n.d.	5.0	0.48
672	9.2	6.4	10.8	7.0	8.8	7.4	9.8	8.1	1.3	8.4	1.49
912	n.d.	14.8	n.d.	23.4	n.d.	22.9	n.d.	24.6	n.d.	21.4	4.45
1152	32.8	27.1	35.6	28.3	28.1	27.7	31.9	31.8	1.3	30.4	3.04
1584	46.1	50.2	65.4	57.6	44.9	42.2	50.4	61.5	1.4	52.3	8.33
3024	156.9	158.6	190.1	176.3	130.2	119.1	95.4	190.6	n.d.	152.2	34.57

Table 14B: SO_4^{2-} concentration (mM) changes of individual cells in MS-A (6°C)

Hour	Flask 1	Flask 2	Flask 3	Flask 4	Flask 5	Flask 6	Flask 7	Flask 8	Control	Average	stdev
0	0.8	0.8	0.8	0.8	0.8	0.8	0.8	0.8	0.8	0.8	0
144	1.3	n.d.	1.2	n.d	1.3	n.d.	1.4	n.d.	1.3	1.3	0.06
480	1.1	1.1	1.1	1.2	1.2	1.1	1.3	1.2	1.2	1.2	0.07
672	1.8	1.1	1.2	1.2	1.2	1.1	1.2	1.2	1.2	1.2	0.22
1152	1.3	n.d.	1.5	n.d	1.6	n.d.	1.2	n.d.	1.3	1.4	0.18
1584	1.5	1.4	1.5	11.4	1.7	1.3	3.1	2.5	1.7	3.0	3.24
3024	n.d.	n.d.	21.7	49.5	28.5	16.9	23.3	n.d.	1.9	28.0	15.54

Table 15B: SO_4^{2-} concentration (mM) changes of individual cells in the MS-C series at 32°C

Hour	Flask 1	Flask 2	Flask 3	Flask 4	Flask 5	Flask 6	Control	Average	Stdev
0	0.8	0.8	0.8	0.8	0.8	0.8	0.8	0.8	0
240	5.9	6.2	6.6	5.1	6.3	6.2	1.0	6.1	0.46
648	15.7	n.d.	18.0	n.d.	18.9	n.d.	1.1	17.5	1.65
1128	48.6	53.6	48.0	55.1	49.9	58.3	1.1	52.3	4.08
1488	83.3	n.d.	82.3	n.d.	91.5	n.d.	1.3	85.7	5.03
1752	106.1	101.5	89.2	101.7	117.1	109.7	1.3	104.2	9.35

Table 16B: SO_4^{2-} concentration (mM) changes of individual cells in the MS-C series at 21°C

Hour	Flask 1	Flask 2	Flask 3	Flask 4	Flask 5	Flask 6	Control	Average	stdev
0	0.8	0.8	0.8	0.8	0.8	0.8	0.8	0.8	0
240	1.8	2.2	1.8	1.9	1.8	1.9	1.1	1.9	0.15
624	n.d.	8.9	n.d.	9.6	n.d.	9.6	1.2	9.4	0.37
984	24.2	24.7	23.8	26.0	21.8	24.3	1.3	24.1	1.38
1344	n.d.	28.8	n.d.	43.8	n.d	38.6	1.3	37.0	7.60
1704	50.9	58.8	58.3	73.2	51.6	58.4	1.4	58.5	8.01

Table 17B: SO_4^{2-} concentration (mM) changes of individual cells in the MS-C series at 12°C

Hour	Flask 1	Flask 2	Flask 3	Flask 4	Flask 5	Flask 6	Control	Average	Stdev
0	0.8	0.8	0.8	0.8	0.8	0.8	0.8	1.0	0.00
264	1.5	1.2	1.7	1.3	1.3	1.5	1.0	1.4	0.18
648	7.7	n.d.	4.1	n.d.	3.9	n.d	1.0	5.2	2.14
1008	11.8	11.9	9.9	14.1	13.3	11.0	1.0	12.0	1.51
1320	25.1	25.1	23.8	n.d.	18.3	n.d.	1.1	23.1	3.20
1752	46.2	38.1	37.0	37.0	31.4	25.6	1.2	35.9	6.94

Table 18B: SO_4^{2-} concentration (mM) changes of individual cells in the DI-A series at 32°C

Hour	Flask 1	Flask 2	Flask 3	Flask 4	Flask 5	Flask 6	Flask 7	Flask 8	Control	Average	Stdev
0	0	0	0	0	0	0	0	0	0	0	0
168	n.d.	0.6	n.d.	3.2	n.d.	2.4	n.d.	0.7	0.00	1.7	1.26
216	n.d.	1.4	4.1	5.5	4.3	4.8	4.4	3.5	n.d.	4.0	1.31
312	n.d.	7.1	n.d.	10.0	n.d.	8.1	n.d.	7.3	0.00	8.1	1.32
480	n.d.	13.9	n.d.	20.8	n.d.	15.5	n.d.	13.5	n.d.	15.9	3.35
768	25.1	31.6	32.6	39.9	26.1	32.9	33.2	26.6	0.01	40.00	4.92
1008	n.d.	45.8	n.d.	64.7	n.d.	53.8	n.d.	37.3	n.d.	50.4	11.68
1296	55.0	61.4	72.6	83.7	66.2	72.2	48.5	44.9	0.03	63.1	13.19
1584	n.d.	95.0	n.d.	136.3	n.d.	105.0	n.d.	75.6	n.d.	102.9	25.35
1992	131.4	133.8	146.1	249.7	158.1	162.3	108.3	109.8	0.29	149.9	44.94

Table 19: SO_4^{2-} concenStration (mM) changes of individual cells in the DI-A series at 20°C

Hour	Flask 1	Flask 2	Flask 3	Flask 4	Flask 5	Flask 6	Flask 7	Flask 8	Control	Average	Stdev
0	0	0	0	0	0	0	0	0	0	0	0
288	n.d.	0.1	n.d.	0.1	n.d.	0.05	n.d.	0.04	n.d	0.05	0.02
504	n.d.	0.1	n.d.	0.1	n.d.	0.06	n.d.	0.05	0.01	0.06	0.02
672	2.2	2.5	2.4	2.6	2.71	0.42	1.37	0.13	n.d.	1.8	1.12
840	n.d.	5.6	n.d.	5.2	n.d.	3.29	n.d.	3.13	0.01	4.3	2.21
1056	4.3	8.0	4.8	6.8	4.76	5.86	5.68	5.87	n.d.	5.8	2.61
1152	n.d.	8.6	n.d.	7.1	n.d.	6.91	n.d.	7.13	0.02	7.4	3.39
1296	n.d.	6.0	n.d.	5.1	n.d.	5.19	n.d.	6.00	n.d.	5.6	2.52
1464	n.d.	6.3	n.d.	5.4	n.d.	6.18	n.d.	6.57	n.d.	6.1	2.76
1632	6.7	6.7	5.6	5.4	6.57	6.21	8.68	6.61	0.03	6.6	2.37
1728	n.d.	6.8	n.d.	5.6	n.d.	6.88	n.d.	6.84	0.02	6.5	2.96
2064	7.4	7.8	6.6	6.1	7.95	7.93	9.11	7.59	0.3	7.56	3.09

Table 20B: SO_4^{2-} concenStration (mM) changes of individual cells in the DI-A series at 12°C

Hour	Flask 1	Flask 2	Flask 3	Flask 4	Flask 5	Flask 6	Flask 7	Flask 8	Control	Average	Stdev
0	0	0	0	0	0	0	0	0	0	0	0
672	0.1	0.1	0.1	0.1	0.1	0.1	0.1	0.1	n.d.	0.1	0.01
840	n.d.	0.1	n.d.	0.2	n.d.	0.1	n.d.	0.1	n.d.	0.1	0.06
984	n.d.	0.1	n.d.	1.1	n.d.	0.3	n.d.	0.8	n.d.	0.6	0.47
1080	0.4	0.2	2.3	2.5	0.3	1.7	0.3	2.5	0.1	1.3	1.08
1224	n.d.	1.4	n.d.	3.1	n.d.	2.8	n.d.	3.4	n.d.	2.7	0.89
1392	n.d.	2.8	n.d.	4.1	n.d.	4.0	n.d.	4.5	n.d.	3.9	0.73
1560	4.2	4.1	4.5	4.7	4.1	4.8	4.1	5.1	n.d.	4.5	0.39
1656	n.d.	4.2	n.d.	5.5	n.d.	5.0	n.d.	5.5	0.1	5.0	0.59
1992	10.7	8.7	6.9	6.7	4.7	6.6	4.9	6.4	0.2	6.9	1.96

Table 21B: $\delta^{18}O_{(H2O)}$ and $\delta^{18}O_{(SO4)}$ of series MS-A

Flask	$\delta^{18}O_{(H2O)}$ (‰)	$\delta^{18}O_{(SO4)}$ (‰)			
		32°C	**20°C**	**12°C**	**6°C**
1	960	916	**800**	924	808
2	960	944	906	924	797
3	536	518	510	**480**	**435**
4	536	523	501	514	466
5	239	220	228	222	188
6	239	224	219	208	186
7	-19.0	-14	-18	-18	-18
8	-19.0	-18	-18	-19	-17

Table 22B: $\delta^{18}O_{(H2O)}$ and $\delta^{18}O_{(SO4)}$ of series DI-A

Flask	$\delta^{18}O_{(H2O)}$ (‰)	$\delta^{18}O_{(SO4)}$ (‰)		
		32°C	**20°C**	**12°C**
1	424	**356**	391	402
2	424	385	**426**	403
3	209	183	205	179
4	209	159	202	205
5	96	105	91	88
6	96	88	86	87
7	-18	-18.3	-20	-18
8	-18	-18.2	-18	-19

Bold values considered outliers

Table 23B: $\delta^{34}S_{(SO4)}$ of series MS-A and DI-A

Series	$\delta^{34}S_{(SO4)}$(‰)
MS-A (32) Flask 1	3.2
MS-A (32) Flask 2	4.5
MS-A (32) Flask 3	4.3
MS-A (32) Flask 4	5.7
MS-A (32) Flask 5	3.7
MS-A (32) Flask 6	5.2
MS-A (32) Flask 7	5.9
MS-A (32) Flask 8	3.2
MS-A (32) Control	4.7
MS-A (20) Flask 1	5.7
MS-A (20) Flask 2	6.3
MS-A (20) Flask 3	4.4
MS-A (20) Flask 4	4.9
MS-A (20) Flask 5	4.9
MS-A (20) Flask 6	4.2
MS-A (20) Flask 7	5.3
MS-A (20) Flask 8	5.1
MS-A (20) Control	5.3
MS-A (12) Flask 1	5.3
MS-A (12) Flask 2	4.2
MS-A (12) Flask 3	5.4
MS-A (12) Flask 4	5.1
MS-A (12) Flask 5	4.7
MS-A (12) Flask 6	4.0
MS-A (12) Flask 7	5.1
MS-A (12) Flask 8	5.0
MS-A (12) Control	5.3
MS-A (6) Flask 1	4.7
MS-A (6) Flask 2	4.4
MS-A (6) Flask 3	4.5
MS-A (6) Flask 4	4.0
MS-A (6) Flask 5	**-8.1**
MS-A (6) Flask 6	3.9
MS-A (6) Flask 7	4.5
MS-A (6) Flask 8	3.2
MS-A (6) Control	3.5
DI-A (32) Flask 1	4.7
DI-A (32) Flask 2	4.3
DI-A (32) Flask 3	4.9

DI-A (32) Flask 4	**-0.5**
DI-A (32) Flask 5	5.2
DI-A (32) Flask 6	5.1
DI-A (32) Flask 7	5.5
DI-A (32) Flask 8	4.5
DI-A (32) Control	5.3
DI-A (20) Flask 1	5.2
DI-A (20) Flask 2	4.6
DI-A (20) Flask 3	5.2
DI-A (20) Flask 4	5.2
DI-A (20) Flask 5	4.6
DI-A (20) Flask 6	**-1.3**
DI-A (20) Flask 7	5.4
DI-A (20) Flask 8	5.5
DI-A (20) Control	5.4
Average	4.9
Standard Deviation	0.78

Bold values considered outliers

Figure 1B: Normality test for S^0 samples ($\delta^{34}S$) prior to oxidation

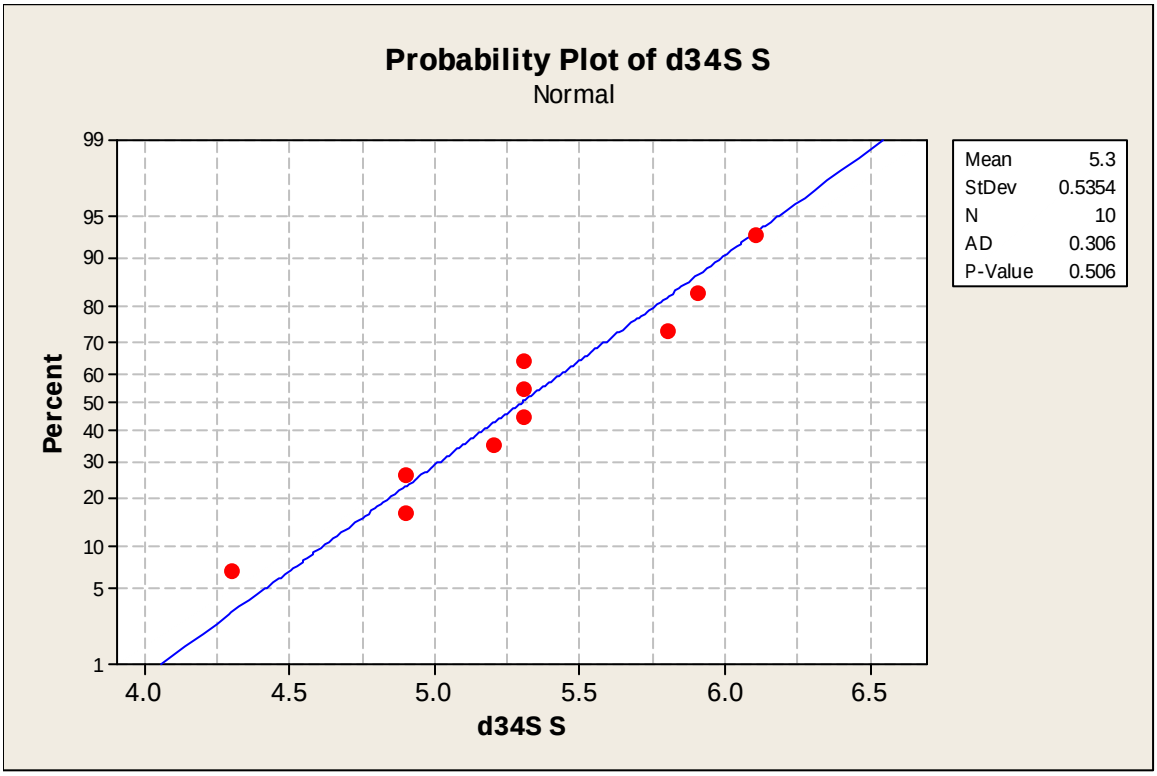

Figure 2B: Normality test for $BaSO_4$ samples ($\delta^{34}S$) after oxidation

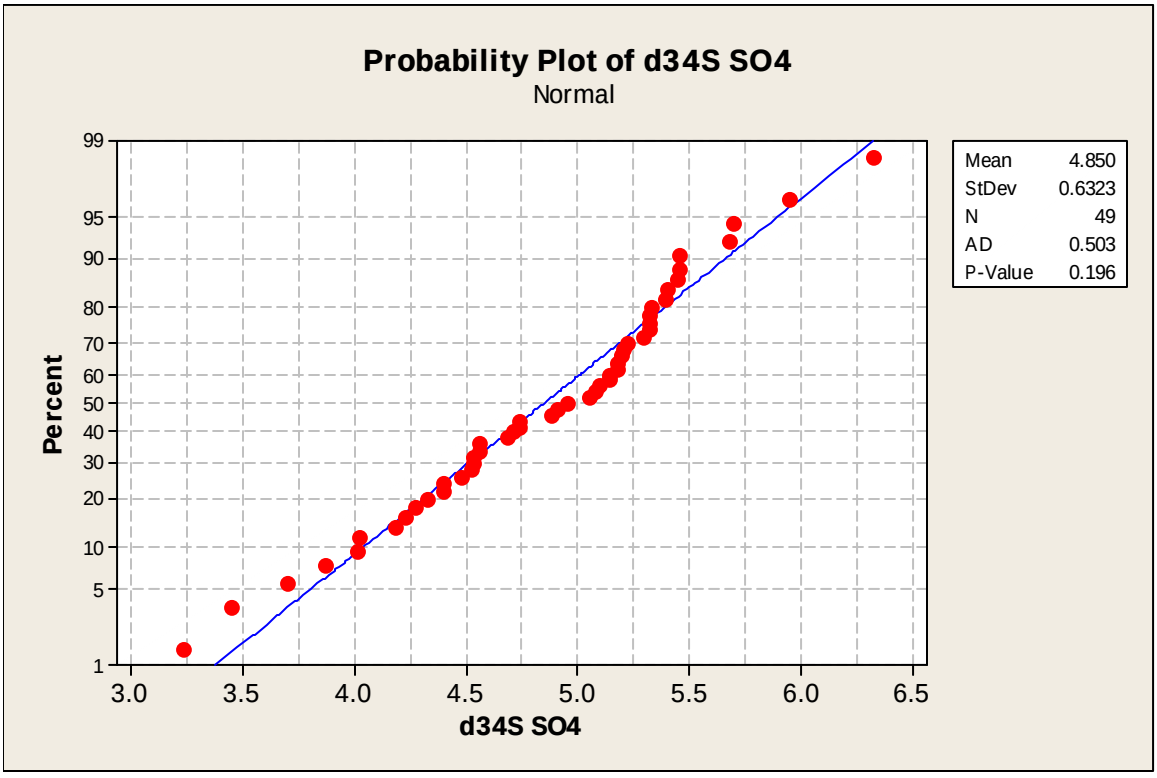

APPENDIX C- Sample calculation µg S^0 oxidized

Example: MS-A (32°C)

Table 1C: Experimental data from MS-A (32°C)

Hour	Average SO_4^{2-} (mg/L)	Average SO_4^{2-} (mg/ml)	Solution remaining in flask (ml)	Cumulative SO_4^{2-} removed (mg)	Cumulative total SO_4^{2-} (mg)	S^0 oxidized (µg)
0	80.1	0.1	100	0	0	0
144	184.4	0.2	96	0.7	10.4	3480.4
312	752.6	0.8	92	3.8	65.0	21661.0
384	1081.2	1.1	88	8.1	95.2	31739.5
480	1681.9	1.7	84	14.8	148.1	49360.1
576	2328.2	2.3	80	24.1	202.4	67456.8
672	3310.8	3.3	76	37.4	280.9	93658.9
912	4919.4	4.9	72	57.0	403.2	134410.9
1152	6677.6	6.7	68	83.7	529.8	176608.1
1584	8668.5	8.7	64	118.4	665.2	221734.9
3024	37593.2	37.6	60	268.8	2516.4	838794.9

Cumulative SO_4^{2-} removed (mg) = volume removed (4 mL) * average mg/ml (SO_4^{2-}) + previous mg SO_4^{2-} removed.

Cumulative total SO_4^{2-} produced (mg) = [(volume remaining * average mg/ml) – initial background SO_4^{2-} concentration] + cumulative SO_4^{2-} removed

S^0 oxidized (µg) = Total g SO_4^{2-} produced at each sampling period / m.w. SO_4^{2-} (96g/mol) * m.w. S^0 (32 g/mol) * 1000000µg

% S^0 oxidized = g S^0 oxidized / initial g S^0 = 0.83 g / 40 g *100 = 2.1%

APPENDIX D: Supplementary data for SCL pilot block study

Table 1D: $\delta^{18}O_{(H2O)}$ and δD of pilot block samples collected between August 2, 2006 and October 16, 2007

Table 2D: LMWL values for Edmonton, Alberta, Canada (IAEA, 2006)

Table 3D: $\delta^{18}O_{(SO4)}$ and $\delta^{18}O_{(H2O)}$ of SO_4^{2-} and H_2O in pilot block effluent samples

Table 4D: $\delta^{18}O_{(SO4)}$ and $\delta^{18}O_{(H2O)}$ of SO_4^{2-} and H_2O in Phase II block effluent samples

Table 1D: $\delta^{18}O_{(H2O)}$ and δD of pilot block samples collected between August 2, 2006 and October 16, 2007

Block	Date	$\delta^{18}O_{(H2O)}$(‰)	$\delta D_{(H2O)}$(‰)
Coletanche	**Aug. 2**	-15.5	-128.7
	Aug. 17	-15.7	-129.9
	Aug. 24	-15.8	-129.9
	Sept. 7	-16.0	-129.1
	Oct. 19	-15.6	-129.5
	Oct. 26	-15.8	-129.9
	June. 26	-19.8	-157.4
	July. 10	-18.5	-147.6
	July. 24	-18.2	-147.5
	Aug. 9	-17.9	-144.3
	Aug-24	-17.9	-145.0
	Sept. 5	-18.2	-146.0
	Sept. 18	-18.0	-147.0
	Oct-16	-17.6	-141.0
	Aug. 2	-17.4	-139.6
	Aug. 17	-17.5	-140.5
	Aug. 24	-17.4	-139.2
	Sept. 7	-17.7	-141.3
	Oct. 19	-17.8	-142.1
Insulated	**Oct. 26**	-17.7	-141.2
	June. 5	-17.2	-139.8
	June. 14	-17.9	-144.5
	June. 26	-17.8	-143.4
	July. 10	-17.7	-141.2
	July. 24	-17.6	-141.9
	Aug. 9	-17.5	-139.6
	Aug-24	-18.3	-144.0
	Sept. 5	-18.2	-144.0
	Sept. 18	-18.0	-140.0
	Oct-02	-17.7	-140.0
	Oct-03	-17.7	-141.0
	Oct-16	-18.1	-141.0
	Aug. 2	-18.1	-142.5
	Aug. 17	-18.1	-143.2
	Aug. 24	-18.0	-141.7
	Sept. 7	-17.2	-139.3
	Oct. 19	-17.9	-141.7
	Oct. 26	-17.8	-141.5

Reclamation	**June. 14**	-18.8	-149.1
	June. 26	-18.5	-147.8
	July. 10	-18.4	-146.3
	July. 24	-18.4	-147.0
	Aug. 9	-18.1	-144.5
	Aug-24	-18.9	-145.0
	Sept. 5	-18.5	-146.0
	Sept. 18	-17.7	-140.0
	Oct-02	-17.5	-138.0
	Oct-16	-17.8	-140.0
	Aug. 2	-16.0	-124.4
	Aug. 17	-15.9	-124.5
	Aug. 24	-15.9	-123.7
	Sept. 7	-16.0	-123.5
	Oct. 19	-16.2	-125.8
	Oct. 26	-15.9	-125.0
	June. 5	-16.4	-137.7
	June. 14	-16.6	-132.0
	June. 26	-16.9	-134.6
	July. 10	-16.8	-132.5
Exposed	**July. 24**	-16.9	-134.0
	Aug. 9	-16.0	-126.2
	Aug. 24	-15.4	-121.0
	Sept. 5	-15.1	-119.0
	Sept. 18	-14.8	-117.0
	Oct-02	-14.6	-115.0
	Oct-03	-16.4	-129.0
	Oct-16	-14.8	-116.0

Table 2D: LMWL values for Edmonton, Alberta, Canada (IAEA, 2006)

δD(‰)	$\delta^{18}O$(‰)
-92.3	-13.2
-86.1	-11.4
-104.6	-14.8
-112.7	-14.1
-122.4	-16.0
-166.3	-20.1
-146.5	-17.8
-114.5	-15.1
-102.8	-11.6
-109.6	-14.0
-124.2	-14.9
-163.8	-22.0
-165.7	-22.3
-180.4	-23.9
-200.1	-26.7
-200.1	-26.0
-153.9	-19.2
-158.2	-19.8
-169.4	-21.3
-126.1	-15.8
-101.6	-12.8
-114.5	-14.7
-113.3	-14.3
-82.4	-10.7
-187.2	-23.9
-178.6	-22.9
-202.0	-25.9
-160.7	-21.4
-174.3	-22.5
-127.4	-17.8
-112.1	-13.8
-92.9	-11.6
-115.7	-16.4
-121.8	-15.2
-124.2	-15.8
-187.2	-24.6
-213.7	-27.0
-203.2	-26.6
-129.2	-17.0
-91.0	-13.1
-98.3	-12.4
-120.7	-16.1
-116.1	-15.7
-125.3	-15.9
-177.5	-24.2
-198.5	-26.7

Table 3D: $\delta^{18}O_{(SO4)}$ and $\delta^{18}O_{(H2O)}$ of SO_4^{2-} and H_2O in pilot block effluent samples

Date	Coletanche $\delta^{18}O_{(SO4)}$(‰)	Coletanche $\delta^{18}O_{(H2O)}$(‰)	Insulated $\delta^{18}O_{(SO4)}$	Insulated $\delta^{18}O_{(H2O)}$	Reclamation $\delta^{18}O_{(SO4)}$	Reclamation $\delta^{18}O_{(H2O)}$	Exposed $\delta^{18}O_{(SO4)}$	Exposed $\delta^{18}O_{(H2O)}$
01-Aug-06	-15.5	-13.6	-17.7	-19.7	-18.1	-15.1	-16.0	-17.7
26-Oct-06	-15.8	-13.6	-17.7	-	-17.8	-18.0	-15.9	-18.9
14-Jun-07	-18.5	-13.2	-17.4	-18.3	-17	-16.2	-16.8	-18.9
07-Sep-07	-17.2	-14.1	-17.7	-17.7	-17.5	-18.4	-14.6	-14.2

Table 4D: $\delta^{18}O_{(SO4)}$ and $\delta^{18}O_{(H2O)}$ of SO_4^{2-} and H_2O in Phase II block effluent samples

Date	Phase II block $\delta^{18}O_{(SO4)}$(‰)	Phase II block $\delta^{18}O_{(H2O)}$(‰)
13-Aug-07	-16.2	-15.9
10-Nov-07	-20.0	-19.8